



Contents lists available at ScienceDirect

# Environmental Technology & Innovation

journal homepage: [www.elsevier.com/locate/eti](http://www.elsevier.com/locate/eti)

## Conducting polymer based visible light photocatalytic composites for pollutant removal: Progress and prospects

Gopalan Saianand<sup>a,b,\*</sup>, Anantha-Iyengar Gopalan<sup>c,1</sup>, Liang Wang<sup>a,b</sup>,  
K. Venkatramanan<sup>d</sup>, Vellaisamy A.L. Roy<sup>e</sup>, Prashant Sonar<sup>f</sup>, Dong-Eun Lee<sup>g,\*\*</sup>,  
Ravi Naidu<sup>a,b,\*</sup>

<sup>a</sup> Global Centre for Environmental Remediation (GCER), College of Engineering, Science and Environment, The University of Newcastle, Callaghan 2308, New South Wales, Australia

<sup>b</sup> Cooperative Research Centre for Contamination Assessment and Remediation of the Environment (CRC CARE), Callaghan 2308, New South Wales, Australia

<sup>c</sup> Intelligent Construction Automation Center, Kyungpook National University, Daegu 41566, South Korea

<sup>d</sup> Department of Physics, SCSVMV Deemed University, Kanchipuram 631561, Tamil Nadu, India

<sup>e</sup> James Watt School of Engineering, University of Glasgow, G12 8QQ, United Kingdom

<sup>f</sup> Centre for Materials Science, School of Chemistry and Physics, Queensland University of Technology (QUT), 2 George Street, 4001 Brisbane, Australia

<sup>g</sup> School of Architecture, Civil, Environment and Energy Engineering, Kyungpook National University, 80

Daehakro, Buk-gu, Daegu 41566, Republic of Korea

### ARTICLE INFO

#### Article history:

Received 24 January 2022

Received in revised form 22 April 2022

Accepted 24 May 2022

Available online 2 June 2022

#### Keywords:

Conducting polymers

Inorganic semiconductors

Visible light mediation

Photocatalysis

### ABSTRACT

Conducting polymers (CPs) have been proved to be instrumental in enhancing photocatalytic efficacy owing to their unique physicochemical properties and energy levels. In this regard, titanium dioxide (TiO<sub>2</sub>) has been investigated in transdisciplinary research areas (like catalysis, energy technologies, health, and environment) due to its desirable characteristics. In the process of developing advanced photocatalysts, novel inorganic–organic heterojunction design based materials have been explored and developed in contrast to conventional, inorganic–inorganic type semiconducting photocatalysts (SCPs). In this context, hybrid/composite SCPs comprising CPs and TiO<sub>2</sub>, have received significant attention for enhancing photocatalytic efficacy in terms of activity as well as visible light activation. The synergistic contribution from CPs (here we focus only on polyaniline (PANI) and polypyrrole (PPy)) and TiO<sub>2</sub> have been proved to enhance light-absorption capability in the visible region, photogenerated extraction, and higher stability. Importantly, the published literature (before 2015) on the photocatalysis of TiO<sub>2</sub>-CP composites mainly discusses in terms of the sensitizing aspects of CP for TiO<sub>2</sub>. However, there is a critical need to review the literature (beyond 2015) to explore the state of art progress concerning the mechanism of photocatalytic performances as phenomenal parallel developments and knowledge gaps have been addressed on new kinds of heterojunction formation (like S-Scheme over traditional ones), band tuning and interfacial contact effects between two SCPs. In particular, this topical review aims

**Abbreviations:** CPs, Conducting polymers; Titanium dioxide, TiO<sub>2</sub>; NC, Nanocomposites; SCPs, Semiconducting photocatalyst; PANI, Polyaniline; PPy, Polypyrrole; VOCs, Volatile organic compounds; PEDOT, Poly(3,4-ethylenedioxythiophene); UV, Ultraviolet; TC, Tetracycline; RhB, Rhodamine B; CV, Crystal violet; HOMO, Highest occupied molecular orbital; LUMO, Lowest unoccupied molecular orbital

\* Corresponding authors at: Global Centre for Environmental Remediation (GCER), College of Engineering, Science and Environment, The University of Newcastle, Callaghan 2308, New South Wales, Australia.

\*\* Corresponding author.

E-mail addresses: [SaiAnand.Gopalan@newcastle.edu.au](mailto:SaiAnand.Gopalan@newcastle.edu.au) (G. Saianand), [Dolee@knu.ac.kr](mailto:Dolee@knu.ac.kr) (D.-E. Lee), [Ravi.Naidu@newcastle.edu.au](mailto:Ravi.Naidu@newcastle.edu.au) (R. Naidu).

<sup>1</sup> Authors contributed equally to this work.

<https://doi.org/10.1016/j.eti.2022.102698>

2352-1864/© 2022 The Author(s). Published by Elsevier B.V. This is an open access article under the CC BY-NC-ND license (<http://creativecommons.org/licenses/by-nc-nd/4.0/>).

to capture and highlight the current advancements (2016–2021) in relevance to the visible light photocatalytic performance of CP–TiO<sub>2</sub> functional composites, which include nanostructures and multi-components. The predominantly available literature over the last five years on the application of CPs–TiO<sub>2</sub> functional composites for monitoring or removal of pollutants under visible light activation is reviewed giving importance to revealing the role of CP in concurrent enhancement in both visible light activation and photocatalytic performances. Finally, we elaborate on the challenges and future outlook for advanced research and development in this area.

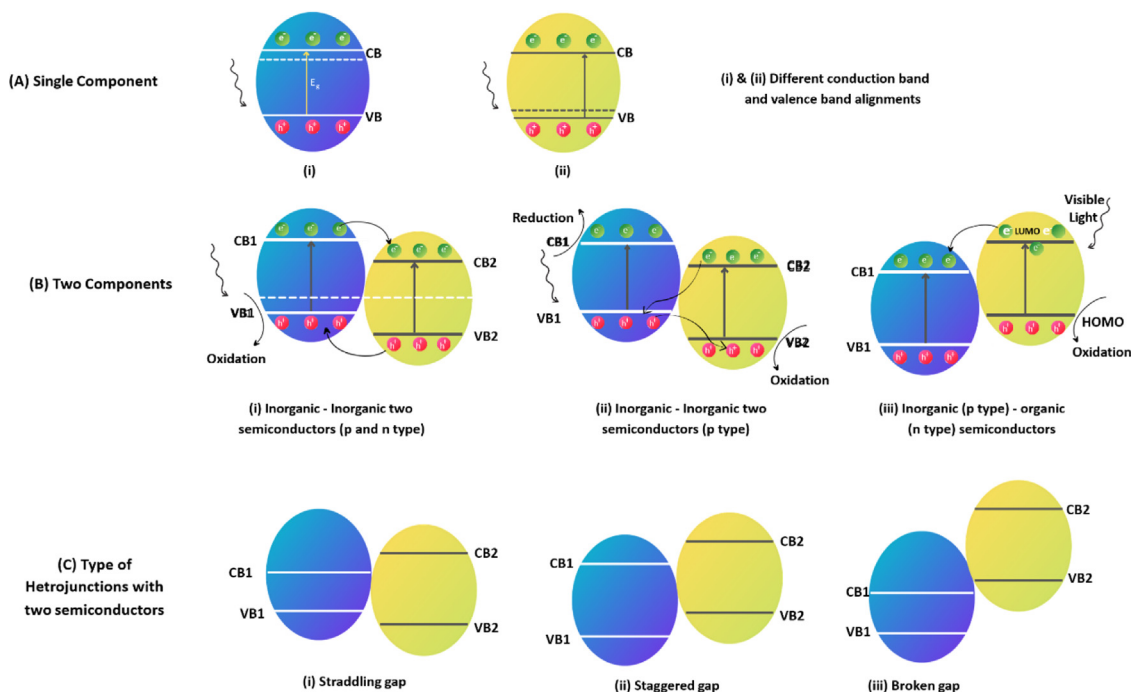
© 2022 The Author(s). Published by Elsevier B.V. This is an open access article under the CC BY-NC-ND license (<http://creativecommons.org/licenses/by-nc-nd/4.0/>).

## Contents

1. Introduction.....	2
1.1. State of the art of the topic.....	4
1.2. Progress beyond the state of the art.....	6
2. Key aspects of the review .....	6
3. Semiconductor photocatalysis.....	7
3.1. TiO <sub>2</sub> as photocatalysts.....	7
3.2. Visible light photocatalysts for environmental remediation .....	7
3.2.1. TiO <sub>2</sub> in visible light photocatalysis .....	8
3.2.2. CPs and photoactivity .....	9
4. PANI/PPy in visible light photocatalysis.....	10
4.1. Methods of preparation of TiO <sub>2</sub> –CP composites.....	10
4.2. Photocatalysis by TiO <sub>2</sub> in conjunction with PANI for photocatalytic pollutant removal.....	10
4.2.1. Mechanism of photodegradation by PANI–TiO <sub>2</sub> composite.....	10
4.2.2. PANI–TiO <sub>2</sub> conventional composites .....	11
4.2.3. Nanostructured PANI–TiO <sub>2</sub> composites.....	12
4.2.4. TiO <sub>2</sub> incorporated PANI ternary composites.....	16
4.2.5. TiO <sub>2</sub> –PANI based multicomponent composites.....	18
4.2.6. PANI–semiconductor (other than TiO <sub>2</sub> ) based photocatalytic systems.....	18
5. Various types of PPy–TiO <sub>2</sub> based visible light photocatalysts .....	18
5.1. PPy–TiO <sub>2</sub> composites.....	18
5.2. PPy–TiO <sub>2</sub> nanostructures .....	19
5.3. PPy–TiO <sub>2</sub> based multicomponent photocatalysts .....	20
5.4. PPy in conjunction with semiconductors other than TiO <sub>2</sub> .....	24
6. Conclusion and prospects.....	24
CRediT authorship contribution statement .....	25
Declaration of competing interest.....	25
Acknowledgments .....	25
References .....	25

## 1. Introduction

Keeping in view of the importance of the increasing need for green energy requirements for human society and towards problems of mitigating environmental deterioration, the development of clean and green photocatalysis technology has been given increasing research interest. Ever since the phenomenon of photocatalysis was first discovered by Honda–Fujishima on the photo–electrochemical water splitting using titanium dioxide (TiO<sub>2</sub>) as the photocatalyst, the utilization of photocatalysis technology has been proved its importance through several photocatalysts in diversified fields, that include, environment, pollution control, energy conservation/production, and chemicals synthesis, etc. (Fujishima and Honda, 1972). Notably, the importance of photocatalysis for human life has been realized steadily. Of course, there exist grand challenges to utilizing photocatalysis for further expanding the practical application of photocatalytic technology, and this aspect is given preference for intensive research activities. Over the past five decades, research activities have been triggered towards the development of several strategies to fine-tune the physico-chemical attributes of photocatalysts in the process of enhancing the efficiency of photocatalysis through various performing improvement strategies (Wu et al., 2021). The general strategies that have been evolved for enhancing the efficiency of photocatalysis revolve around engineering the semiconductor interfaces in composite photocatalytic systems via the inclusion of diverse individual components (coupling two inorganic semiconductors, compositing inorganic–polymer, etc) to form heterojunctions, p–n junctions, and Z-scheme systems, etc (Scheme 1). In particular, solar energy, the abundant natural and low-cost energy source can be utilized for the removal of harmful organic compounds in the process of mitigating pollution as well for sustainable and clean energy production from water splitting (Xing et al., 2020), photocatalytic degradation of pollutants

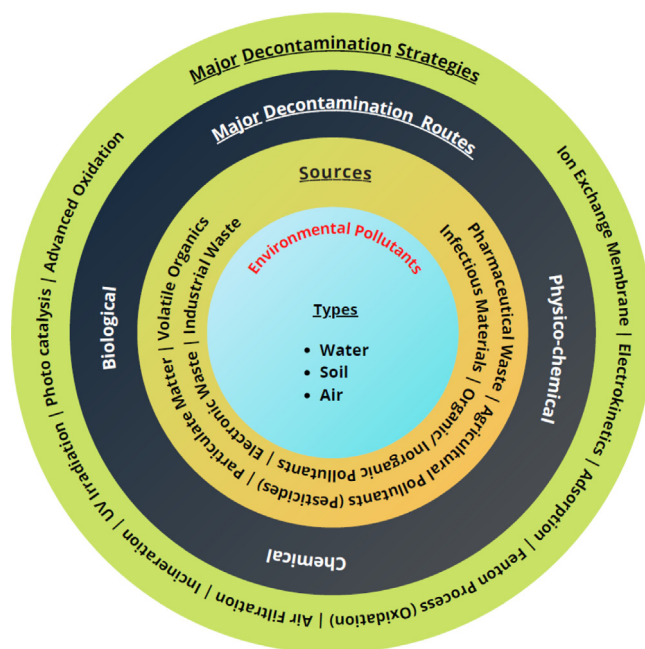


**Scheme 1.** (a, b) single/two components, (c) heterojunction, (d) Z-scheme and (e–g) type I/II/III heterojunctions.

(Ayodhya and Veerabhadram, 2018), energy conversion/storage (Abdelnasser et al., 2021) and to provide a sustainable pathway for green synthesis of important chemicals (Molinari et al., 2017).

In recent years, one significant challenge facing environmental scientists has been to mitigate the increasing health issues arising from air/water/soil pollution through practical or viable methodologies, especially *via* green technologies, toward a sustainable future (Hou et al., 2020). The research activities for removing or controlling toxic (organic and inorganic) pollutants (mainly released from industrial and anthropogenic activities) are given utmost importance (Carolin et al., 2017). Water pollutants reach the earth's environment predominantly *via* industrial origin (textile, tannery, pharmaceutical, agricultural, etc.). The expulsion of effluents from these industrial resources could cause pollution of water at the surface and ground levels. One must note that pharmaceutical industries and hospitals' waste expulsion, especially antibiotics, can also contaminate soil or water through complexation with other pollutants, such as organics and heavy metals, and pose a serious threat to a biological organism. Conversely, air pollutants can also be gaseous substances (particulate matter, carbon monoxide, carbon dioxide, and volatile organic compounds (VOCs)) that are released from automobiles, factories, and pesticide usage that exceed the permissible limit in the air which can lead to health issues. These primary pollutants can as well generate secondary pollutants such as ozone, sulfuric acid, nitric acid, and hydrogen peroxide and further increase the pollutant effects. While conventional techniques have been attempted over the years, the development of newer and practical methods is essential and warranted to minimize environmental contaminants and toxic pollutants that include waterborne pesticides, textile and tannery effluents, organics (phenolic and non-phenolic), inorganics (heavy metal ions), gaseous nitrogen/sulfur oxides, VOCs, and solid wastes (Biswas et al., 2019b; Hassan et al., 2020).

Scheme 2 illustrates the types of environmental pollutants and the predominant methodologies adopted for contaminant remediation. Considering the different approaches that are available for pollutant removal in air/water, the use of photocatalysts has emerged as one of the latest developments to mitigate pollutants (Boyjoo et al., 2017). In these pursuits, several photocatalytic materials have been developed can mainly be divided into metal oxides (TiO<sub>2</sub>, zinc oxide, iron oxide, copper oxide, tungsten(VI) oxide, and others) and non-metal oxide-based (tungstates, bismutates, vanadates, complex oxyhalides, carbon nanostructures, etc.) materials toward treating diverse pollutants in various media. In recent literature, the potential roles of various photocatalytic materials on the photocatalytic abatement of both organic and inorganic pollutants have been reviewed (Talaiekhazani et al., 2021). Among the photocatalysts, TiO<sub>2</sub> has been extensively investigated because it possesses several advantages that include high photocatalytic activity, appropriate physical and chemical stability, non-corrosiveness, non-toxic nature, and high abundance. The ground-breaking investigation on conducting polymers (CP) in 1977 opens up the horizon of technological application prospects for CPs branching out into various disciplines. The diverse molecular structures and the feasibility of tuning the physico-chemical properties provide unparalleled opportunities for CPs in developing highly efficient photocatalysts.



**Scheme 2.** Environmental Pollutants: Types, Sources, Decontamination Routes and Strategies.

### 1.1. State of the art of the topic

There has been increasing interest in extending research on advanced green technologies and processes toward developing different types of photocatalytic materials possessing enhanced visible light (solar) absorption properties and evaluating their utilities in various applications that include environmental remediation. As a consequence, one could notice the emergence of many reviews on photocatalysts for pollutant removal (Zhang et al., 2020). Due to the exceedingly high research activities on  $\text{TiO}_2$  photocatalysis, a sufficiently larger number of reviews have been published (Courtesy: Web of Science) on  $\text{TiO}_2$  photocatalysis in recent years (over 350 reviews since 2016) and out of which more than 50% (nearly 176) reviews have been focused on visible or solar photocatalysis. Around 35 reviews are available in the literature on “visible light-mediated  $\text{TiO}_2$  photocatalysis on pollutant removal” (Table 1). Those reviews cover the developments in  $\text{TiO}_2$  based visible light photocatalysis either focusing on “modified  $\text{TiO}_2$ ” or as a part of the topic related to all the semiconductor photocatalysts. In the past 5 years (since 2016), a considerable number of research papers (nearly 1100 since 2016) have been published on “ $\text{TiO}_2$ -CP composite/hybrids”, however, an exclusive and comprehensive review on the topic “ $\text{TiO}_2$ -CP composite/hybrids” as “visible light-mediated photocatalysts for pollutant removal” is not available until now.

In this review, we focus on providing novel perspectives as well a concise description of the developments and key strategies used on “ $\text{TiO}_2$  – CP composite/hybrids as visible light photocatalysts” and their utilities for environmental pollutant removal. We specifically emphasize the different points of view concerning the issue of visible light activation by CPs in conjunction with  $\text{TiO}_2$  by providing a clear description of the shortcomings and strategies to tackle the grand challenges using selected examples. Further to note, among many CPs available, most research activities on  $\text{TiO}_2$  – CP composite/hybrids have been focused on two of the CPs, namely, polyaniline (PANI) and polypyrrole (PPy). Typically, out of the nearly 1100 papers published on “ $\text{TiO}_2$ - CP composite/hybrids”, the predominance of PANI (580 research papers since 2016) and PPy (80 research papers since 2016) is significant. We understand that a comprehensive overview over a short time frame may not be a particularly useful task because that may sometimes mask the primary issues that need to be highlighted. Hence, we focus on the research activities that provide advancement of knowledge in this field.

Poly(3,4-ethylenedioxythiophene) (PEDOT) exhibits desirable characteristics such as environmental stability, biocompatibility, and high optical transparency that are needed for the development of the highly efficient photocatalytic system (Ghosh et al., 2015a). The perfect conjugation structure in PEDOT augments electron transfer processes during photoexcitation and the electronic conductivity in PEDOT provides the basis for applications in optoelectronic devices (Reza et al., 2020; Saianand et al., 2021; Xu et al., 2017) and biosensors (Khodagholy et al., 2013). When PEDOT is nanostructured, it possesses a narrow bandgap ( $E = 1.69$  eV) which in turn is suitable for absorbing light in the visible and near-infrared region. It has been demonstrated that PEDOT based photocatalysts can be stable and suitable for multiple reuses without a significant loss in photoactivities (Ghosh et al., 2015b). Most importantly the inherent redox properties in PEDOT and stability in the presence of oxidative species like hydroxyl radicals form the basis for the

**Table 1**  
Reviews on visible light-mediated TiO<sub>2</sub> photocatalysis for pollutant degradation.

Modified TiO <sub>2</sub>	Application	Reference
TiO <sub>2</sub> -based photocatalysts	Air treatment/purification (Removal of VOCs, inorganic gas pollutants)	Boyjoo et al. (2017)
TiO <sub>2</sub> based photocatalysts	Organic and inorganic pollutants in the air	Talaiekhozani et al. (2021)
Modified TiO <sub>2</sub> (with layered double hydroxides)	Organic pollutants (azo dyes, phenol compounds)	Zhang et al. (2020)
Fe <sub>2</sub> O <sub>3</sub> /TiO <sub>2</sub>	Organic pollutant removal (Dyes, pharmaceuticals, pesticides)	Fawzi Suleiman Khasawneh and Palaniandy (2021)
Ag <sub>3</sub> PO <sub>4</sub> /TiO <sub>2</sub>	Gaseous environment (VOCs, acetaldehyde, formaldehyde, trichloroethylene, NO <sub>x</sub> )	Naciri et al. (2021)
Doped TiO <sub>2</sub> /Composite TiO <sub>2</sub>	Industrial chemicals (phthalate esters) (Atmosphere, water, soil, and sediment)	Pang et al. (2021)
Doped TiO <sub>2</sub>	Water disinfection and micro-pollutant abatement	Venieri et al. (2020)
TiO <sub>2</sub> based photocatalysts	Decomposition of acetaldehyde	Tryba et al. (2020)
TiO <sub>2</sub> doped films	Aqueous bisphenol A oxidation	Žerjav et al. (2020)
Modified TiO <sub>2</sub> (Nanostructured, doped, composites)	Water pollutant removal (Dyes, pharmaceuticals, and others)	Gopinath et al. (2020)
TiO <sub>2</sub> /g-C <sub>3</sub> N <sub>4</sub>	Photocatalytic conversion of CO <sub>2</sub> , pollutant degradation	Acharya and Parida (2020)
Chitosan supported TiO <sub>2</sub>	Wastewater pollutant remediation	Mohd Adnan et al. (2020)
Aerogel based TiO <sub>2</sub> (TiO <sub>2</sub> @carbon, Fe <sub>3</sub> O <sub>4</sub> @TiO <sub>2</sub> )	Organic dyes using aerogels from wastewater	Hasanpour and Hatami (2020)
TiO <sub>2</sub> -based heterojunctions	Degradation of personal care products & pharmaceuticals	Kumar et al. (2020)
Modified TiO <sub>2</sub>	Aqueous pharmaceutical pollutants	Majumdar and Pal (2020)
TiO <sub>2</sub> -based photocatalysts	Aqueous pollutants and degradation of pesticides	Kanan et al. (2020)
Plasmonic/TiO <sub>2</sub>	Organic/inorganic pollutants (liquid/gaseous media) and inactivation of pathogenic microorganisms	Wang et al. (2018)
TiO <sub>2</sub> : From Engineering to Applications	Aqueous pollutants and air pollutants	Kang et al. (2019)
TiO <sub>2</sub> /porous adsorbents	Dye degradation and others	MiarAlipour et al. (2018)
Graphene embedded TiO <sub>2</sub>	Degradation of dyes synthetic	Giovannetti et al. (2017)
Modified TiO <sub>2</sub> -based photocatalysts	Air quality, disinfection	Binas et al. (2017)

excellent photocatalytic activities (Casado et al., 2016). In general, PEDOT in its nascent neutral form has a low electronic bandgap of 1.6–1.7 eV, and the onset of the  $\pi - \pi^*$  absorption starts from 610 nm. The  $\pi$ -conjugated polythienyl group in PEDOT and the electronic state of PEDOT support hole mobility and hence PEDOT can function as an efficient hole transport material (Jeong et al., 2020). Notably, PEDOT has higher charge injection ability and lower impedance than metals and hence can be effectively coupled with inorganic semiconductor materials which are suitable for the fabrication of composite photocatalysts (Kayser and Lipomi, 2019). However, the literature reveals that the major use of PEDOT is not on photocatalysis but rather is based on the doping nature of PEDOT backbone with a myriad of synthetic or biological counter-ions, leading to bioelectronic, flexible electronics, and biosensors (Boehler et al., 2019; Gueye et al., 2020; Hui et al., 2018). PEDOT in conjunction with poly(styrene sulfonate) (PSS), an anionic polymer electrolyte (PEDOT:PSS) possesses good film-forming characteristics, high transparency, and excellent stability (Anantha-Iyengar et al., 2019; Sun et al., 2015). Thus, PEDOT:PSS has been widely used in diversified applications including displays, transistors, various sensors, and photovoltaics (del Agua et al., 2018; Fan et al., 2019; Kim et al., 2018). Nevertheless, the photocatalytic applications of PEDOT in composite forms are scarce. Few studies are highlighted here. The composite photocatalyst made of TiO<sub>2</sub> and PEDOT (TiO<sub>2</sub>-PEDOT) has been explored for the removal of bisphenol A (Katančić et al., 2020). The ternary photocatalyst PEDOT@ZnO@MWCNTs was fabricated using the chemical oxidative method of polymerization and the photodegradation of the dye was studied with the visible source of light (Khan and Narula, 2019). The enhanced photocatalytic activity is attributed to the increased visible light absorption and separation of photogenerated charge carriers to the redox surface.

The review published in 2021 (Amorim et al., 2021) mainly detailed the synthesis and characterization aspects of TiO<sub>2</sub>-PPy composites, however, no highlighted chapter focused on the visible light photoactivities including the information pertaining to the photocatalytic mechanisms. This review will present an overview of “TiO<sub>2</sub>-CP composite/hybrids as visible light-mediated photocatalysts for pollutant removal” focusing on the use of PANI and PPy, within a short time frame (2016 till present).

## 1.2. Progress beyond the state of the art

In the year 2015, a short review on “Role of Conducting Polymers in Enhancing TiO<sub>2</sub>-based Photocatalytic Dye Degradation” has been published (Riaz et al., 2015). The review mainly focused on the role of CP as the sensitizer for TiO<sub>2</sub> towards enhancing the photoactivity of TiO<sub>2</sub>. Until 2015, the literature on visible light active TiO<sub>2</sub>-CP composites was limited and hence the review in 2015 covered the sparingly available studies on visible light photocatalytic properties of TiO<sub>2</sub>. Hence, the distinct role of CPs in enhancing the visible light photoactivities has not been dealt with separately in that review. In the case of TiO<sub>2</sub>-CP composites, the extended visible light photoactivation needs to be coupled with enhanced redox activities for the photogenerated carriers for achieving high performance for the photodegradation of pollutants. Besides the role of CP as a sensitizer for TiO<sub>2</sub>, additional features such as heterojunction formation and interfacial contacts need to be present in the TiO<sub>2</sub>-CP composites. Such features have not been covered in that contribution. In recent years, heterojunction construction favors visible light photoactivity to TiO<sub>2</sub> which can not only solve the charge recombination problems but also decouple oxidation and reduction reactions for the photogenerated carriers (Chen et al., 2022; Wang et al., 2022). While considering the two semiconductor based composite/hybrid photocatalysts, in general, two types of heterojunctions (type-II (comprised of semiconductor photocatalyst I (SPC I) and SPC II), and Z-scheme (Lu et al., 2021) are predominantly used. The formation and ultimate photocatalytic properties of type-II heterojunction are dependent on valence band (VB)/conduction band (CB) energy levels of constituent SPC 1 and SPC 2. The Z-scheme originates by mimicking the photosynthetic processes. The Z-scheme family is further subdivided into traditional, all-solid-state, and direct Z-scheme heterojunctions (Tada et al., 2006). It has been well demonstrated that factors such as the semiconducting nature (n-type or p-type) of SPC, Fermi level position of the semiconductors, and CB/VB potentials of the constituent semiconductors determine the heterojunction properties, carrier transfer efficiency, and the photocatalytic mechanism of the photocatalytic process (Yang, 2021). By critically analyzing the shortcomings and limitations of type II and Z-scheme heterojunctions (Fu et al., 2019), brought forward a new heterojunction concept, namely S-scheme heterojunction, composed of oxidation photocatalysts (OP) and reduction photocatalysts (RP), with spatially separated reduction and oxidation units. The photoinduced electrons (e<sup>-</sup>) and holes (h<sup>+</sup>) accumulate in the semiconductor with a more negative conduction band CB position and the other semiconductor with the more positive VB position, respectively. In the S-scheme heterojunction, RP and OP are energetically positioned with staggered band structures. Though this kind of band structure is similar to type-II heterojunction, the charge transfer process is entirely different. In the S-Scheme heterojunction, the charge transfer process is driven mainly through the internal electric field between SPC I and SPC II. The work function and Fermi level of oxidation photocatalyst (SPC I) and the reduction photocatalyst (SPC II) are tuned because of the intrinsic features of novel heterojunction. The S-Scheme favors simultaneously visible light absorption, enhanced charge separation, and higher charge carrier redox capacity. More importantly, an intimate interfacial contact and band structure alignment between the SCPs, are crucial factors for forming the S-scheme charge transfer pathway across the interface (namely, S-scheme heterojunction). As well, PANI can behave as a p-type reductive SCP and can have band bending which is favorable for transferring e<sup>-</sup> and h<sup>+</sup> between reductive SCP and oxidative SCP in the S-Scheme heterojunction (Zhao et al., 2015).

## 2. Key aspects of the review

To our knowledge, there is a need to critically review the recent literature (published beyond 2015) on photocatalytic studies on TiO<sub>2</sub>-CPs given the latest developments in the coupled effects of SCP based heterojunction, bandgap tuning, and intimate interfacial contacts between the SC components. While visible light photoactivity has been witnessed for TiO<sub>2</sub>-CPs composites, the explanations for the photocatalytic enhancement mechanism need to be reviewed thoroughly based on the latest developments in the mechanistic pathways for the photocatalytic processes. Furthermore, the steady advances in concepts and design on the visible light-mediated photocatalysis using TiO<sub>2</sub>-CP based materials that include complicated ternary or quaternary photocatalysts and their uses for environmental pollutant removal applications will also be detailed. While there has been significant progress in the synthesis and application of nanoscale or nanostructured (nanowire, nanotube, etc) TiO<sub>2</sub> or CP, the development of photocatalysts based on the combination of these materials are gaining importance in recent years. The literature on the role of CPs for enhancing photocatalytic performances in TiO<sub>2</sub> has not been reviewed so far in relevance to ternary or quaternary photocatalysts and the role of nanostructured components. There is an urgent necessity to cover and update the recent developments and challenges in the TiO<sub>2</sub>-CP based hybrid photocatalysis focusing on the role of CPs. This review presents the description of the visible light-activated photocatalytic processes detailing the role of PANI in PPy - TiO<sub>2</sub> aided photocatalysis. We particularly illustrate the importance of these hybrids for the photodegradation of various aqueous pollutants. We emphasize on bringing out how the modification of TiO<sub>2</sub> with CPs could influence the optoelectronic properties, charge carrier separation efficiency, charge transport, and the enhancement of the photocatalytic activities. Nevertheless, this review also presents the literature available on visible light-mediated CP based photocatalysts. Finally, we propose perspectives for exploring newly modified TiO<sub>2</sub>-CPs for photocatalytic applications, which is expected to trigger more exciting research activities in this field. As a result of the proven importance of green technology developments and decontamination of the environment, photocatalysis has witnessed increasing consideration in recent years. The developments in this thriving area are expected to resolve the grand challenges concerning clean energy toward realizing a decarbonized society.

### 3. Semiconductor photocatalysis

Among the various methodologies available to remove environmental pollutants, photocatalysis has been regarded as an eco-friendly technology that depends on irradiated light in degrading the contaminants and converting them into their non-toxic component (Hisatomi et al., 2014; Jo et al., 2019). The photocatalyst participates in the various stages of photocatalytic transformation: generation of transient state intermediate through absorption of light (photon energy), charge carrier ( $e^-$  and  $h^+$ ) production, and photocatalytic chemical transformations (resulting products).

The interest in photocatalysis has been steadily increasing after the seminal works that were published by Kraeutler et al. (1979), Reiche and Bard (1979) and Fujishima and Honda (1972). Since then, various photocatalytic materials and their applications have been investigated. The widespread commercial applications are typically limited due to the low photocatalytic activity of these photocatalytic materials under visible or solar illumination. Popular photocatalytic materials, such as single component photocatalysts or multi-component heterojunctions (including Z-scheme systems), include  $TiO_2$  and its composite counterparts (Lee et al., 2015a, 2019, 2020; Meng et al., 2019), zinc oxide (Ong et al., 2018), graphitic carbon nitride (Mishra et al., 2019; Dong et al., 2019), metal-organic framework compounds (Mehla et al., 2020), black phosphorus (Liu et al., 2019; Wen et al., 2019), zinc ferrite (Huang et al., 2017) and others. Regarding these classes of materials, the most prominent approaches include using judiciously designed heterojunction (including Z-scheme) photocatalysts, and complex multi-component systems by combining co-catalysts and/or plasmonic particles. Over the last three decades, there has been plenty of research activities on advanced oxidation processes using semiconductor photocatalysis for water treatment. Semiconductor photocatalysis could be applied to the development of air purification strategies, besides the most prevalent water treatment. The pollutants of interest include nitrogen oxide, sulfur oxide, carbon monoxide, hydrogen sulfide, and VOCs. It has been evident through literature that unlike water treatment and fuel generation, the utilization of photocatalysis for air purification is challenging both economically and technologically. For a detailed review of this application, readers are advised to refer to reference (Boyjoo et al., 2017). The design and development of non-noble, metal-free catalytic active material receive importance to reduce the cost of photocatalysts (Yi et al., 2018).

#### 3.1. $TiO_2$ as photocatalysts

Among the different photocatalysts, semiconductor photocatalysts have shown significant efficiency in degrading organic and inorganic pollutants (Rahimi et al., 2016). The bottlenecks that must be considered in terms of mass scale-up for practical application include limited solar light spectrum absorption, charge recombination, low electronic transport, and low photostability. (Lang et al.)  $TiO_2$  is one of the important commercial and efficient photocatalyst materials for degrading many pollutants because of its versatility, ease in synthesis, and excellent controllability and stability (Lang et al., 2020; Lee et al., 2015b). Anatase and rutile are the most thoroughly explored  $TiO_2$  phases; while anatase exhibits superior photocatalytic activity, rutile has better thermodynamic stability (Lee et al., 2020; Luttrell et al., 2014). Few other phases, such as brookite, also receive attention mainly based on their surface structure characterization and photoactivity (Henderson, 2011). Hence, the photoactivity of  $TiO_2$  is initiated in the ultraviolet (UV) region, and hence the utility for photoactivity is restricted to  $< 5\%$  in the solar light. Knowing these drawbacks, many researchers have focused on preparing  $TiO_2$  in its different phases and its composites/hybrids, and used it as the photocatalyst for the removal/degradation of pollutants in water/air and wastewater with enhanced photoactivities in the UV region.  $TiO_2$  nanostructures with different shapes (nanorod, nanowire, nanotube, nanofiber, etc.) possess diverse physicochemical characteristics and a particular review (Reghunath et al., 2021) details the decomposition of contaminants from water/wastewater (Amin et al., 2014). However, there is a need to fully utilize the remaining spectrum (visible region) for photocatalysis, and to achieve that the bandgap of  $TiO_2$  needs to be decreased to have visible light absorptions. This is normally achieved by incorporating a suitable dopant (metal, non-metal, or ion). Doping modulates the photoactivity of  $TiO_2$  through surface modification and energy level (conduction and valence band) alterations (Barkul et al., 2016). The photocatalytic efficiency of  $TiO_2$  can be improved by the modifications to the surface area, sizes, shapes, and surface properties. The enhancement in photoactivity has been achieved *via* chemical modifications, by incorporating additional components in the  $TiO_2$  structure (Hanaor and Sorrell, 2011). Various approaches have been evolved for improving the visible light-mediated photoactivity of  $TiO_2$  that comprises doping (metal/non-metal/multiple metals/multiple non-metals/metal-non-metal co-doping), surface modifications (coating or chemical), structural modification (generating impurity sites or enhancing oxygen vacancies or oxygen-rich sites or phase changes), morphological modifications (tube, wires, rods, etc.) and heterojunction generation (using other semiconductors or metal complexes). Readers are suggested to refer to a few of the recently published reviews that describe the visible light activation strategies or approaches for  $TiO_2$  (Table 1) (Gomes et al., 2019; Schneider et al., 2014; Xu et al., 2019; Zhang et al., 2019).

#### 3.2. Visible light photocatalysts for environmental remediation

Taking note of the depth of high-quality research conducted on advanced photocatalysis materials for environmental remediation, it is worth informing that there exist challenges for developing energy-efficient and cost-effective photocatalytic systems for lowering or removing air/water pollutants from the environment. Visible light-activated photocatalytic technology holds great promise in this regard.

### 3.2.1. TiO<sub>2</sub> in visible light photocatalysis

The current progress and achievements in photocatalytic materials have primarily given attention to utilizing inorganic semiconductors (metal oxides and chalcogenides) based photocatalysts for environmental remediation applications. Thus far, the most widely used semiconductor is TiO<sub>2</sub> and its application is in the photo-induced oxidation of organic compounds for its application in water/air treatment or purification. However, the main demerits of TiO<sub>2</sub> are the high band-gap energy (around 3.2 eV) and the rapid e<sup>-</sup> - h<sup>+</sup> recombination rate. *What kind of improvement in TiO<sub>2</sub> modification can then enhance photocatalysis performances?* Taking into account the advantages of using renewable resources for photocatalysis, the use of sunlight as a preferential energy source receives paramount interest. In this context, visible light-mediated photocatalysis, which takes into account of absorption of visible light and participates in photocatalysis via single-electron transfer or energy transfer processes with pollutant substrates, has been considered attractive to researchers in recent years.

Different approaches that have been designed and developed to improve the photoactivities and the charge transport characteristics include (i) band-gap engineering (Chen et al., 2017), (ii) usage of co-catalysts (Ran et al., 2018), (iii) incorporation of plasmonic nanoparticles (gold, platinum, copper), (iv) formation of heterojunction based on two or more inorganic semiconductors (Abe, 2010) or (v) designing controlled nanostructures for heterogeneous catalysts (Li et al., 2019). A new approach to improving the visible light photocatalytic performance of TiO<sub>2</sub> is to develop inorganic-organic hybrid materials (Mir et al., 2018). The development of inorganic-organic type TiO<sub>2</sub>-organic hybrid/composite materials includes the incorporation of organic macromolecules or polymers, as the organic counterpart. Especially, a class of polymers, namely, CPs which generally possess extended  $\pi$ -electron systems exhibiting high mobility for charge carriers and hence can be coupled as sensitizers for enhancing the absorption capability in the visible region for wide bandgap metal oxide semiconductors (Riaz and Ashraf, 2014).

To enable the UV photoactive metal oxide based SCP towards visible light activity, the bandgap energy of the metal oxides needs to be narrowed or decreased. While various bandgap engineering strategies were attempted by the researchers worldwide, defect or introduction of lattice disorder has been attempted and its influences on the photocatalytic performance of metal oxide photocatalysts are investigated. Considering the various possible forms of defects, point defects leading to the formation of oxygen vacancies and/or Ti<sup>3+</sup> interstitials in the rutile and anatase structures are proved to enhance the photocatalytic properties of TiO<sub>2</sub> (Gopalan et al., 2020; Lee et al., 2020). There can be three probable cases in the defect generation in TiO<sub>2</sub>: (i) possible balancing of the electric charges of Ti<sup>3+</sup> species in TiO<sub>2</sub> through the generation of oxygen vacancies. It must be noted that these modifications can be transitory as Ti<sup>3+</sup> and oxygen vacancies appear/disappear simultaneously, (ii) in addition to the formation of Ti<sup>3+</sup> and oxygen vacancies, other kinds of structural defects can compensate for the charges arising from the inequalities between Ti<sup>3+</sup> and oxygen vacancies and, (iii) the possible balancing of electric charges of Ti<sup>3+</sup> species in TiO<sub>2</sub> through photon inclusions.

Defect engineering has been given importance because the inclusion of any external species (in the form of external doping) to titania structure can introduce heterojunction between the modifier/dopant and titania through interactions which in turn can cause issues related to intrinsic stability and the constraints in the commercialization of the designed visible-light active photocatalysts. The introduction of ionic defects in TiO<sub>2</sub> generates donor and acceptor levels energy levels in TiO<sub>2</sub> (Nowotny et al., 2008). The extent and type of intrinsic defects influence the energy levels in TiO<sub>2</sub>. The approach of the inclusion of Ti<sup>3+</sup> in self-doped TiO<sub>2</sub> is considered to be advantageous due to its simplicity, safer procedures (no harsh external chemical treatments), and visible light photocatalytic activity. In an interesting study by Tang et al. (2021b), a new kind of p-n heterojunction based on p-type Bi<sub>2</sub>O<sub>3</sub> and n-type Ti<sup>3+</sup> self-doped porous TiO<sub>2</sub> photocatalyst (Bi<sub>2</sub>O<sub>3</sub>/Ti<sup>3+</sup>-TiO<sub>2</sub>) was explored through a facile method (photodeposition followed by calcination) and successfully demonstrated the near-complete removal (100%) of tetracycline (TC) in many water streams under visible light. The as-developed material showed light absorption with a narrow bandgap (2.89 eV). Due to the synergistic role of p-n heterojunction and Ti<sup>3+</sup> self-doping, the resultant Bi<sub>2</sub>O<sub>3</sub>/Ti<sup>3+</sup>-TiO<sub>2</sub> exhibited excellent recyclability (98%) and complete degradation (Tang et al., 2021b). The photoelectrochemical/photocatalytic measurements and degradation pathway confirm that superoxide radical formation and photoinduced holes play a key role in the removal of TCs. Similarly, the same group has demonstrated complete removal of TCs (100%) by preparing a novel p-n heterojunction (Bi<sub>2</sub>O<sub>3</sub> sensitized hollow TiO<sub>2</sub>) type photocatalysts in an air atmosphere (Shi et al., 2020). Besides, in both these works (Shi et al., 2020; Tang et al., 2021b), the influence of pH, inorganic ions, various water matrices, and outdoor light conditions were investigated and discussed in detail. In one of their earlier works (Xiao et al., 2019), the authors demonstrated the beneficial role of doping carbon into N-doped TiO<sub>2</sub> (C-N/TiO<sub>2</sub>) hollow spheres through a unique approach and demonstrated excellent photocatalytic activity/recyclability for TC degradation. Importantly, the complete removal of phenolic contaminants from bismuth-modified TiO<sub>2</sub> single-crystal (Bi-SCTiO<sub>2</sub>) photocatalysts through judicious design and development have also been demonstrated (Tang et al., 2021a). The authors concluded the synergistic roles of the surface plasmon effect of Bi, highly conductive SC-TiO<sub>2</sub>, and the Schottky barrier formation contributed to the enhanced photocatalytic degradation under visible light irradiation.

After the pioneering work of Chen et al. (2011), self-doped TiO<sub>2</sub> (i.e., Ti<sup>3+</sup> species) has been utilized as an alternative strategy for modifying the properties, especially the bandgap of inorganic semiconductors. The inclusion of Ti<sup>3+</sup> species and subsequent charge balancing via the formation of oxygen vacancies can result in bandgap narrowing and the separation of photogenerated electrons and holes (Wang et al., 2013b). The synthetic techniques that have been adopted to include the oxygen vacancy in TiO<sub>2</sub> include hydrogen plasmas (Wang et al., 2013a), aluminum reduction (Wang et al.,



2013b), chemical oxidation (Liu et al., 2013), and electrochemical reduction (Xu et al., 2013). To date, methods to induce  $Ti^{3+}$  have generally been energy-intensive and involve the utilization of unstable Ti raw materials (such as  $Ti(II)O$  Pei et al., 2013 and  $TiH_2$  Liu et al., 2013). In this context, it is highly desirable to develop an alternative method for preparing  $Ti^{3+}$  self-doped  $TiO_2$ . A large number of studies inform that the inclusion of defects such as oxygen vacancies or  $Ti^{3+}$  can modify the properties of semiconductors via 'self-modification/self-doped titania' (Di Valentin et al., 2009; Etacheri et al., 2015; Liu et al., 2013; Nowotny, 2008). Furthermore, the presence of defects can also affect charge transport and surface properties of the semiconductor (Nowotny, 2008). The  $Ti^{3+}$  included  $TiO_2$  (mostly referred to as reduced  $TiO_2$ ), has been demonstrated to exhibit extended light absorption to visible light and increase the charge mobility (Akter et al., 2021; Saari et al., 2022). The inclusion of oxygen vacancies in  $TiO_2$  has been reported to influence photocatalytic properties, such as the electronic structure, charge transport, and surface properties (Lai et al., 2012). The oxygen vacancies including  $TiO_2$  can function as adsorption and active site, and impact the suppression of the charge recombination process in photocatalysis (Polarz et al., 2006).

Besides the advantageous aspects of defect engineering, several issues need to be dealt with through future studies. One of the issues is that defect engineering does not always result in visible light absorption or an increase in photocatalytic activity improvements. The other issue is the restriction in the exhaustive characterization of the lattice structure of  $TiO_2$  after defect engineering and difficulties in establishing a correlation between the extent of properties enhancements and defect concentrations. As a consequence of these issues, the explanation of photocatalytic mechanisms with defect engineered  $TiO_2$  is often overlooked or conceived (Huang et al., 2019).

### 3.2.2. CPs and photoactivity

CPs possess sequential alternating double and single bonds. CPs have been extensively explored in photocatalytic applications owing to their outstanding charge-transport and light-harvesting properties (Anantha-lyengar et al., 2019). CPs have been given special focus to create a new platform in the field of photocatalysis considering their inherent advantages: ease of preparation, tunability in the band structure, and adequate stability. CPs, in general, contribute to the increased light absorption capability, limit the charge recombination and result in high stability. The chief advantages of CPs include preparation under ambient conditions, chemical stability against photobleaching, and molecular structural modifications via functionalization (Wang and Yu, 2019). The  $\pi$ -conjugation in CP backbone chains supports photogenerated charge carrier separation and improves transport properties, which are essential requirements for triggering photo-redox reactions. The delocalized  $\pi$ -electrons generated through the overlapping of  $p$ -orbitals endow special electronic properties for CPs to form a basis for various light activation-based applications (organic optoelectronics) (Liu et al., 2016a; Ostroverkhova, 2016). The combinational properties in CPs which include light absorption, tunable emission over the spectrum (solar), hole injection and electron-blocking abilities, processability, etc. suit for light activated applications. Many scientists have reported exciting achievements in photocatalysis through modifications of CPs at the molecular level and/or composite formation, and a review covering important aspects on this research topic is sought after.

The sequence of basic steps involved in the polymer semiconductor-based light-driven redox reactions is detailed in many reviews, and the general pathway is well known. Upon irradiation of light, the semiconductor absorbs incident photons and generates charges ( $h^+$ - $e^-$  pairs) carriers. The photogenerated charge separation and transport to the semiconductor surface, cause redox reactions to occur. Conversely, the competing process is the recombination of photogenerated  $e^-$  and  $h^+$  at the bulk or surface of the polymeric semiconductor. In general, CPs to have an efficient photocatalytic efficiency should possess at least a few of the following properties: (a) broad and strong light absorption (visible region); (b) efficient charge separation and transportation to the surface of the photocatalyst; and (c) suitable alignment of energy-levels. To sum up, the prominent factors that influence the efficiency of the photocatalytic process in CPs are the appropriate energy levels, efficient charge separation, and transportation of photogenerated charges. For achieving these requirements, rational design in the synthesis of CPs and coupling with photoactive metal oxides have been attempted.

Extensive studies have been made on soluble polymers that contain linear structures having functional groups such as ether, alcohol, amide, etc. and these polymers can dissolve, disperse, or swell in solvent to specifically find interesting applications in environmental pollutant removal (Vajihinejad et al., 2019). These soluble CPs are known to be easily processable and hence fabrication of thin films could be feasible. However, as explained before, the chain structures in CPs are susceptible to degradation in the presence of light illumination. Specifically, the carbon atom adjacent to the CP backbone is vulnerable to radical formation (e.g., poly(hexylthiophene)). Also, the existence of exocyclic double bonds along the polymer backbone is prone to degradation. To quote an example, the chain scission can occur for poly(*p*-phenylenevinylene)s via oxidation in the presence of oxygen. The photostability of CPs has been dependent on their structure-property relation (Manceau et al., 2011). In general, the presence of aromatic polycyclic units and the absence of side chains in CPs can cause good photochemical stability. Based on this, CPs that have polycyclic aromatic units without the presence of side chains in the polymer backbone are highly photostable. There has been a resurgence in research activities toward developing newer CPs having efficient photocatalytic properties by tuning their optoelectronic, microstructural properties, and photostability (Park, 2017). The emerging research area in this direction is the development of composites/hybrids comprising inorganic semiconductors and CP for achieving enhanced photo-reactivity (Lin et al., 2012).

#### 4. PANI/PPy in visible light photocatalysis

Among many CPs, PANI and/or a few of the derivatized counterparts are known to possess unique combinational properties due to their efficient electronic properties and chemical/photostability leading to the suitability for application in multi-disciplinary areas (Kim et al., 2015; Komathi et al., 2017; Shanmugasundaram et al., 2016). Moreover, PANI exhibits p-type semiconducting and excellent  $h^+$  transporting properties (Gopalan et al., 2018; Sai-Anand et al., 2016). PANI possesses a high electron-hole carrying capacity and hence when it is mixed with transition metal oxide, the enhanced photocatalytic properties were witnessed in the decomposition of organic dyes, etc. (Zhang et al., 2006). Specifically, PANI when combined with transition metal oxide decrease the optical band gap of metal oxides and shifts the absorption maxima (Mohamed and Aazam, 2014). Besides, PANI can increase the separation between charge carriers and hence contribute to enhanced visible light photo-activity (Li et al., 2008).

The development of heterojunction between a semiconductor nanocrystal (having a narrow bandgap) and a CP is an effective approach for achieving enhanced charge carrier separation and improved visible light activity (Nallal et al., 2017). In this regard, PANI suits the integration with inorganic semiconductors owing to its high charge carrier mobility and light absorption coefficients. Further, after excitation under light, PANI can function both as an electron donor as well an excellent hole acceptor. Due to these beneficial properties, PANI suits for the use toward achieving enhanced charge-separation efficiency for photocatalysis. Efforts have been focused on combining PANI and inorganic semiconductors toward the preparation of advanced photocatalysts. Turning to another important CP, PPy has a bandgap of 2.2–2.4 eV (Pan et al., 2016) and composite photocatalysts were designed and developed using PPy (Yang et al., 2020; Zhu et al., 2016). In the forthcoming headings, the literature details on the role of most prevalently used CPs, PANI and Ppy, in conjunction with  $TiO_2$  for the enhanced and visible light photocatalysis are reviewed. With relevance to the application, abundant research works on pollutant removal are considered for discussion.

##### 4.1. Methods of preparation of $TiO_2$ -CP composites

The preparation of  $TiO_2$ -CP composites/hybrids has been carried out in general by any of the following methods: in-situ polymerization (Yu et al., 2019; Zhang et al., 2006) of the respective monomer in the presence of  $TiO_2$ , template-assisted polymerization (Xiong et al., 2004; Zhang and Wan, 2003), sol-gel synthesis (Katoch et al., 2012; Pawar et al., 2010) and physical mixing of  $TiO_2$  and CP (Chen et al., 2018; Gu et al., 2012). In a recent review, the reports on the synthesis of  $TiO_2$ -PPy composites have been detailed (Amorim et al., 2021).

##### 4.2. Photocatalysis by $TiO_2$ in conjunction with PANI for photocatalytic pollutant removal

When PANI combines with  $TiO_2$ , the optical and photocatalytic properties of the resultant composites rely on two factors. Firstly, the microstructural and phase composition of  $TiO_2$ . Secondly, the chemical composition of PANI chains and the electronic bandgap of PANI ( $E_g$ -PANI), evolved from the HOMO and LUMO energy level positions. PANI, in general, is considered to comprise  $C_6H_4-N$  repeating units which are represented in terms of emeraldine base (EB), leucoemeraldine base (LB), or pernigraniline base (PB). These structural units arise based on the extent of oxidation of the nitrogen atoms and the creation of imine structures. The processes such as oxidative doping of LB and protonation of EB with protonic acids can lead to the formation of more conductive PANI forms such as emeraldine salt (ES). The bandgap value of the PANI value is predicted to be in the range of 1.53 to 2.52 eV, depending on the chain length of the EB, LB, and PB units in PANI. The  $E_g$ -PANI decreases when the undoped PANI changes to PANI-ES from 2.52 to 1.5 eV (Alemán et al., 2008; Liu et al., 1999).

The composite formation between  $TiO_2$  with PANI can decrease its bandgap and/or extend its light capability in the visible light region. In general, PANI in association with  $TiO_2$  can photosensitize  $TiO_2$  particles through the absorption of visible light photons and transfer electrons to the CB of  $TiO_2$ . PANI hybrids/composites can be photocatalytically active under visible light due to the energy level (HOMO – LUMO) electronic excitation and the possibility of increased separation of  $e^-/h^+$  pairs (Yang et al., 2017). The electronic transitions that can be resulted upon irradiation of PANI by light in the presence of  $TiO_2$  are as follows; the irradiation of PANI results in the injection of  $e^-$  in CB of  $TiO_2$ . Subsequently, the  $e^-$  can be transferred into the CB of  $TiO_2$ . The  $h^+$  can be pooled into the VB of  $TiO_2$ . Under UV or visible irradiation, the slowing of the charge carrier recombination process and increases in  $TiO_2$  photoactivity due to the synergistic influence arising from PANI- $TiO_2$  interactions. Thus, the visible light photocatalysis of  $TiO_2$ -PANI composite can be in the general process through the mechanism. The  $e^-$  of CB in  $TiO_2$  and/or  $h^+$  in VB of PANI can participate in the reaction with  $H_2O$  and  $O_2$  and generate  $OH^-$  radicals.

##### 4.2.1. Mechanism of photodegradation by PANI- $TiO_2$ composite

The mechanism of photocatalytic degradation by PANI- $TiO_2$  composites involves the initial excitation and subsequent charge carrier transfer/reactions suggested for semiconducting polymer by Heeger (2001). The majority of research activities on the PANI- $TiO_2$  composites have been centered on the removal or photodegradation of dyes such as methylene blue (Ahmad and Mondal, 2012) and Rhodamine B (Pan et al., 2018) (aqueous-based). Limited studies have been directed on the photocatalytic activity of PANI- $TiO_2$  composites (gas phase) (Wei et al., 2011). The gas-phase pollutant degradation

is useful for improving indoor air quality maintenance. In this review, the discussions are centered on the research activities of  $\text{TiO}_2$ -PANI composite materials for photocatalytic degradation of pollutants. The discussions are arranged on the materials that include PANI- $\text{TiO}_2$  composite, PANI combined with nanostructured (nanotube, nanowire, etc.)  $\text{TiO}_2$  and PANI in combination with  $\text{TiO}_2$ , and more additional component(s) such as carbon nanostructures, transition metal oxides, etc., and presented under the subheadings: PANI-composite, PANI- $\text{TiO}_2$  nanostructure composites, and multicomponent composites.

CPs like PANI and PPy can greatly enhance the photoresponse of  $\text{TiO}_2$  under visible light/solar irradiation. Firstly, the extended  $\pi$ -conjugated electronic structures in CPs support strong light absorption over the wide spectral region ranging from ultraviolet, visible, and NIR, and this feature provide the basis for their functioning as efficient photosensitizers for  $\text{TiO}_2$ . Similar to the majority of semiconductors including  $\text{TiO}_2$ , the energy bandgap between CB and VB ranges ranging between 1.5 and 3.0 eV (Muthirulan et al., 2013). Thus, CPs can be photoexcited under visible light irradiation and transfers the VB into the CB band of  $\text{TiO}_2$ , leading to an increase in the number of photoexcited charges that can support photoreactions. This feature also favors the effective transport of photons through the polymer layer to the surface of  $\text{TiO}_2$ . It must be noted that the thickness of CP coating plays an important factor as the photogenerated charge carriers need to be transported from the external CP interface in contact with the aqueous solution to the inner  $\text{TiO}_2$  layer. Combining CPs with  $\text{TiO}_2$  is therefore an effective strategy for enhancing the visible light-driven formation of active intermediate free radicals like hydroxyl ( $\text{HO}\bullet$ ) and superoxide radicals ( $\text{O}_2^-\bullet$ ) for triggering the photooxidation of organic pollutants in water (O'Neal Tugaon et al., 2018). A reduction reaction can occur if electron acceptors are present on the surface of the  $\text{TiO}_2$  or in the environment, however, the reactive intermediates like hydroxyl radicals can be generated through the reaction of holes with surface hydroxyls/water in the catalyst surface or medium (Ahmad and Mondal, 2012). The photogenerated  $\text{h}^+$  can also be directly involved in the oxidation of any organic molecule (pollutants). Likewise, the photogenerated  $\text{e}^-$  can either be involved in the reaction with electron acceptors to generate superoxide radical cations or directly can participate in the reduction reaction of polluting species.

#### 4.2.2. PANI- $\text{TiO}_2$ conventional composites

We refer to the PANI- $\text{TiO}_2$  conventional composites as the composites derived from bulk (non-nanostructured) PANI and  $\text{TiO}_2$ . The improved photocatalytic activity for the discoloration of the dye and Reactive Red was witnessed for PANI- $\text{TiO}_2$  composite under solar irradiation, whilst pristine  $\text{TiO}_2$  showed poor photocatalysis (Gilja et al., 2017). PANI- $\text{TiO}_2$  composites were prepared by varying the two components through oxidative polymerization (in-situ) along with  $\text{TiO}_2$  precursors. The optimum composition that produces the enhanced photocatalytic effect by the synergistic effects from  $\text{TiO}_2$  and PANI was deduced. Also, the photocatalytic activity of 15PANI/ $\text{TiO}_2$  was superior at the combined UV/Vis irradiation than solar irradiation or UV irradiation only (Fig. 1(A)). The explanation for the increased photocatalytic activity was detailed in terms of the formation of coordination bonds between nitrogen atoms of PANI and Ti atoms in  $\text{TiO}_2$  implying the Ti-N interaction, and consequent red shift in the PANI bands absorption. The composition of PANI in the PANI- $\text{TiO}_2$  composite determines the extent of light reflection. While the highest adsorption capacity of the dye degradation was reported for 10PANI/ $\text{TiO}_2$ , the lowest was witnessed for 25PANI/ $\text{TiO}_2$ . The differences in the light absorption capabilities of PANI- $\text{TiO}_2$  composites are attributed to factors like the types of structural units (EB, ES, PB) in the PANI chains, the difference in PANI amount in the composite, and the extent of interaction between the positively charged nitrogen in PANI and negatively charged dye (Fig. 1A) (Gilja et al., 2017). The presence of a homogeneous PANI layer on the  $\text{TiO}_2$  surface functions as the  $\text{h}^+$  acceptor and promotes the oxidative photodegradation for the dye as well as enables the synergistic effect from PANI- $\text{TiO}_2$  caused a significant decrease in the  $\text{h}^+$  and  $\text{e}^-$  recombination process.

PANI- $\text{TiO}_2$  composite, prepared as the 3D network hydrogel, exhibited an enhanced photocatalytic removal of organic contaminants (MB dye) due to the combined effects of improved photocatalytic degradation (in-situ) and adsorption (Jiang et al., 2016). The PANI- $\text{TiO}_2$  composite hydrogel was prepared by the polymerization of aniline with  $\text{TiO}_2$  particles and phytic acid as the cross-linker. The photocatalytic activity was evident for the dye degradation both in static and dynamic systems. The photocatalytic mechanism describes the photocatalytic degradation and adsorption enrichment through synergistic effects from PANI and  $\text{TiO}_2$  (Fig. 1(B)) (Jiang et al., 2016).

The first step involves the adsorption of the dye and enrichment onto the  $\text{TiO}_2$  surface assisted by the 3D network of PANI hydrogel. In the second step, the dye was in-situ degraded under light irradiation. Upon irradiation of light,  $\text{e}^-$  and  $\text{h}^+$  are photogenerated on the CB and VB of  $\text{TiO}_2$ . The photogenerated  $\text{h}^+$  are transferred to the HOMO of PANI as the VB of  $\text{TiO}_2$  is lower than the HOMO of PANI and the 3D network PANI hydrogel improves the separation efficiency of charge carriers and results in enhancement in the photocatalytic activity. PANI- $\text{TiO}_2$  composites were synthesized by the chemical polymerization of aniline with  $\text{TiO}_2$ , and the photocatalytic activity again degradation of congo red was demonstrated (Ali et al., 2017). The photocatalytic activity comprised of adsorption through pseudo-second-order kinetics for removal.

The acrylic pseudo-paints were prepared based on PANI- $\text{TiO}_2$  composite and tested for the photo-oxidative degradation of gaseous benzene in the air under visible light (Hashemi Monfared and Jamshidi, 2019). During the preparation of the photo paint, dodecylbenzene sulfonic acid (DBSA) was used which played multiple roles such as dopant for PANI, surfactant, and stability improver. The PANI present in  $\text{TiO}_2$ -PANI composites caused higher absorption at longer wavelengths ( $>380$  nm) due to the lower energy bandgap of PANI. It is interesting to note that the absorption of PANI- $\text{TiO}_2$  composite is more than pristine PANI (about 40%) due to the interactions between  $\text{TiO}_2$  particles and PANI. The bandgap

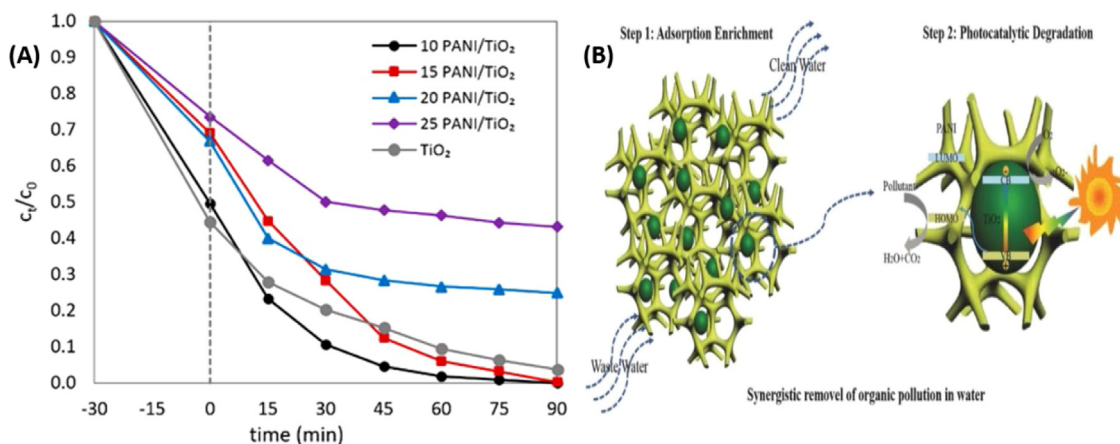


**Fig. 1.** (A) Concentration variation for various studied composite photocatalysts ( $\text{pH} = 4$ ;  $\gamma_{\text{cat}} = 1 \text{ g/L}$ ,  $\gamma_{\text{RR45}} = 30 \text{ mg/L}$ ) (Gilja et al., 2017). Reproduced with permission: Copyright 2017, Multidisciplinary Digital Publishing Institute and (B) Picture illustrating the synergistic removal of PANI/TiO<sub>2</sub> composite hydrogel. Reproduced with permission: Copyright 2016, Wiley-VCH (Jiang et al., 2016).

was reduced to 2.20 eV for the composite as compared to pure TiO<sub>2</sub> particles. The amount of TiO<sub>2</sub> in the composite determines the photoactivity which was optimized by further experiments. Typically, the optimized photocatalytic paints demonstrated ~31% benzene removal efficiency, which is acceptable compared to those of conventional VOCs removal technologies.

A transparent polyacrylic film formation containing PANI–TiO<sub>2</sub> composites with various TiO<sub>2</sub> to PANI ratios was prepared and the self-cleaning properties of the coating were evaluated in terms of an indoor and outdoor application under LED light irradiation (Nosrati et al., 2017). The polyacrylic coating containing 1% PANI–TiO<sub>2</sub> composites has been reported to be more than the photodecolorization ability of that of a coating having pristine 1% TiO<sub>2</sub> particles. In another study, a TiO<sub>2</sub>/PANI bilayer photocatalyst prepared by Bahrudin's group was reported to have enhanced photocatalytic decolorization of methyl orange (MO) (Bahrudin et al., 2019). The existence of TiO<sub>2</sub> on the top layer and adsorption by PANI synergistically caused the enhanced photoactivity for decolorization of MO. The authors analyzed the intermediates of photocatalysis through total organic carbon and ion chromatography techniques, which confirmed the initiation process followed by the aromatic ring opening to generate CO<sub>2</sub> and H<sub>2</sub>O as by-products.

#### 4.2.3. Nanostructured PANI–TiO<sub>2</sub> composites

PANI-wrapped TiO<sub>2</sub> nanotubes (NT) were prepared by combined vacuum impregnation and anodic oxidation methods and the photoelectrocatalytic (PEC) removal of phenol was evaluated under simulated sunlight irradiation of the photoelectrode (Wang et al., 2020a). Interestingly, the PANI-wrapped TiO<sub>2</sub> NT exhibited enhanced photoelectrocatalytic degradation of phenol (83.0%) as compared to photocatalytic (22.0%) and electrocatalytic (0.3%) processes, which implied the predominance of synergistic photo-electro catalytic combined properties for the PANI wrapped TiO<sub>2</sub> NT. The synergistic effect (both photo/electrocatalytic) was reported because PEC degradation of phenol (83.0%) is more than the total of the photocatalytic process (22.0%) and electrocatalytic process (0.3%) at 1.0 V (Fig. 2). The increased surface properties between PANI and TiO<sub>2</sub> NT, hybridization, and well-matched band energy result in a synergistic effect. PANI plays not only the role of visible light response enhancer but also promotes charge separation efficiency. The importance of PANI and TiO<sub>2</sub> NT for the photoelectrocatalytic degradation process, the role of composition, applied potential, morphology and mechanism of photoelectrocatalytic degradation are reported (Fig. 2) (Wang et al., 2020a).

The oxidative polymerization (*in-situ*) was used for the preparation of high-stability PANI–TiO<sub>2</sub> nanocomposite (NC) photocatalysts and used to decolorize and mineralize Azo (Reactive Red [RR]) dye in wastewater samples under solar light irradiation (Gilja et al., 2017). The optimized photocatalyst was identified by manipulating the pH of the solution (15% PANI/TiO<sub>2</sub>) and comparing it with TiO<sub>2</sub> for varying amounts of CP and PANI (10, 15, and 20%). Similarly, the highly active, visible solar light-induced PANI–TiO<sub>2</sub> NC (crystallite size: 46 nm, 2.1 eV) photocatalysts were prepared through the *in-situ* polymerization method and experimented for the photocatalytic decolorization of Reactive Blue-19 (RB19), and a comparative study was performed under simulated solar and UV irradiation (Kalikeri et al., 2018). The various aspects like the influence of pH, dye concentration, and catalyst loading on dye mineralization of RB19, were analyzed to ascertain the optimal conditions for efficient photocatalysis. Further, the authors found that the degradation kinetics of the reaction followed the Langmuir–Hinshelwood (L–H) model with an apparent rate constant of 0.251 mM min<sup>-1</sup>. The authors could produce very efficient NC through thermal treatment of PANI–TiO<sub>2</sub> at 650 °C in an inert atmosphere as well could manipulate the ratio of TiO<sub>2</sub>/PANI (20, 50, and 80) (designated as TPC-20, TPC-50, and TPC-80) by the chemical oxidative polymerization process (Fig. 3) (Radoičić et al., 2017). The as-developed composite and the carbonized PANI–TiO<sub>2</sub> were further assessed for their photocatalytic efficacy for the removal of MB and rhodamine B (RhB). The results

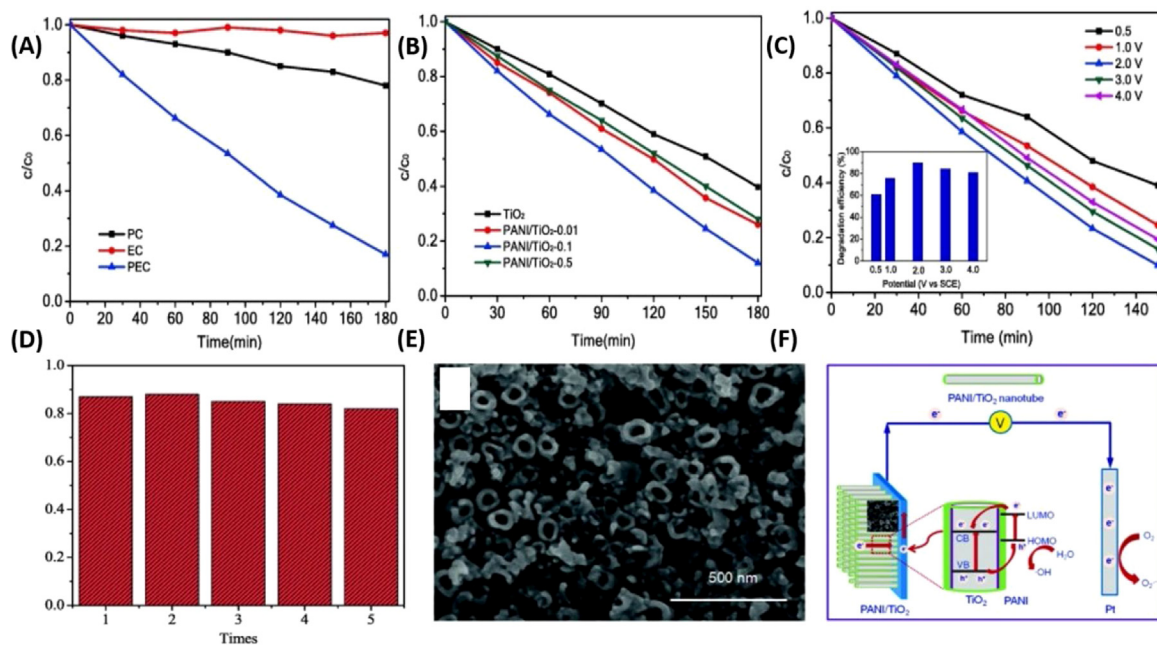


**Fig. 2.** (A) Degradation for PANI/TiO<sub>2</sub>-0.1, (B) PEC degradation for studied samples, TiO<sub>2</sub> and PANI/TiO<sub>2</sub> (at 1.0 V), (C) influence of bias, (D) stability, (E) SEM image of PANI/TiO<sub>2</sub>-0.1, and (F) plausible degradation mechanism. Reproduced with permission: Copyright 2020, Elsevier (Wang et al., 2020a).

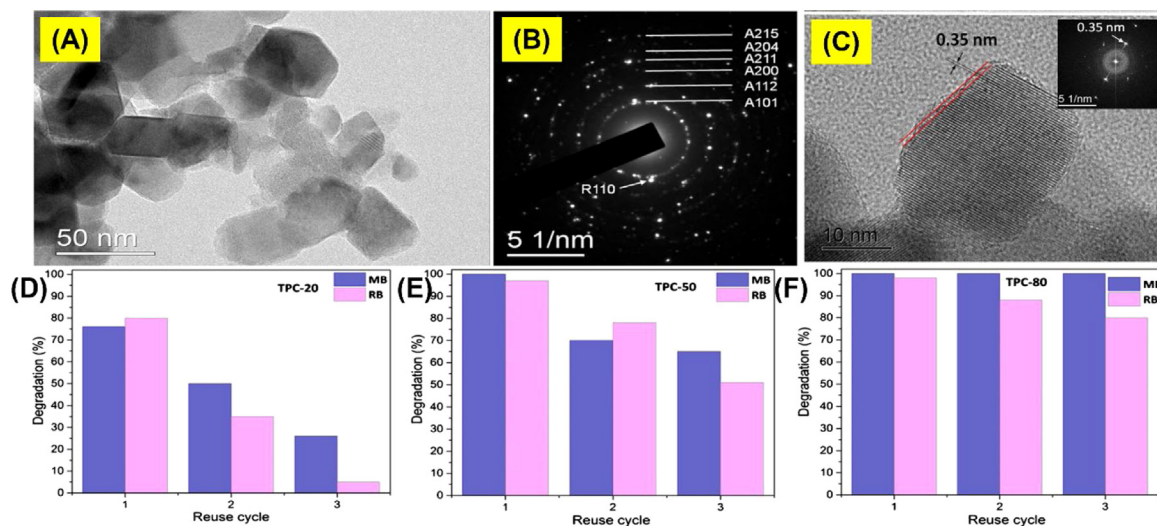


**Fig. 3.** (A) TEM image of optimized TPC-80 nanocomposite and their corresponding (B) SAED pattern, (C) TEM at higher magnification of TPC-80 with inset showing the Fast Fourier transform pattern, and (D–F) removal efficiencies of MB and RB in the presence of TPC – 20/50/80 nanocomposites (10 mg/mL) post three cycles (Illumination time, 60 min for MB and 90 min for RB, initial dye concentration:  $1 \times 10^{-5}$  mol L<sup>-1</sup>). Reproduced with permission: Copyright 2017, Elsevier (Radoičić et al., 2017).

indicated that carbonized PANI–TiO<sub>2</sub> NC witnessed superior photocatalytic degradation compared with pristine TiO<sub>2</sub> and simple PANI–TiO<sub>2</sub>. The mechanism for photocatalysis details the transfer of photogenerated electrons to create an electron sink, thus boosting the formation of superoxide radicals. Similarly, the holes are pooled at the HOMO of PANI through the transfer of photogenerated holes in TiO<sub>2</sub> nanoparticles (NP). Besides, the possibility of drifting the holes generated in the VB of TiO<sub>2</sub> to the orbital of PANI and its contribution to the tuning of oxidation status of PANI is also considered.

PANI can act as a photosensitizer to enhance the light-mediated activity of TiO<sub>2</sub>-based catalysts various promising properties and its suitable bandgap to sensitize TiO<sub>2</sub> have prompted researchers to design and develop nanostructured PANI based PANI–TiO<sub>2</sub> composites to abate organic pollutants (Reza et al., 2019). PANI NT arrays (electrochemical anodic

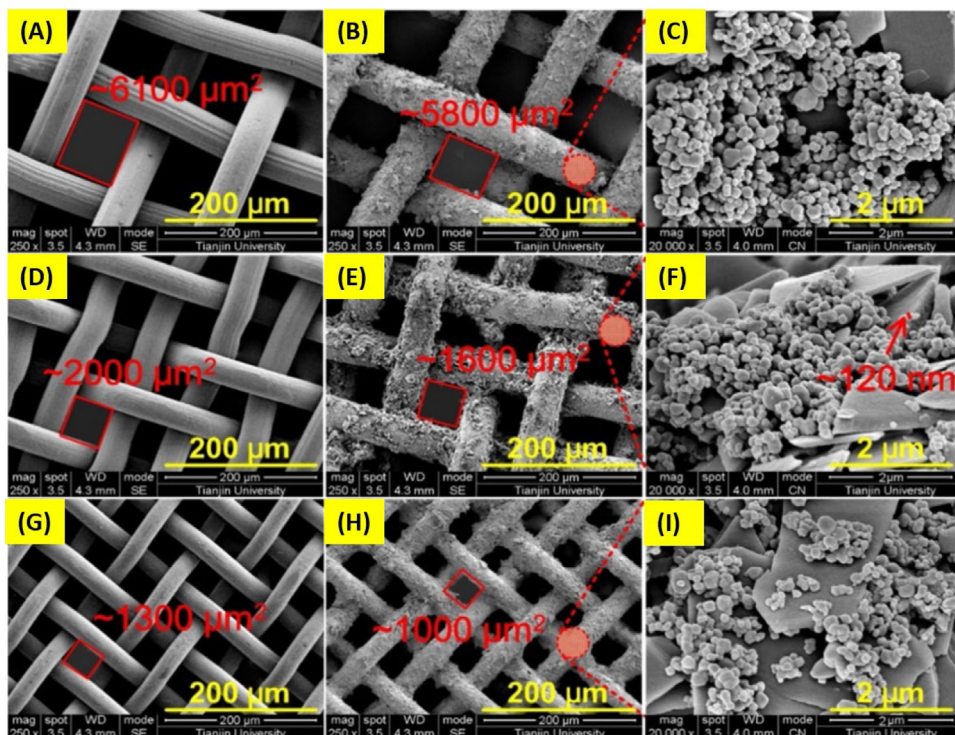


**Fig. 4.** SEM images of stainless steel mesh (A–C) and PANI/TiO<sub>2</sub>-modified meshes (D–I) with different mesh numbers (A, D, G: 200/B, E, H: 300/C, F, I: 400). Reproduced with permission: Copyright 2020, Elsevier (Wang et al., 2020b).

oxidation method) were wrapped onto TiO<sub>2</sub> photoelectrodes *via* a vacuum-assisted impregnation method, resulting in excellent photo electrocatalytic degradation under simulated sunlight irradiation to degrade phenol (Wang et al., 2020a). Another recent study demonstrated that robust superhydrophobic stainless steel mesh-coated PANI/TiO<sub>2</sub> nanoclusters have excellent application in oil & water separation and are expected to have high self-cleaning, flux, anti-corrosion and abrasive resistance achieved through a facile dip-coating technique (Fig. 4) (Wang et al., 2020b). Thin films of PANI were successfully grown on the surface of TiO<sub>2</sub> NT (designated as TNT–PANI) *via* the rotating bed plasma-enhanced chemical vapor deposition technique at various plasma powers for the heterogeneous photocatalytic degradation of Reactive Black (RB) under visible light and compared with unmodified TNT. The energy band gap was dramatically reduced to 2.54 eV from 3.23 eV for TNT–PANI. TNT–PANI displayed remarkably enhanced photocatalytic efficiency, with 56.40% after 240 min, and was able to retain 91% after five cycles, indicating excellent recyclability and reusability.

In recent years, core-shell nanostructured materials received importance for application as these materials can be endowed with different functional components to impart improved physical and chemical properties, which cannot be witnessed in either of the individual components (Li et al., 2018a). The heterojunction or active interfaces that are generated in a core-shell structure can contribute to synergistic functions and new properties for core-shell materials. These concepts have been utilized for enhancing the catalytic efficiency by assembling PANI and TiO<sub>2</sub> into core-shell structures (Hu et al., 2020).

The double-shell TiO<sub>2</sub>/PANI hollow spheres (TAHSs) (Fig. 5(A)) were prepared by Sun et al., wherein PANI was employed as a sensitizer to boost photocatalytic activity (Fig. 5(B)) under UV and visible light for MO degradation (Fig. 5) (Sun et al., 2019). The synthetic procedure of the double-shell structured TAHS is shown in Fig. 5(A). The photocatalytic efficiencies, kinetic simulations (fitted using an apparent L–H first-order kinetic model), and photostability tests were compared between pure TiO<sub>2</sub> and TAHS having various loadings of PANI with TiO<sub>2</sub> hybrids (TAHSs-1 to 4) under UV and visible light irradiation. Among the investigated materials, TAHSs-3 displayed high photodegradation efficiencies for MO after four hours under visible light (97.1%). Taking into account the band gaps of TiO<sub>2</sub> and PANI as approximately 3.2 and 2.8, respectively (Razak et al., 2014), the photocatalytic mechanism proposed under UV and visible light irradiation is shown (Fig. 6). The mechanism details the plausible synergetic effect between TiO<sub>2</sub> and PANI, due to well-aligned HOMO and LUMO energy levels (Sun et al., 2019).

Simple interfacial-engineered heterojunction core-shell-type structured TiO<sub>2</sub>@PANI-based composite photocatalysts were prepared on titanium glycolate (TG) spheres by using electrostatic attraction, resulting in the PANI-grafted TG. The as-prepared TiO<sub>2</sub>@PANI photocatalysts exhibited dramatically improved photodegradation for removing MO under visible light activation because of the synergistic contributions from each of the components (Chen and Yang, 2018). PANI absorbs

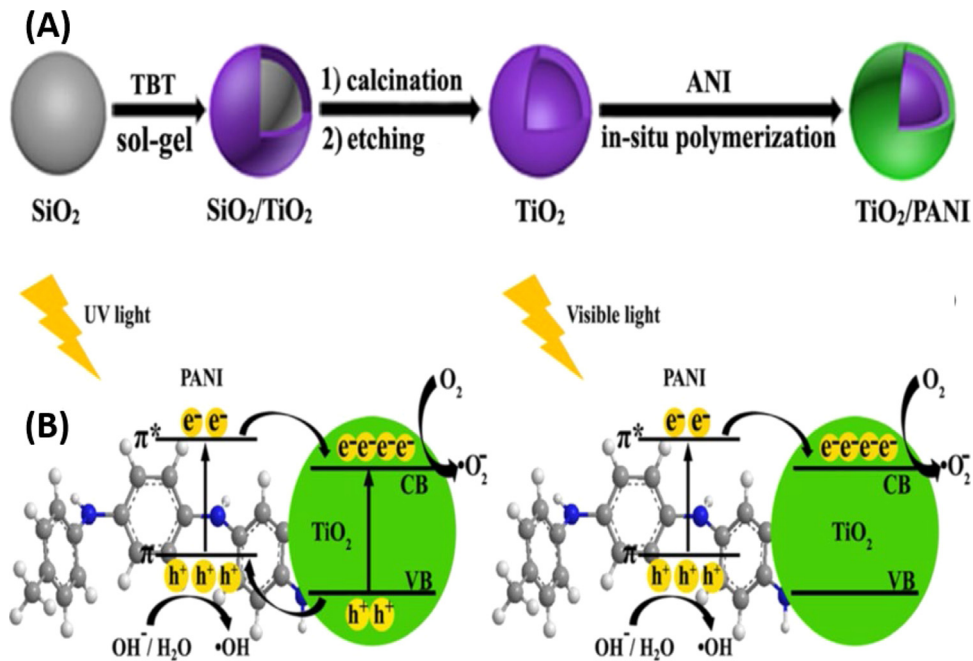


**Fig. 5.** (A) Preparation scheme and (B) degradation mechanism for double-shell  $\text{TiO}_2/\text{PANI}$  hollow spheres under UV light and (B) visible light. Reproduced with permission: Copyright 2019, Springer Nature (Sun et al., 2019).

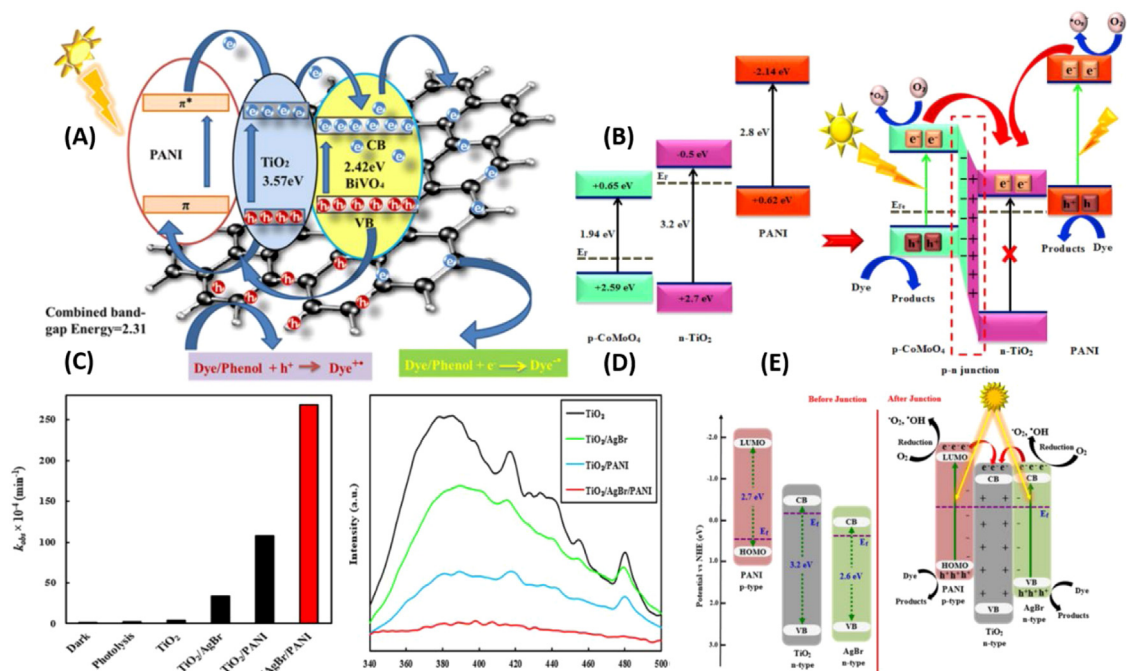


**Fig. 6.** Energy-level diagram of the (A) dye/phenol degradation process and (B) ternary  $\text{TiO}_2/\text{CoMoO}_4/\text{PANI}$  nanocomposites. Reproduced with permission: Copyright 2019, Springer Nature<sup>112</sup> and Elsevier (Feizpoor et al., 2019; Zhao et al., 2019a,b). (C) Rate constants for various photocatalysts (RhB), (D) photoluminescence spectra for the  $\text{TiO}_2$ ,  $\text{TiO}_2/\text{AgBr}$ ,  $\text{TiO}_2/\text{PANI}$  and  $\text{TiO}_2/\text{AgBr}/\text{PANI}$  photocatalysts and (E) plausible mechanism for MB degradation by  $\text{TiO}_2/\text{AgBr}/\text{PANI}$  nanocomposite. Reproduced with permission: Copyright 2019, Springer Nature (Zeynali and Taghizadeh, 2019).

visible light due to the excitation of  $e^-$  from the HOMO level to the LUMO. The excited  $e^-$  from the PANI transfers into the CB of  $\text{TiO}_2$ . The reactions of the electrons in  $\text{TiO}_2$  CB with adsorbed oxygen and water result in the formation of active superoxide radicals and hydroxyls, respectively, leading to the photoreduction of the dye molecules. PANI-wrapped  $\text{TiO}_2$

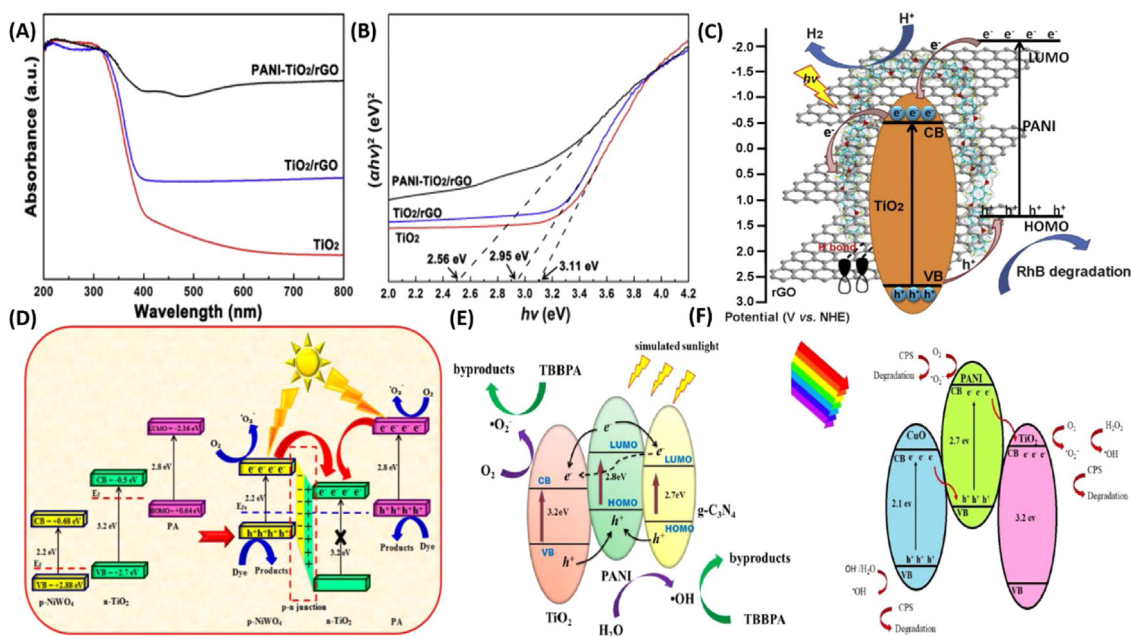


**Fig. 7.** (A) UV-Vis DRS, (B) Kubelka–Munk graphs, (C) photocatalytic activity of hybrid composite, PANI–TiO<sub>2</sub>/rGO. Reproduced with permission: Copyright 2020, Elsevier (Ma et al., 2020). Photogenerated charge separation of (D) TiO<sub>2</sub>/NiWO<sub>4</sub>/PANI hybrids (Zhou et al., 2020), (E) TiO<sub>2</sub>/PANI/g–C<sub>3</sub>N<sub>4</sub> and (F) mechanism for the degradation of CuO/TiO<sub>2</sub>/PANI. Reproduced with permission: Copyright 2021, Elsevier (Nekooie et al., 2021).

nanorods were prepared *via* the oxidative polymerization of aniline and hydrothermally prepared TiO<sub>2</sub> nanorods and the degradation studies of Bisphenol A (BPA) were carried out to evaluate the photocatalytic efficiencies (Sambaza et al., 2020). PANI contributes to the enhancement of photoactivity by transferring electrons to the CB of TiO<sub>2</sub> and also improving charge separation.

#### 4.2.4. TiO<sub>2</sub> incorporated PANI ternary composites

Upon illumination of the ternary nanocomposite, NiWO<sub>4</sub>@PANI@TiO<sub>2</sub> by visible light, the lower energy gap semiconductors, NiWO<sub>4</sub> and PANI are photoexcited and generate e<sup>−</sup>/h<sup>+</sup> pairs. Thus generated e<sup>−</sup> on the CB and LUMO of NiWO<sub>4</sub> and PANI subsequently transfer to the CB of TiO<sub>2</sub> (Fig. 7(D)). Through these processes, the e<sup>−</sup> accumulated in the CB of TiO<sub>2</sub> reduces O<sub>2</sub> into ·O<sub>2</sub><sup>−</sup>. Also, the migrated h<sup>+</sup> and present in the VB of NiWO<sub>4</sub> and HOMO of PANI can oxidize RhB molecules. Importantly, the mechanism explains the efficient separation of photoinduced e<sup>−</sup>/h<sup>+</sup> pairs as well the enhanced photocatalytic efficiency. The magnetic g-Fe<sub>2</sub>O<sub>3</sub> core–shell heterojunction nanocomposite has been reported as visible light active photocatalyst (Wang et al., 2020c). The preparation involves deposition of Fe<sub>2</sub>O<sub>3</sub>@PANI shell at the surface of hydrothermal pre-synthesized TiO<sub>2</sub>. A mechanism for visible light photocatalysis was suggested. Upon visible light irradiation, the e<sup>−</sup> of VB level of TiO<sub>2</sub> are excited and the photogenerated h<sup>+</sup> are concurrently transferred to HOMO of PANI, which is at a higher level than VB of TiO<sub>2</sub>. The LUMO of PANI is higher than the CB of TiO<sub>2</sub> and hence the e<sup>−</sup> are transferred to the CB of TiO<sub>2</sub>. These electronic transitions involving h<sup>+</sup> and e<sup>−</sup> cause efficient separation of the charge carriers.

Mousli et al. (2019) reported a PANI-grafted, mixed oxide-coated PANI (ruthenium dioxide [RuO<sub>2</sub>]-TiO<sub>2</sub>/PANI) heterostructure for the improved catalytic degradation of MO under both visible light and darkness. The explanation for the enhanced photocatalytic activities for RuO<sub>2</sub>-TiO<sub>2</sub>/PANI was based on the nature of the heterostructure developed in the composite as well the new physico-chemical properties evolved from the components. The factors such as the similar tetravalent cationic nature of RuO<sub>2</sub> and TiO<sub>2</sub>, the difference in the electronic configurations between Ti and Ru, and the difference in conducting characteristics, while TiO<sub>2</sub> is an n-type semiconductor, but RuO<sub>2</sub> is metallic. These nanoparticles were further coated with 4-diphenylamine diazonium to endow diphenyl amino groups (DPA) on PANI (RuO<sub>2</sub>-TiO<sub>2</sub>/DPA/PANI). The RuO<sub>2</sub>-TiO<sub>2</sub>/DPA/PANI exhibits a higher photodegradation percentage for MO as compared to RuO<sub>2</sub>-TiO<sub>2</sub>/PANI under dark. The electron exchange between TiO<sub>2</sub> and RuO<sub>2</sub> as well as between RuO<sub>2</sub>-TiO<sub>2</sub> and PANI contribute to the exceptional photocatalytic activity for the former. The role of PANI as an electron donor is important to note for the catalytic activity in the dark. Through various experimental results, the authors reported that RuO<sub>2</sub>-TiO<sub>2</sub>/DPA/PANI possessed better thermal/chemical stability with high reusability (more than nine times).

Feizpoor et al. fabricated multiple heterojunctions–type TiO<sub>2</sub>/cobalt molybdate (CoMoO<sub>4</sub>)/PANI nanocomposites (refluxing route) as efficient photocatalysts with enhanced activity for the removal of organic (RhB, MO, MB, and C<sub>20</sub>H<sub>20</sub>N<sub>3</sub>·HCl) and inorganic pollutants (photoreduction of hexavalent chromium in the presence of simulated visible



light, Fig. 6(B)) (Feizpoor et al., 2019). Various factors include the formation of the p–n junction between n-type TiO<sub>2</sub> and p-type CoMoO<sub>4</sub>, generation of positive and negative charges at the interface, the effective transfer of photoinduced e<sup>-</sup> of PANI and CoMoO<sub>4</sub> into the CB of TiO<sub>2</sub> and efficient separation of h<sup>+</sup>/e<sup>-</sup> pairs contribute to the excellent photoactivity for TiO<sub>2</sub>/CoMoO<sub>4</sub>/PANI as compared to TiO<sub>2</sub>/CoMoO<sub>4</sub> (for RhB).

Similarly, Zeynali et al. prepared the visible light-mediated, highly efficient photocatalyst nanocomposites with a combination of TiO<sub>2</sub>, silver bromide (AgBr), and PANI and evaluated them. Other pollutants, such as MB and MO, were also studied to prove the practical utility of the prepared photocatalysts. The photocatalytic efficiencies were compared for studied photocatalysts (TiO<sub>2</sub>/AgBr/PANI, TiO<sub>2</sub>/PANI, TiO<sub>2</sub>/AgBr, and TiO<sub>2</sub>) for 140 min. The TiO<sub>2</sub>/AgBr/PANI displayed excellent photostability as compared to the TiO<sub>2</sub>/PANI, TiO<sub>2</sub>/AgBr, and TiO<sub>2</sub> and possess better reusability (Fig. 6). Considering that once the contact is established between the three components, the region of TiO<sub>2</sub> becomes positive, and that of PANI and AgBr become negative charges leading to the formation of p–n heterojunction with visible light irradiation, the excitation of e<sup>-</sup> in VB of AgBr and HOMO of PANI can move to the CB, leaving h<sup>+</sup> in VB. The photoexcited electrons present on the surface of AgBr and PANI are effectively transferred into CB of TiO<sub>2</sub> which causes the photodegradation of RhB under visible light irradiation (Fig. 6(C–E)) (Zeynali and Taghizadeh, 2019).

A visible light active ternary nanocomposite was prepared by coupling copper oxide nanoparticles (CuO) having bandgap energy of 2.1 eV with TiO<sub>2</sub> and PANI (CuO/TiO<sub>2</sub>/PANI) and evaluated the aqueous photodegradation of chlorpyrifos (Nekooie et al., 2021). TiO<sub>2</sub> nanoparticles were prepared by solvothermal method and TiO<sub>2</sub>/CuO was prepared by chemical reduction method. The CuO/TiO<sub>2</sub>/PANI ternary was then synthesized by chemical oxidative polymerization of aniline with TiO<sub>2</sub>/CuO composite. The bandgap of the individual components, band alignment, generation of intermediate species, and efficient charge separation possibilities are explained in the mechanism (Fig. 7(F)) (Nekooie et al., 2021).

Carbon-based nanostructured materials (fullerenes, carbon nanotubes, graphenes, and their hybrid counterparts) have gained substantial attention in transdisciplinary applications (energy and environmental) (Benzigar et al., 2019; Joseph et al., 2020; Saianand et al., 2020). To this end, in another study, PANI and carbon dots (CDs) were integrated with TiO<sub>2</sub> nanoparticles (TiO<sub>2</sub>/CDs/PANI) to prepare a new kind of ternary nanocomposites–type visible light active photocatalytic material via a simple synthetic procedure (Feizpoor et al., 2018). The authors witnessed substantial improvement in the photodegradation efficiencies and rate constant for TiO<sub>2</sub>/CDs/PANI (20%) for the removal of RhB, MO, MB, and C<sub>20</sub>H<sub>20</sub>N<sub>3</sub>-HCl dyes. It should be noted that the rate constant of TiO<sub>2</sub>/CDs/PANI (20%) (RhB) was ~36 times better than pure TiO<sub>2</sub> and ~2.6 times better than TiO<sub>2</sub>/CDs because of the beneficial role of O<sub>2</sub><sup>-</sup>. Upon visible light irradiation of TiO<sub>2</sub>/CDs/PANI nanocomposites, PANI absorbs the light and generates e<sup>-</sup>/h<sup>+</sup> pairs through excitation of e<sup>-</sup> from its HOMO to LUMO, and the photogenerated e<sup>-</sup> moves to CB of TiO<sub>2</sub> through the intermediary role of efficient transfer by the CD. The improved photocatalytic responses correlated with the high surface area increased visible light absorption and reduced charge carrier recombination.

The g-C<sub>3</sub>N<sub>4</sub>/TiO<sub>2</sub>@polyaniline (g-C<sub>3</sub>N<sub>4</sub>/TiO<sub>2</sub>@PANI) nanocomposite was used for the degradation of the Congo red (CR) under solar light illumination (Alenizi et al., 2019). The enhanced photocatalytic degradation of the CR was explained based on the synergistic behavior of TiO<sub>2</sub>, PANI and g-C<sub>3</sub>N<sub>4</sub> in the g-C<sub>3</sub>N<sub>4</sub>/TiO<sub>2</sub>@PANI. A different kind of photocatalytic mechanism for charge separation is presented. The h<sup>+</sup> are transmitted to the PANI surface. The efficiently separated e<sup>-</sup> remained in the CB of g-C<sub>3</sub>N<sub>4</sub> and participate in the reaction with O<sub>2</sub> to generate reactive superoxide radicals (•O<sub>2</sub><sup>-</sup>) which degrade the dye molecules. The PANI/TiO<sub>2</sub>/rGO photocatalysts exhibited narrow bandgap energy as against TiO<sub>2</sub> (Fig. 7(A, B)) and improved capability to harness visible region (Ma et al., 2020). A photocatalytic mechanism that suggests the improved charge carrier separation involving the roles of graphene, TiO<sub>2</sub>, and PANI, the oxidation of the dye through superoxide anion radicals generated by the reaction with surface oxygen, and e<sup>-</sup> in the CB of TiO<sub>2</sub> (Fig. 7(C)).

The g-C<sub>3</sub>N<sub>4</sub> and PANI co-modified TiO<sub>2</sub>NTs array exhibited excellent simulated solar radiation initiated photocatalytic degradation for tetrabromobisphenol (TBBPA) (Zhou et al., 2020). TiO<sub>2</sub>NT arrays were generated by anodizing titanium sheets. PANI and g-C<sub>3</sub>N<sub>4</sub> were sequentially coated on the TiO<sub>2</sub>NTs. The mechanism of visible light photocatalytic degradation of TBBPA by g-C<sub>3</sub>N<sub>4</sub> and PANI modified TiO<sub>2</sub>NT arrays involves the formation of oxidative species such as h<sup>+</sup>, OH, and O<sub>2</sub><sup>-</sup>. The reactive intermediates formation was augmented by the generation, transportation, and reaction of photoinduced e<sup>-</sup> and h<sup>+</sup> (Fu et al., 2017). The efficiency enhancements are contributed by the predominant and efficient charge separation. In addition, the heterojunction formation and energy level matching among g-C<sub>3</sub>N<sub>4</sub>/PANI and TiO<sub>2</sub>NTs resulted in effective formation and photo-induced charge separation carriers under visible light (Fig. 7(E)) (Zhou et al., 2020).

In an interesting study, Zarrin and Hesmatpour effectively synthesized highly active NCs comprising TiO<sub>2</sub> modified with niobium oxide (Nb<sub>2</sub>O<sub>5</sub>), reduced graphene oxide (RGO), and PANI through combined hydrothermal and *in-situ* oxidative polymerization and investigated their photocatalytic performance for the successful removal of MB and MO (Zarrin and Heshmatpour, 2018). The authors purposefully used a range of sophisticated instrumentations (such as XRD, FT-IR, SEM/TEM, and BET) to ascertain the physico-chemical properties of as-developed photocatalysts. Among them (TiO<sub>2</sub>/Nb<sub>2</sub>O<sub>5</sub>, TiO<sub>2</sub>/Nb<sub>2</sub>O<sub>5</sub>/PANI, TiO<sub>2</sub>/Nb<sub>2</sub>O<sub>5</sub>/RGO, and pure TiO<sub>2</sub>), TiO<sub>2</sub>/Nb<sub>2</sub>O<sub>5</sub>/RGO displayed a dramatically higher photocatalytic response compared with the studied nanocomposites owing to its high conductivity and excellent photogenerated charge-separation efficiency. The results were ascribed to the complementary beneficial properties of the chosen photocatalytic materials. The TiO<sub>2</sub>/Nb<sub>2</sub>O<sub>5</sub> surface is sensitized by RGO (TiO<sub>2</sub>/Nb<sub>2</sub>O<sub>5</sub>/RGO), which causes effective charge separation.

Graphene (G) TiO<sub>2</sub>-PANI (G-TiO<sub>2</sub>-PANI) composites were synthesized through a sol-gel method and photodegradation of 4-Nitrophenol under visible light in an aqueous phase was investigated (Thakare et al., 2020). The photodegradation

mechanism involves capturing photogenerated  $e^-$  from PANI by graphene and transferring it to VB of  $TiO_2$ , which consequently decreases the recombination of charge carriers formed by the G- $TiO_2$ -PANI composite. The increase in the quantity of  $e^-$  in the excited levels contributes to the enhanced photoactivity of the photocatalyst.

The functional cotton fabrics (CF) based visible light photocatalyst was designed by depositing the mixed metal oxide  $RuO_2$ - $TiO_2$  and PANI on the fabric surface and investigated for the organic pollutants photodegradation (Mousli et al., 2020). The photocatalytic activity of the nanocomposites showed strong dependence on the amount of PANI in the composite. Table 1 summarizes the key parameters affecting the performance of  $TiO_2$ -PANI based composite photocatalytic materials.

#### 4.2.5. $TiO_2$ -PANI based multicomponent composites

In this review, we designated and grouped the  $TiO_2$ -PANI included composites comprising two or more components than the  $TiO_2$  and PANI as  $TiO_2$ -PANI based multicomponent composites. Heshmatpour et al. prepared the ceramic type (C: silicon dioxide [ $SiO_2$ ]/iron(III) oxide [ $Fe_2O_3$ ]/zirconium dioxide [ $ZrO_2$ ]) hybrid NCs comprising n-type  $TiO_2$ , carbon, and PANI (n- $TiO_2$ /C/PANI) through the combination of sol-gel and *in-situ* chemical oxidative polymerization and demonstrated its efficient photocatalytic properties (Heshmatpour and Zarrin, 2017). The authors subsequently evaluated and compared the visible light-mediated photocatalytic performances between various materials like n- $TiO_2$ /C, n- $TiO_2$ /C/PANI, and  $TiO_2$ , concerning the removal of MB and crystal violet (CV). The photocatalytic efficiencies follow the order of n- $TiO_2$ /C/PANI > n- $TiO_2$ /C >  $TiO_2$ . The enhanced photocatalytic activity for  $TiO_2$ /C/PANI is due to the effective separation of  $e^-$  and  $h^+$  pairs at the interface of PANI and n- $TiO_2$ /C as well as on the effective  $e^-$  donor and  $h^+$  accepting properties of PANI. Also, the enhanced surface area, high conductivity, and reduced agglomeration of  $TiO_2$ /C/PANI contribute to improved photostability.

Zhao prepared the multi-component composite comprising bismuth vanadate ( $BiVO_4$ ), graphene oxide (GO),  $TiO_2$ , and PANI (BVGTA-PANI) through a facile one-pot hydrothermal method and investigated its photocatalytic performance under visible light for the degradation of MB and phenol (Fig. 6(A)) (Zhao et al., 2019b). Interestingly, BVGTA-PANI displayed a satisfactory photocatalytic performance (higher rate constant) over its BVG ( $BiVO_4$ -GO) counterparts. The authors further evaluated toxicity tests for the studied photocatalysts hybrids (BVGTA, BVG, and others) and found no significant activity for *Staphylococcus aureus* and *Bacillus subtilis*. The increased photocatalytic performance can be attributed to the suitable tailoring of the combined band gaps and the beneficial role of PANI for efficient charge separation and  $e^-$  trapping. It is to be noted that the transfer of photoinduced  $e^-$  in the LUMO of PANI to the CB of  $TiO_2$  and  $BiVO_4$  energy levels is feasible because both the HOMO and the LUMO of PANI are higher than that of  $TiO_2$  or  $BiVO_4$ . Also, the more acidic characteristic of CB of  $BiVO_4$  CB provided the feasibility of injection of the photogenerated  $e^-$  from the CB of  $BiVO_4$  to that of  $TiO_2$  (Fig. 6(A)).

#### 4.2.6. PANI-semiconductor (other than $TiO_2$ ) based photocatalytic systems

The readers can refer to Table 2 and the details within to refer to the literature on the visible light-activated photocatalysis by PANI-semiconductor (other than  $TiO_2$ ) catalytic materials.

## 5. Various types of PPy- $TiO_2$ based visible light photocatalysts

PPy is one of the most studied CPs in energy, environment, and health, due to its ease of synthesis, electronic properties, excellent electrochemical properties, and the availability of strong binding or anchoring sites for subsequent modifications (Yuan et al., 2019). Recently, hybrid photoactive materials based on PPy-semiconductors have been tailor-designed and developed for practical application in environmental remediation (Zhao et al., 2019a; Zia et al., 2019). It must be noted that PPy has been combined with  $TiO_2$  to generate composites, nanostructures, and multicomponent based visible light photocatalysts. However, the literature is limited for PPy as compared to PANI.

### 5.1. PPy- $TiO_2$ composites

Sangareswari et al. designed and developed the PPy-modified  $TiO_2$  NCs through facile chemical oxidative polymerization and used them for the photocatalytic degradation of MB. Further, the factors affecting photocatalytic degradation, which include initial dye concentration, exposure time, the role of pH, loadings of PPy- $TiO_2$ , and reusability, have also been investigated. In one study, it was observed that the efficiency obtained for PPy- $TiO_2$  was far higher than that of pristine  $TiO_2$  (Sangareswari and Meenakshi Sundaram, 2017). PPy is a p-type narrow bandgap semiconductor, whilst  $TiO_2$  is an n-type narrow bandgap semiconductor. The LUMO of PPy is at a higher energy level than that of the CB edge of  $TiO_2$ . The combination of these two aspects provides desirable photocatalytic performance for the PPy- $TiO_2$  NC. The photocatalytic mechanism involves the transfer of excited  $e^-$  in the LUMO levels of PPy into the CB of the  $TiO_2$  and thus generates more photo energized  $e^-$  at the  $TiO_2$ .  $TiO_2$  was immobilized on PPy support by reverse microemulsion polymerization has been proved to be an efficient nano-photocatalyst for the photocatalytic elimination of phenylhydrazine (PHZ) (Sheikhsamany and Faghihian, 2019). PPy- $TiO_2$  NC exhibited a higher photocatalytic activity under solar light than pristine  $TiO_2$ . Likewise, g PPy- $TiO_2$  NCs were prepared to have a proportion of PPy to  $TiO_2$  as 1:100 by keeping the reaction mixture under stirred conditions at 90, 180, and 270 °C (250 rpm) and showed good photocatalysis of the RR45 dye under UVA and

**Table 2**Visible light-activated and enhanced photocatalysis by PANI-semiconductor (other than TiO<sub>2</sub>) materials.

Material	Synthetic procedure	Application	Reason for the enhanced effects	Reference
BiOBr-GO-PANI	In-situ chemical oxidative polymerization	Photodegradation of phenol	Establishment of double Z-scheme	Liu and Cai (2019)
NiO-doped polyaniline	Electrochemical deposition	Degradation of MB and rhodamine B dyes	PANI acts as a sensitizer and semiconductor	Haspulat Taymaz et al. (2021)
BiVO <sub>4</sub> /GO/PANI	Interfacial coupling	Degradation of MB and safranin O	Synergetic effect of PANI and BiVO <sub>4</sub> /GO	Biswas et al. (2020)
MoS <sub>2</sub> -PANI	Oxidative polymerization of aniline with MoS <sub>2</sub> nanosheets	Degradation of MB and 4-chlorophenol	LUMO of PANI is higher than MoS <sub>2</sub>	Saha et al. (2019)
LaNiSbWO <sub>4</sub> -G-PANI	Hydrothermal method	Degradation of MO	Relative energy level of PANI and LaNiSbWO <sub>4</sub>	Biswas et al. (2019a)
PANI/SrSnO <sub>3</sub> nanocomposites	Mechanical grinding, heat treatment, and ultrasonication	Photodegradation of MB	Synergetic doping of PANI (electron donor) into the SrSnO <sub>3</sub> framework	Faisal et al. (2019)
PANI/BiOCl nanosheets	PANI formation on the surface of the BiOCl nanosheets	Photocatalytic activity for reactive blue	Photoexcited electrons on CB of PANI could easily be transferred to that of BiOCl	Mansor et al. (2021)
PANI supported CdS/CeO <sub>2</sub> /Ag <sub>3</sub> PO <sub>4</sub> nanocomposite	Co-precipitation method	Photodegradation of methyl orange	"A-B" type tandem n-n ternary heterojunction formation and PANI as the sensitizer	Tadesse et al. (2021)
PANI-Pt co-catalyzed CdS	Interfacial polymerization	Hydrogen production	S-C, S-Pt, and Pt-N formation facilitated charge transfer	Zhu et al. (2020)

solar irradiation (Kratofil Krehula et al., 2019). The resultant photocatalysts were designated as PPy/TiO<sub>2</sub>-90/180/270 and validated by optimizing various experimental parameters. It was found that organic carbon values were significantly lower for PPy/TiO<sub>2</sub>-270, with high photocatalytic mineralization and stability for RR45 dye (81.6% and apparent rate constant: 0.0289/min). The presence of the PPy surface mitigates the aggregation of TiO<sub>2</sub>NPs and provides conditions for boosting photocatalytic degradation. Similarly, NCs based on PPy-TiO<sub>2</sub> were synthesized via *in-situ* oxidative polymerization of pyrrole using ferric chloride as an oxidant and the composite was evaluated for visible light-mediated photocatalysis of RhB (Gao et al., 2016). The RhB degradation efficiency of PPy-TiO<sub>2</sub> attained 97% at eight hours (41% more than TiO<sub>2</sub>). Similarly, Guan et al. reported a sol-gel route for the preparation of PPy-TiO<sub>2</sub> and evaluated its adsorption and photocatalytic decolorization of salicylic acid (Wang et al., 2015a). The adsorption kinetics using different models (Langmuir, Freundlich, Temkin, and Dubinin-Radushkevich) were carefully studied at various temperatures ranging from 5 to 25 °C (50 mg/L salicylic acid) for the composite PPy-TiO<sub>2</sub>. The PPy-TiO<sub>2</sub> composite (5 °C) (48.6%) (adsorption capacity: 32.4 mg/g) displayed more enhanced photocatalytic activity than PPy-TiO<sub>2</sub> (10 °C) (42.4%) and PPy-TiO<sub>2</sub> (25 °C) (35.7%) under visible light irradiation (Wang et al., 2015a).

4-chlorophenol (4-CP) and diclofenac (2-[2-(2,6-dichloroanilino)phenyl]acetic acid) (DCF) are considered the most important compounds in the paper (bleaching) and pharmaceutical (pesticides) industries (Orias and Perrodin, 2013). In a recent study, the PPy-TiO<sub>2</sub> composite was prepared and used for the photocatalytic conversion of 4-CP and DCF under simulated solar light (Xe lamp, 600 W/m<sup>2</sup>) (Silvestri et al., 2020). To achieve this, traditional polymerization was used, and the as-developed materials were analyzed for their inherent physicochemical properties. The experimental data suggest that the PPy-TiO<sub>2</sub> composite was able to convert >90%, DCF (15 min) and 40%, 4-CP (60 min), demonstrating excellent stability and conversion efficiency (five cycles) (Silvestri et al., 2020). An interesting computational study (density functional theory) investigated the intermolecular interaction mechanism between clusters of Ti<sub>16</sub>O<sub>32</sub> (as an acceptor) and pyrrole (Py) oligomers (as a donor) of optimized geometries and optoelectronic properties (bandgap/edge, molecular orbitals, the density of states, electrostatic surface potential, charge carrier dynamics) of the simulated PPy-TiO<sub>2</sub> composites based on some valid models (Fig. 8) (Ullah et al., 2017). It was found that Py-Ti<sub>16</sub>O<sub>32</sub> possesses enhanced optical absorption and narrow bandgap. The authors concluded that the oligomeric length (eight or nine) is an optimum choice for designing PPy-TiO<sub>2</sub> composites.

## 5.2. PPy-TiO<sub>2</sub> nanostructures

The core-shell nanobelt, TiO<sub>2</sub>@vanadium pentoxide (V<sub>2</sub>O<sub>5</sub>)-PPy was utilized as an active visible-light photocatalyst (Liu et al., 2020). Earlier, the same group of researchers developed TiO<sub>2</sub> nanobelts with V<sub>2</sub>O<sub>5</sub> nanosheets heterojunction photocatalyst and witnessed an enhanced reaction area, improved solar light photocatalysis efficiency increased charge transfer rate and efficient separation of photogenerated charge carrier (Bayati et al., 2010). However, TiO<sub>2</sub> nanobelts-V<sub>2</sub>O<sub>5</sub>

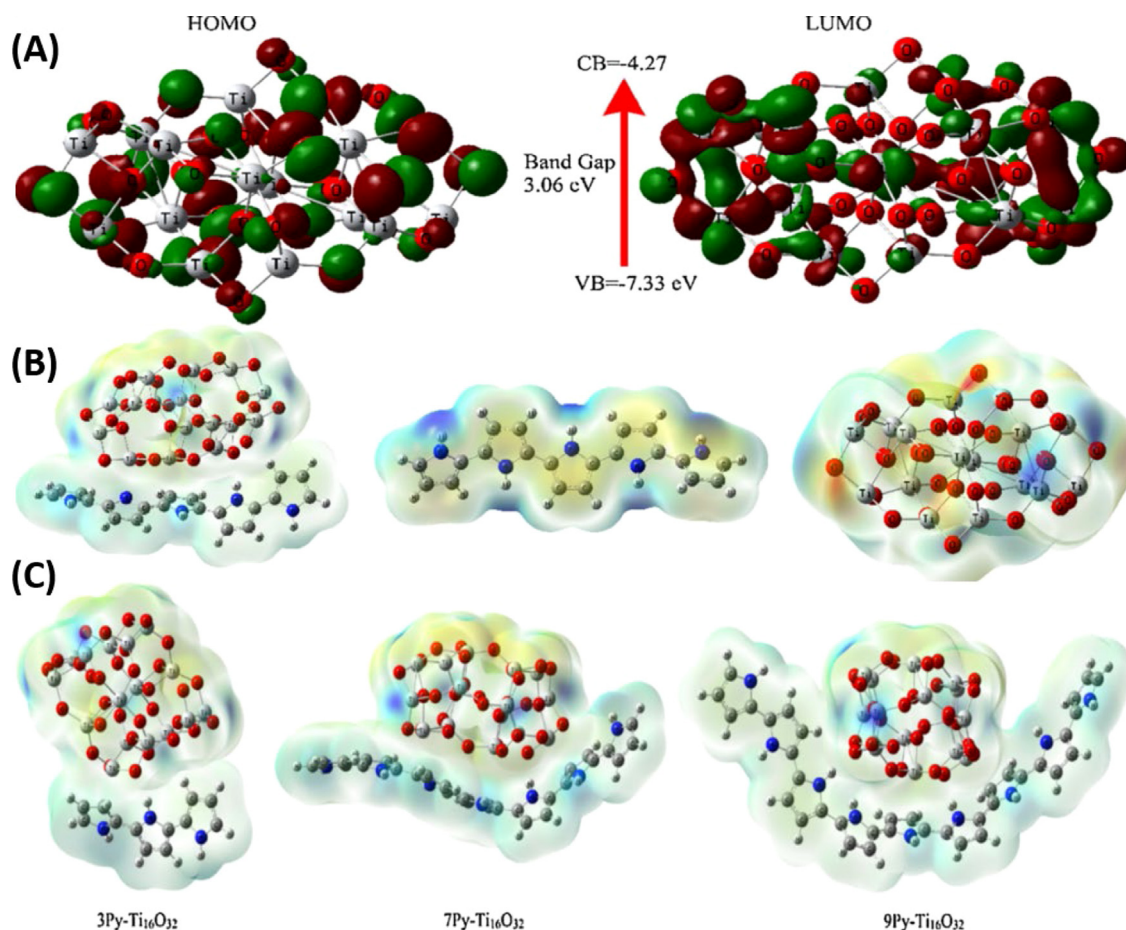


**Fig. 8.** (A) Contours of  $\text{Ti}_{16}\text{O}_{32}$ , molecular electrostatic potential plots of (B)  $\text{Ti}_{16}\text{O}_{32}$ , 5Py and 5Py- $\text{Ti}_{16}\text{O}_{32}$ , and (C) 3, 7, and 9Py- $\text{Ti}_{16}\text{O}_{32}$  composites. Reproduced with permission: Copyright 2017, Elsevier (Ullah et al., 2017).

nanosheets based composites were constrained with the associated leakage of  $\text{V}_2\text{O}_5$  during the application stage. In the  $\text{TiO}_2@V_2O_5$ -PPy ternary composite, PPy primarily plays the role of controlling the leakage of  $\text{V}_2O_5$ . The  $\text{TiO}_2@V_2O_5$ -PPy ternary composite exhibited 98%, 96% and 85% photocatalytic removal efficiencies for TC, doxycycline and oxytetracycline respectively, within 120 min. Similarly, the core-shell PPy-Ag/ $\text{TiO}_2$  ternary composite having an optical band gap of 3.06 eV exhibited high visible-light photocatalytic activity for RhB and MB dyes (Liu et al., 2016b). The efficiency of MB, the pH influence (3 to 9), and the initial dye concentration (4 to 20 mg/L) (Kumar et al., 2016).

Different from other reports, a unique visible light-activated photocatalytic structure composed of yolk-shell structure iron(II),(III) oxide ( $\text{Fe}_3\text{O}_4$ )/poly(methacrylic acid) (MAA)-N, N'-Methylenebisacrylamide-(MBAA)-PPy/Au/void/ $\text{TiO}_2$  magnetic microspheres were synthesized and evaluated for photocatalytic decolorization of RhB (5 mg/mL) (400 W metal halide lamp) (Fig. 12(A)-(C), (D)) (Ma et al., 2019). Herein, the authors used the affinity property of PPy to bind with the surface plasmon resonance (Au), widening the adsorption of  $\text{TiO}_2$ 's visible light capability (Fig. 12(D)). The unique yolk-shell structure arising from  $\text{Fe}_3\text{O}_4$ /P(MAA-MBAA)-PPy/Au/void/ $\text{TiO}_2$  enhanced light use and capture, resulting in highly efficient recyclable photocatalysts with an efficiency of 70.2% (after six cycles) (Fig. 12(D), (F)) (Ma et al., 2019).

### 5.3. PPy- $\text{TiO}_2$ based multicomponent photocatalysts

Hybrid multi-functional nanostructure materials comprising more than two distinct components have become an efficient approach for tailor designing novel functional materials for environmental remediation applications. In a report,  $\text{TiO}_2/\text{SiO}_2$  membranes (PPy@TS) were coated by nanofibrous PPy using a combination of various techniques, such as electrospinning, calcination, sol-gel, subsequent *in-situ* polymerization and evaluated for photocatalytic investigation of aqueous MO degradation. The photocatalytic performance of various membranes (TS400, PPy@TS400, TS600, PPy@TS600, TS800, and PPy@TS800) was compared and analyzed. As a result of the synergistic contributions of PPy and  $\text{TiO}_2$ , PPy@TS800 displayed an outstanding photocatalytic response over the others (Li et al., 2018b). The *in-situ* polymerization

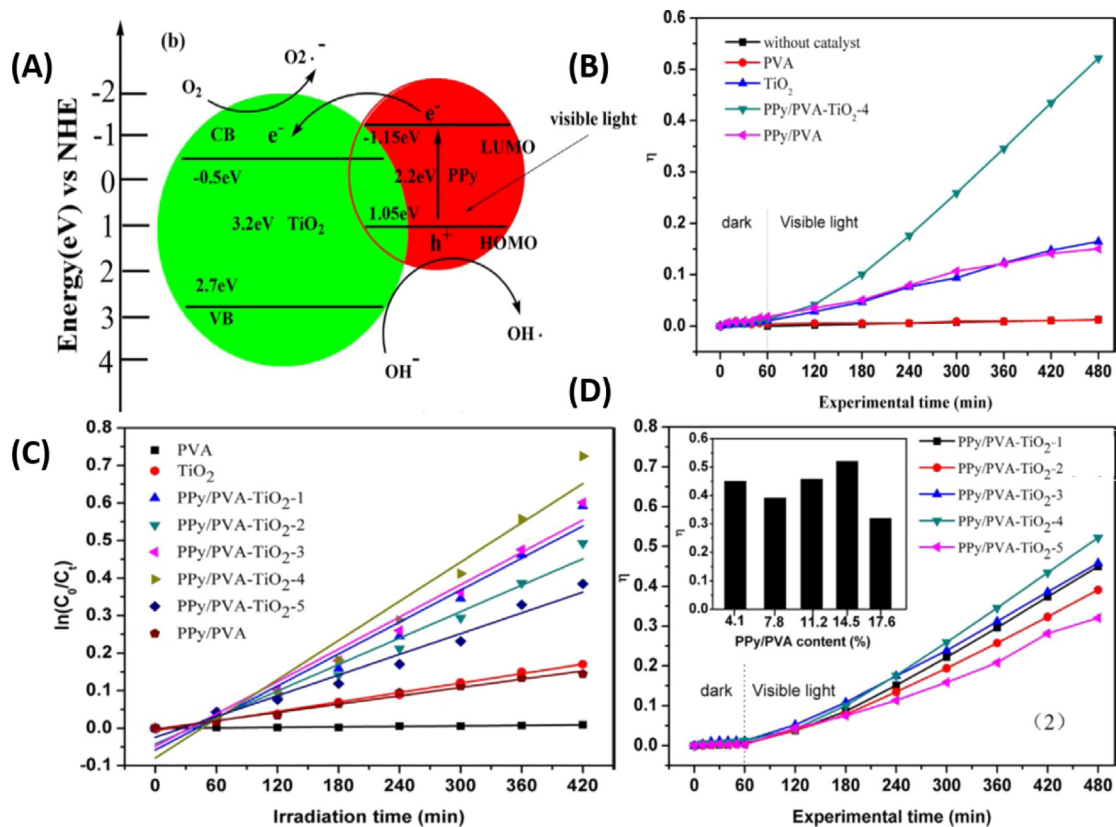


**Fig. 9.** (A) The possible degradation mechanisms of PPy/PVA-TiO<sub>2</sub> composites (B) influence of decolorization ratio of RhB (10 mg/L) for various photocatalysts, (C) pseudo first-order kinetic plots, and (D) PPy/PVA with various TiO<sub>2</sub> contents. Reproduced with permission: Copyright 2020, Elsevier (Liu et al., 2020).

of PPy resulted in the layer formation of PPy particles both on the surface of TiO<sub>2</sub> and within the TS nanofibers matrix. The excellent photocatalytic activity of the PPy@TS arises from the individual contributions of TiO<sub>2</sub> and PPy.

A group of researchers led by Dan used traditional chemical oxidative polymerization and sol-gel synthesis to investigate PPy-polyvinyl alcohol-TiO<sub>2</sub> (PPy/PVA-TiO<sub>2</sub>) composite films for the photocatalysis of RhB (Fig. 9) (Cao et al., 2015) and analyzed various photocatalytic composites (PPy/PVA-TiO<sub>2</sub>-1 to 5) by varying the ratio of PPy to PVA (g) (from 0.038 to 0.0195) and their role influence of the variations in the concentration on the photocatalytic performance (Fig. 9(A, B, C)). The experimental data suggest that the adsorption efficiency under visible light follows this order: PPy/PVA-TiO<sub>2</sub>-4 (52.1%) (14.5 wt%) > PPy/PVA-TiO<sub>2</sub>-3 (45.8%) > PPy/PVA-TiO<sub>2</sub>-1 (45%) > PPy/PVA-TiO<sub>2</sub>-2 (39.1%) > PPy/PVA-TiO<sub>2</sub>-5 (32%). These activities were compared with pure TiO<sub>2</sub>, PVA, and unmodified PPy/PVA. The reusability tests indicated that PPy-PVA-TiO<sub>2</sub>-4 possesses higher photocatalytic performance for UV/visible light irradiation primarily because of higher optical absorption (200–800 nm) and efficient electron shuttling between TiO<sub>2</sub> and PPy (Fig. 9) (Cao et al., 2015) (see Fig. 13).

The multicomponent TiO<sub>2</sub>/Ag-AgCl@PPy has been reported to exhibit an improved photodegradation activity for RhB under visible-light illumination (Yao et al., 2016). The remarkable visible light activity was explained based on combined effects arising from TiO<sub>2</sub> nanofibers, Ag-AgCl nanoparticles, and the PPy shell. The photocatalytic mechanism that explains the enhanced visible-light activity and good charge separation has been proposed. Typically, the charge carrier separation efficiency was improved due to the plasmonic effect of Ag-AgCl nanoparticles, and the heterojunction formed between PPy and TiO<sub>2</sub>. A nanocomposite based on TiO<sub>2</sub> and nanostructured polypyrrole (PPyNS-TiO<sub>2</sub>) was prepared and its visible-light photocatalytic activity was demonstrated (Yuan et al., 2020). The improved visible-light photoactivity was attributed to the heterojunction formation between PPyNS and TiO<sub>2</sub>, broadening of the absorption to the visible light region, and efficient charge carriers' separation. The optical band gap of PPyNS-TiO<sub>2</sub> photocatalyst as derived from the Kubelka-Munk method indicated a decrease to 1.95 eV from 2.93 eV for the pristine TiO<sub>2</sub>. In another study, a metal-organic framework (MOFs)-based PPy (TiO<sub>2</sub>/Cu-MOF/PPy) was developed as the visible light photocatalyst and tested for the removal of dyes (organic) (Liu et al., 2021). The optical energy gaps were in the order: TiO<sub>2</sub> > TiO<sub>2</sub>/Cu-MOF > TiO<sub>2</sub>/Cu-MOF/PPy. The significant decrease in band gap for the PPy included composite is attributed to significant light absorption arising from organic ligand (PPy)-to-metal (Cu) and d-d transition of Cu ions.

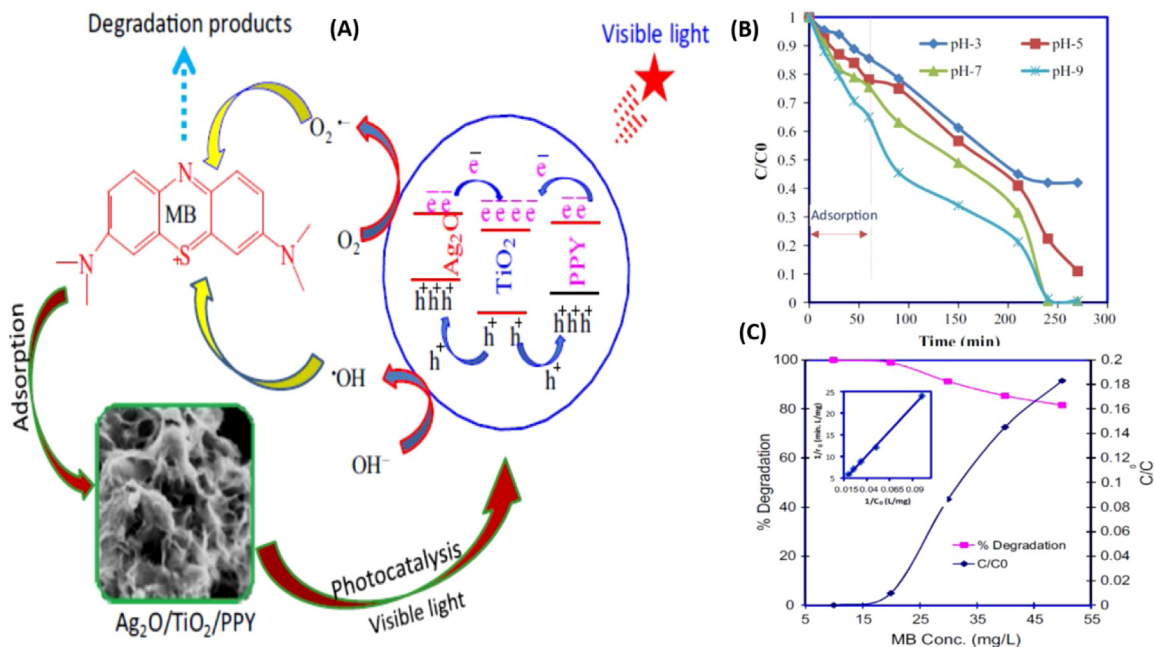


**Fig. 10.** (A) Illustration showing the mechanism involved for Ag<sub>2</sub>O/TiO<sub>2</sub>/PPy, (B) Adsorption behavior at different pH (3, 5, 7, and 9), and (C) Influence of MB concentration on photodegradation activity (inset: plot showing L-M kinetic model). Reproduced with permission: Copyright 2016, Elsevier (Kumar, 2016).

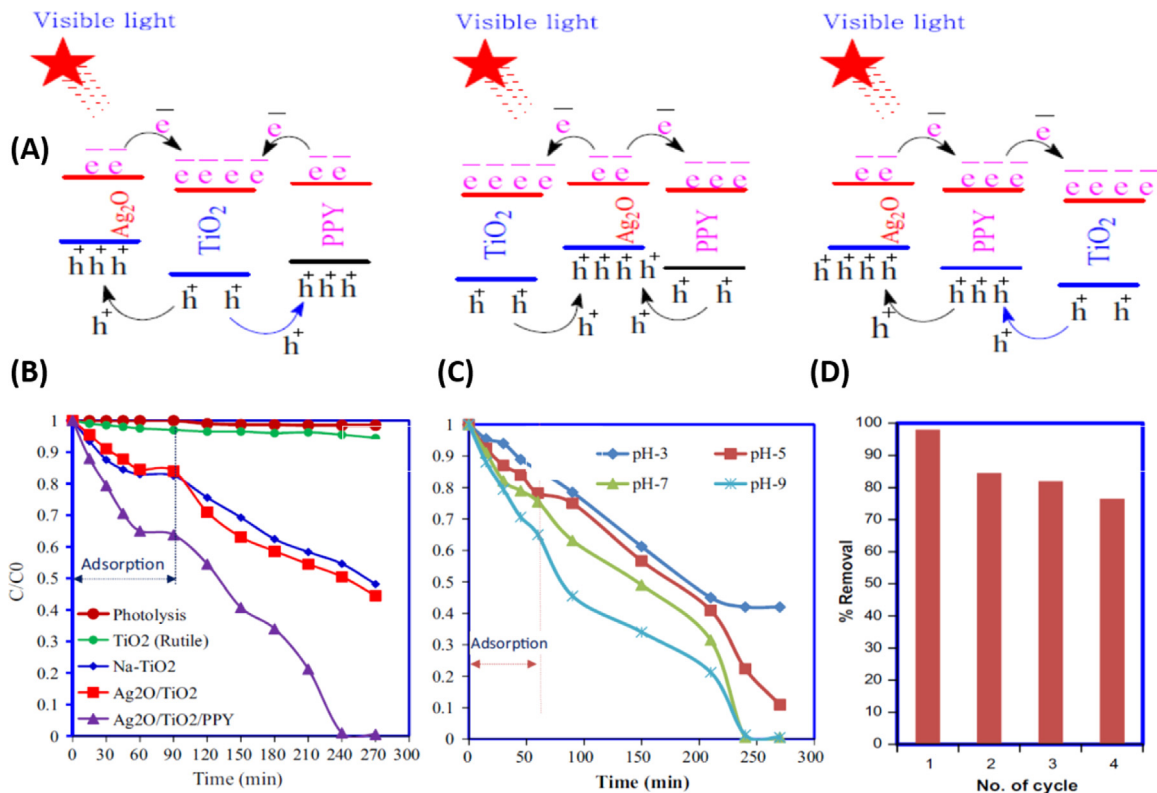


**Fig. 11.** (A) Charge-separation mechanism at the Ag<sub>2</sub>O/TiO<sub>2</sub>/PPy interface, (B) adsorption behavior and degradation trend for MB at different pH (0.05 g, concentration of MB: 20 mg/L, volume: 100 ml, pH-9), (C) influence of pH, and (D) reusability. Reproduced with permission: Copyright 2016, Elsevier (Kumar, 2016).

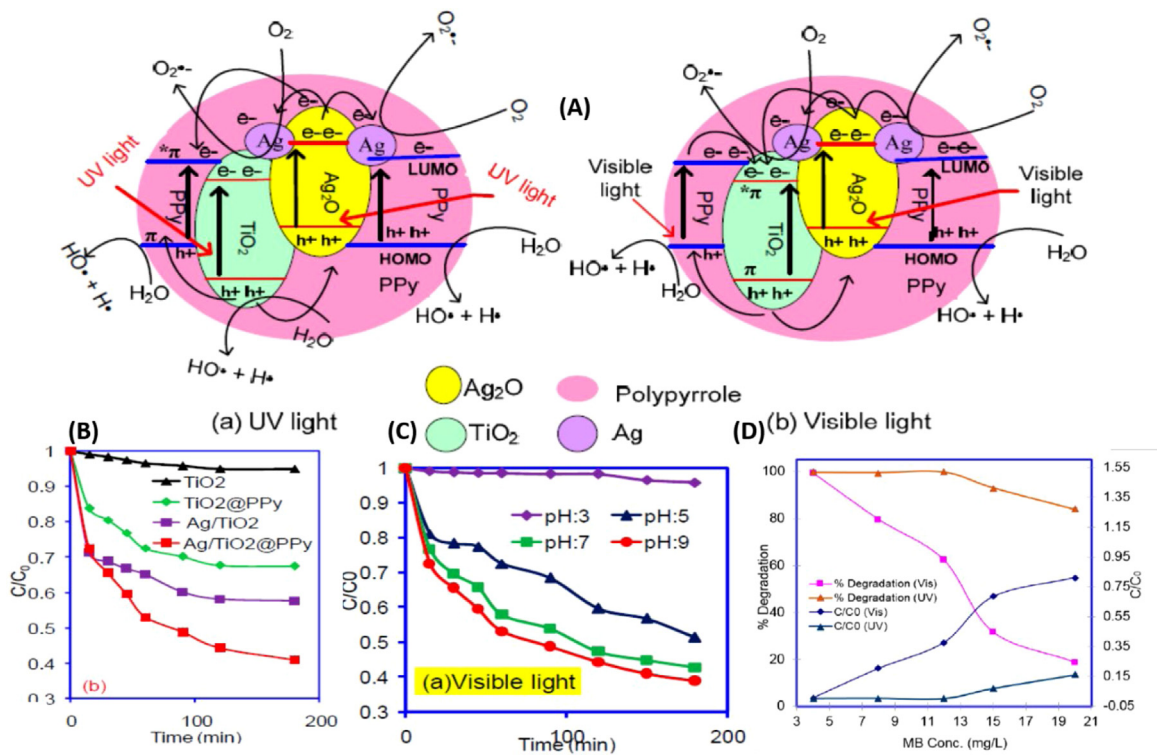


**Fig. 12.** (A) Mechanism showing charge separation of Ag–Ag<sub>2</sub>O/TiO<sub>2</sub>@PPy heterostructure, (B) photocatalytic degradation efficiency of MB, (C) the corresponding pH influence, and (D) effect of initial dye concentration. Reproduced with permission: Copyright 2016, Multidisciplinary Digital Publishing Institute (Kumar et al., 2016).

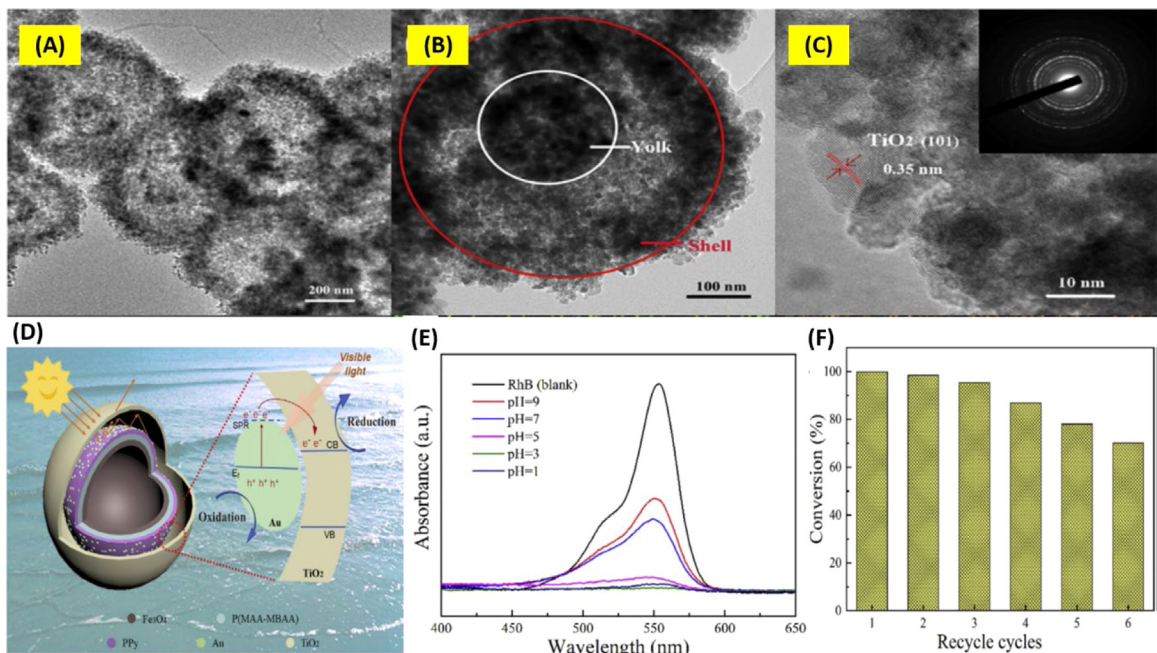


**Fig. 13.** (A, B, C) TEM images (D) plausible degradation mechanism, (E) influence of pH (1 to 9), and (F) reusability test of Fe<sub>3</sub>O<sub>4</sub>/P(MAA-MBAA)-PPy/Au/void/TiO<sub>2</sub> catalyst for RhB. Reproduced with permission: Copyright 2019, Elsevier (Ma et al., 2019).

**Table 3**  
Visible light-activated and enhanced photocatalysis by polypyrrole-semiconductor (other than TiO<sub>2</sub>) catalytic system.

Material	Synthetic procedure	Application	Reason for the enhanced effects	Reference
ZnO/PPy	Oxidative polymerization of PPy with ZnO	Photodegradation of MB	MB acts as a photosensitizer and is adsorbed on ZnO	Ovando-Medina et al. (2015)
PPy/AgFeO <sub>2</sub> nanohybrids	In-situ polymerization with AgFeO <sub>2</sub>	Sonophotocatalytic degradation of TCP	Formation of hydroxyl radicals by photoelectron trapping	Kashyap and Riaz (2018)
ZnO/PPy composite	Oxidative polymerization of the monomer with ZnO nanoparticles	Degradation of Orange II azo dye	p-n heterojunction formation and accumulation of charges in the VB of ZnO	Escobar-Villanueva et al. (2020)
PPy/Co-ordination complex C/Polyoxometalate nanohybrids	In-situ chemical oxidation polymerization	Degradation of RhB	PPy/ZnP <sub>2</sub> Mo <sub>5</sub> nanorod VB and CB align well with LUMO and HOMO of PPy	Xu et al. (2015)
MoSe <sub>2</sub> -PPy nanocomposite	Combined hydrothermal and in-situ polymerization	Degradation of cationic and anionic dyes	Excited MoSe <sub>2</sub> and PPy transferred to the CB	Mittal and Khanuja (2021)
Anthraquinone-2-sulfonate doped ZnIn <sub>2</sub> S <sub>4</sub> - PPy	Hydrothermal and oxidative polymerization	Removal of TC	Photogenerated holes and electrons occurred at the different active sites	Gao et al. (2017)
α-Fe <sub>2</sub> O <sub>3</sub> /PPy composite	Simultaneous gelation and polymerization process	Degradation of MB	Rapid migration of photosensitized PPy into CB of α-Fe <sub>2</sub> O <sub>3</sub> and to the surface of the catalyst	Harraz et al. (2015)
CdS/PPy composite	Room temperature chemical oxidative polymerization	Degradation of MB	The CB of CdS lies below the LUMO level of PPy	Hiragond et al. (2018)
NiS-PPy-Fe <sub>3</sub> O <sub>4</sub> nano-photocatalyst And Fe <sub>3</sub> O <sub>4</sub> @PPy Core/Shell	Oxidative polymerization with metal oxide	Removal of cephalixin	Bandgap reduction of NiS after immobilizing with the catalyst	Torki and Faghihian (2017)
PPy/Bi <sub>2</sub> O <sub>2</sub> CO <sub>3</sub> composite	Hydrothermal method and chemical oxidative polymerization	Degradation of RhB	Rapid charge separation and slow charge recombination.	Wang et al. (2015b)
PPy-ZnO composite	Oxidative polymerization	Degradation of diclofenac	Enhanced charge migration and electronic transport	Silvestri et al. (2019)

Rajeev Kumar judiciously designed and developed a composite made of mixed-phase lamellar TiO<sub>2</sub>-titanate anchored with silver oxide (Ag<sub>2</sub>O) and PPy toward superior adsorption and visible light photocatalytic activity (MB degradation) by modifying the chemistry of materials involving rutile TiO<sub>2</sub>, hydrothermal treatment (100 °C for 12 h), ion exchange and hydrogen peroxide oxidative polymerization (Kumar, 2016). It was identified that MB's adsorption capacity has the following order: TiO<sub>2</sub> < Ag<sub>2</sub>O/TiO<sub>2</sub> < sodium (Na)-TiO<sub>2</sub> < Ag<sub>2</sub>O/TiO<sub>2</sub>/PPy (Lagergren), whereas photocatalytic decontamination takes the following order: TiO<sub>2</sub> < Na-TiO<sub>2</sub> < Ag<sub>2</sub>O/TiO<sub>2</sub> < Ag<sub>2</sub>O/TiO<sub>2</sub>/PPy (L-H kinetic model) (Fig. 10(A)-(D)) (Kumar, 2016).

Hybrid multiple heterojunctions-type photocatalytic composites comprising Ag/TiO<sub>2</sub>@PPy have been prepared by using combined oxidation polymerization (PPy), AgNO<sub>3</sub> with TiO<sub>2</sub> NPs and comparing these with those of p-n type Ag/TiO<sub>2</sub> and TiO<sub>2</sub>@PPy (n-p) heterojunctions (Fig. 11) (Kumar et al., 2016). Ag/TiO<sub>2</sub>@PPy composites were primarily prepared and tested for significant degradation of MB under illumination (visible light). Herein, PPy was used as a photosensitizer as well as an electron acceptor. The studied materials were thoroughly analyzed for their physicochemical material characterization, and it was found that the activity of Ag/TiO<sub>2</sub>@PPy outperformed Ag/TiO<sub>2</sub> and TiO<sub>2</sub>@PPy.

#### 5.4. PPy in conjunction with semiconductors other than TiO<sub>2</sub>

In recent years, semiconductors other than TiO<sub>2</sub> like ZnO as well metal oxy compounds were individually combined with semiconducting polymers, and visible light photocatalysts were designed. In this sub-section, the research studies published on such PPy based photocatalysts are reviewed and tabulated providing the synthetic approaches, and the type of application for which they are seeking for the role of PPy in providing visible light photoactivities. The readers can refer to Table 3 for the details on the PPy based photocatalysts for additional information.

## 6. Conclusion and prospects

In the recent past, notable efforts have been attempted toward the development of advanced green chemical processes for their prospective utilities in environmental remediation. One of the proven approaches is designing a photocatalytic system involving the photosensitization of the respective semiconducting material in the presence of visible



light/simulated solar light activation. The importance of developing such visible-light-responsive photocatalysts is based on the fact that such catalysts can harness solar energy and offer a facile solution to mitigate environmental issues. Semiconductors in conjunction with CPs have been extensively studied for photocatalytic applications. A wide variety of CP (PANI, PPy)-semiconductor (especially TiO<sub>2</sub>) hybrid photocatalysts have been developed and demonstrated their improved activities under visible light for environmental remediation applications. In the process of establishing progressive motifs for developing semiconductor materials with enhanced photoactivities over a wider wavelength domain, different families or categories of CP-semiconductor based photocatalysts are utilized, which include nanocomposites, Z-scheme systems, and multi-component architectures. This review comprehensively presents the latest reports on a wide range of PANI/PPy-TiO<sub>2</sub> photocatalysts that were developed in the last five years focusing on aspects such as visible light activity, efficiency, mechanistic explanations on the role of sensitizing materials or other components on the enhancement of photoactivities and practical utility of the catalysts.

The literature over the past five years (2016–2021) gives a clue that for advanced photocatalyst developments, TiO<sub>2</sub> dominates as the inorganic semiconductor, and PANI and PPy were predominantly used as the sensitizing semiconducting polymer interfaces. The literature on other inorganic semiconductors in conjunction with PANI/PPy is still limited and requires intensive and extensive consideration. Among visible light photocatalyst materials, it has been well demonstrated that the most promising approaches to derive enhanced photocatalytic activities utilize complex multicomponent systems, that include Z-scheme heterojunction photocatalysts having other metal components as co-catalysts with plasmonic particles. However, considering the cost of the resultant photocatalysts, there has been significant interest in the design and development of metal particles (non-noble) and co-catalysts, keeping in mind that there is a great challenge to attain efficient targets toward application performances.

Extensive research activities are thus needed in this promising area of research giving attention to the outcome of such exploration to benefit the commercial sector from both an ecological and an economic perspective. There are plenty of scopes that the application of CP-semiconductor based hybrid active visible-light mediated photocatalysts can be widely extended to the transdisciplinary research areas such as hydrogen generation using water splitting, mitigation of carbon dioxide to produce sustainable liquid fuels which in turn alleviate global warming, reduction of carbonyls in organic synthesis, hydrogenation of nitro compounds and important photo-oxidation systems. In summary, we envisage that this review will be a useful guide for those seeking to pursue advanced research on PANI/PPy-based hybrid photocatalysts and may also generate ideas to develop smart and innovative next-generation photocatalysts.

### CRediT authorship contribution statement

**Gopalan Saianand:** Conceptualization, Writing – original draft, Investigation, Writing – review & editing. **Anantha-Iyengar Gopalan:** Conceptualization, Writing – original draft, Investigation, Writing – review & editing. **Liang Wang:** Writing – review & editing. **K. Venkatraman:** Writing – review & editing. **Vellaisamy A.L. Roy:** Writing – review & editing. **Prashant Sonar:** Writing – review & editing. **Dong-Eun Lee:** Writing – review & editing. **Ravi Naidu:** Writing – review & editing, Resources, Investigation, Formal analysis, Funding acquisition, Supervision.

### Declaration of competing interest

The authors declare that they have no known competing financial interests or personal relationships that could have appeared to influence the work reported in this paper.

### Acknowledgments

The authors (G.S and R.N) appreciate the funding support from Cooperative Research Centre for Contamination Assessment and Remediation of the Environment (CRC CARE) to carry out this literature review. This work was also supported by the National Research Foundation of Korea (NRF) grant funded by the Korean government (MSIP) (No. NRF-2019R1A2C3003890). The contributions of the Ministry of Science, ICT, and Future Planning are gratefully acknowledged.

### References

- Abdelnasser, S., Al Sakkaf, R., Palmisano, G., 2021. Environmental and energy applications of TiO<sub>2</sub> photoanodes modified with alkali metals and polymers. *J. Environ. Chem. Eng.* 9 (1), 104873.
- Abe, R., 2010. Recent progress on photocatalytic and photoelectrochemical water splitting under visible light irradiation. *J. Photochem. Photobiol. C: Photochem. Rev.* 11 (4), 179–209.
- Acharya, R., Parida, K., 2020. A review on TiO<sub>2</sub>/g-C<sub>3</sub>N<sub>4</sub> visible-light- responsive photocatalysts for sustainable energy generation and environmental remediation. *J. Environ. Chem. Eng.* 8 (4), 103896.
- Ahmad, R., Mondal, P.K., 2012. Adsorption and photodegradation of methylene blue by using PANi/TiO<sub>2</sub> nanocomposite. *J. Dispers. Sci. Technol.* 33 (3), 380–386.
- Akter, J., Hanif, M.A., Islam, M.A., Sapkota, K.P., Hahn, J.R., 2021. Selective growth of Ti<sub>3</sub>+TiO<sub>2</sub>/CNT and Ti<sub>3</sub>+TiO<sub>2</sub>/C nanocomposite for enhanced visible-light utilization to degrade organic pollutants by lowering TiO<sub>2</sub>-bandgap. *Sci. Rep.* 11 (1), 9490.
- Alemán, C., Ferreira, C.A., Torras, J., Meneguzzi, A., Canales, M., Rodrigues, M.A.S., Casanovas, J., 2008. On the molecular properties of polyaniline: A comprehensive theoretical study. *Polymer* 49 (23), 5169–5176.

- Alenizi, M.A., Kumar, R., Aslam, M., Alseroury, F.A., Barakat, M.A., 2019. Construction of a ternary g-C<sub>3</sub>N<sub>4</sub>/TiO<sub>2</sub>@polyaniline nanocomposite for the enhanced photocatalytic activity under solar light. *Sci. Rep.* 9 (1), 12091.
- Ali, S.M., Emran, K.M., Al-Oufi, A.L.L., 2017. Adsorption of organic pollutants by nano-conducting polymers composites: Effect of the supporting nano-oxide type. *J. Molecular Liquids* 233, 89–99.
- Amin, M.T., Alazba, A.A., Manzoor, U., 2014. A review of removal of pollutants from water/wastewater using different types of nanomaterials. *Adv. Mater. Sci. Eng.* 2014, 825910.
- Amorim, S.M., Steffen, G., de S Junior, J.M., Brusamarello, C.Z., Romio, A.P., Domenico, M.D., 2021. Synthesis, characterization, and application of polypyrrole/TiO<sub>2</sub> composites in photocatalytic processes: A review. *Polym. Polym. Compos.* 29 (7), 1055–1074.
- Anantha-Iyengar, G., Shanmugasundaram, K., Nallal, M., Lee, K.-P., Whitcombe, M.J., Lakshmi, D., Sai-Anand, G., 2019. Functionalized conjugated polymers for sensing and molecular imprinting applications. *Prog. Polym. Sci.* 88, 1–129.
- Ayodhya, D., Veerabhadram, G., 2018. A review on recent advances in photodegradation of dyes using doped and heterojunction based semiconductor metal sulfide nanostructures for environmental protection. *Mater. Today Energy* 9, 83–113.
- Bahrudin, N.N., Nawi, M.A., Nawawi, W.I., 2019. Enhanced photocatalytic decolorization of methyl orange dye and its mineralization pathway by immobilized TiO<sub>2</sub>/polyaniline. *Res. Chem. Intermed.* 45 (5), 2771–2795.
- Barkul, R.P., Koli, V.B., Shewale, V.B., Patil, M.K., Delekar, S.D., 2016. Visible active nanocrystalline N-doped anatase TiO<sub>2</sub> particles for photocatalytic mineralization studies. *Mater. Chem. Phys.* 173, 42–51.
- Bayati, M.R., Golestani-Fard, F., Moshfegh, A.Z., 2010. Photo-degradation of methylene blue over V<sub>2</sub>O<sub>5</sub>-TiO<sub>2</sub> nano-porous layers synthesized by micro arc oxidation. *Catal. Lett.* 134 (1), 162–168.
- Benzigar, M.R., Joseph, S., Saianand, G., Gopalan, A.-I., Sarkar, S., Srinivasan, S., Park, D.-H., Kim, S., Talapaneni, S.N., Ramadass, K., Vinu, A., 2019. Highly ordered iron oxide-mesoporous fullerene nanocomposites for oxygen reduction reaction and supercapacitor applications. *Microporous Mesoporous Mater.* 285, 21–31.
- Binas, V., Venieri, D., Kotzias, D., Kiriakidis, G., 2017. Modified TiO<sub>2</sub> based photocatalysts for improved air and health quality. *J. Mater.* 3 (1), 3–16.
- Biswas, M.R.U.D., Cho, K.Y., Jung, C.-H., Oh, W.-C., 2019a. Novel synthesis of LaNiSbWO<sub>4</sub>-G-PANI designed as quaternary type composite for high photocatalytic performance of anionic dye and trihydroxybenzoic acid under visible-light. *Process Saf. Environ. Prot.* 126, 348–355.
- Biswas, M.R.U.D., Ho, B.S., Oh, W.-C., 2020. Eco-friendly conductive polymer-based nanocomposites, BiVO<sub>4</sub>/graphene oxide/polyaniline for excellent photocatalytic performance. *Polym. Bull.* 77 (8), 4381–4400.
- Biswas, B., Warr, L.N., Hilder, E.F., Goswami, N., Rahman, M.M., Churchman, J.C., Vasilev, K., Pan, G., Naidu, R., 2019b. Biocompatible functionalisation of nanoclays for improved environmental remediation. *Chem. Soc. Rev.* 48 (14), 3740–3770.
- Boehler, C., Aqrawe, Z., Asplund, M., 2019. Applications of PEDOT in bioelectronic medicine. *Bioelectron. Med.* 2 (2), 89–99.
- Boyjoo, Y., Sun, H., Liu, J., Pareek, V.K., Wang, S., 2017. A review on photocatalysis for air treatment: From catalyst development to reactor design. *Chem. Eng. J.* 310, 537–559.
- Cao, S., Zhang, H., Song, Y., Zhang, J., Yang, H., Jiang, L., Dan, Y., 2015. Investigation of polypyrrole/polyvinyl alcohol-titanium dioxide composite films for photo-catalytic applications. *Appl. Surf. Sci.* 342, 55–63.
- Carolin, C.F., Kumar, P.S., Saravanan, A., Joshiba, G.J., Naushad, M., 2017. Efficient techniques for the removal of toxic heavy metals from aquatic environment: A review. *J. Environ. Chem. Eng.* 5 (3), 2782–2799.
- Casado, N., Hernández, G., Veloso, A., Devaraj, S., Mecerreyes, D., Armand, M., 2016. PEDOT radical polymer with synergetic redox and electrical properties. *ACS Macro Lett.* 5 (1), 59–64.
- Chen, F., An, W., Li, Y., Liang, Y., Cui, W., 2018. Fabricating 3D porous PANI/TiO<sub>2</sub>-graphene hydrogel for the enhanced UV-light photocatalytic degradation of BPA. *Appl. Surf. Sci.* 427, 123–132.
- Chen, X., Liu, L., Yu, P.Y., Mao, S.S., 2011. Increasing solar absorption for photocatalysis with black hydrogenated titanium dioxide nanocrystals. *Science* 331 (6018), 746–750.
- Chen, S., Takata, T., Domen, K., 2017. Particulate photocatalysts for overall water splitting. *Nat. Rev. Mater.* 2 (10), 17050.
- Chen, J., Tang, T., Feng, W., Liu, X., Yin, Z., Zhang, X., Chen, J., Cao, S., 2022. Large-scale synthesis of p-n heterojunction Bi<sub>2</sub>O<sub>3</sub>/TiO<sub>2</sub> nanostructures as photocatalysts for removal of antibiotics under visible light. *ACS Appl. Nano Mater.* 5 (1), 1296–1307.
- Chen, L., Yang, S., 2018. Interface engineering of TiO<sub>2</sub>@PANI nanostructures for efficient visible-light activation. *Bull. Mater. Sci.* 41 (6), 146.
- del Agua, I., Mantione, D., Ismailov, U., Sanchez-Sanchez, A., Aramburu, N., Malliaras, G.G., Mecerreyes, D., Ismailova, E., 2018. DVS-crosslinked PEDOT:PSS free-standing and textile electrodes toward wearable health monitoring. *Adv. Mater. Technol.* 3 (10), 1700322.
- Di Valentín, C., Pacchioni, G., Selloni, A., 2009. Reduced and n-type doped TiO<sub>2</sub>: Nature of Ti<sup>3+</sup> species. *J. Phys. Chem. C* 113 (48), 20543–20552.
- Dong, J., Shi, Y., Huang, C., Wu, Q., Zeng, T., Yao, W., 2019. A new and stable Mo-Mo<sub>2</sub>C modified g-C<sub>3</sub>N<sub>4</sub> photocatalyst for efficient visible light photocatalytic H<sub>2</sub> production. *Appl. Catal. B* 243, 27–35.
- Escobar-Villanueva, A.G., Ovando-Medina, V.M., Martínez-Gutiérrez, H., Militello, M.P., 2020. Fast photodegradation of Orange II azo dye under visible light irradiation using a semiconducting n-p heterojunction of ZnO nanoparticles/polypyrrole as catalyst. *J. Mater. Sci., Mater. Electron.* 31 (2), 1317–1327.
- Etacheri, V., Di Valentín, C., Schneider, J., Bahnemann, D., Pillai, S.C., 2015. Visible-light activation of TiO<sub>2</sub> photocatalysts: Advances in theory and experiments. *J. Photochem. Photobiol. C: Photochem. Rev.* 25, 1–29.
- Faisal, M., Harraz, F.A., Ismail, A.A., Alsaiari, M.A., Al-Sayari, S.A., Al-Assiri, M.S., 2019. Novel synthesis of Polyaniline/SrSnO<sub>3</sub> nanocomposites with enhanced photocatalytic activity. *Ceram. Int.* 45 (16), 20484–20492.
- Fan, X., Nie, W., Tsai, H., Wang, N., Huang, H., Cheng, Y., Wen, R., Ma, L., Yan, F., Xia, Y., 2019. PEDOT:PSS for flexible and stretchable electronics: Modifications, strategies, and applications. *Adv. Sci.* 6 (19), 1900813.
- Fawzi Suleiman Khasawneh, O., Palaniandy, P., 2021. Removal of organic pollutants from water by Fe<sub>2</sub>O<sub>3</sub>/TiO<sub>2</sub> based photocatalytic degradation: A review. *Environ. Technol. Innov.* 21, 101230.
- Feizpoor, S., Habibi-Yangjeh, A., Yubuta, K., 2018. Integration of carbon dots and polyaniline with TiO<sub>2</sub> nanoparticles: Substantially enhanced photocatalytic activity to removal various pollutants under visible light. *J. Photochem. Photobiol. A: Chem.* 367, 94–104.
- Feizpoor, S., Habibi-Yangjeh, A., Yubuta, K., Vadivel, S., 2019. Fabrication of TiO<sub>2</sub>/CoMoO<sub>4</sub>/PANI nanocomposites with enhanced photocatalytic performances for removal of organic and inorganic pollutants under visible light. *Mater. Chem. Phys.* 224, 10–21.
- Fu, C., Li, M., Li, H., Li, C., Wu, X.g., Yang, B., 2017. Fabrication of Au nanoparticle/TiO<sub>2</sub> hybrid films for photoelectrocatalytic degradation of methyl orange. *J. Alloys Compd.* 692, 727–733.
- Fu, J., Xu, Q., Low, J., Jiang, C., Yu, J., 2019. Ultrathin 2D/2D WO<sub>3</sub>/g-C<sub>3</sub>N<sub>4</sub> step-scheme H<sub>2</sub>-production photocatalyst. *Appl. Catal. B* 243, 556–565.
- Fujishima, A., Honda, K., 1972. Electrochemical photolysis of water at a semiconductor electrode. *Nature* 238 (5358), 37–38.
- Gao, F., Hou, X., Wang, A., Chu, G., Wu, W., Chen, J., Zou, H., 2016. Preparation of polypyrrole/TiO<sub>2</sub> nanocomposites with enhanced photocatalytic performance. *Particuology* 26, 73–78.
- Gao, B., Safaei, Z., Babu, I., Iftekhar, S., Iakovleva, E., Srivastava, V., Doshi, B., Hammouda, S.B., Kalliola, S., Sillanpää, M., 2017. Modification of ZnIn<sub>2</sub>S<sub>4</sub> by anthraquinone-2-sulfonate doped polypyrrole as acceptor-donor system for enhanced photocatalytic degradation of tetracycline. *J. Photochem. Photobiol. A: Chem.* 348, 150–160.

- Ghosh, S., Kouamé, N.A., Ramos, L., Remita, S., Dazzi, A., Deniset-Besseau, A., Beaunier, P., Goubard, F., Aubert, P.-H., Remita, H., 2015a. Conducting polymer nanostructures for photocatalysis under visible light. *Nature Mater.* 14 (5), 505–511.
- Ghosh, S., Kouame, N.A., Remita, S., Ramos, L., Goubard, F., Aubert, P.-H., Dazzi, A., Deniset-Besseau, A., Remita, H., 2015b. Visible-light active conducting polymer nanostructures with superior photocatalytic activity. *Sci. Rep.* 5 (1), 18002.
- Gilja, V., Novaković, K., Travas-Sejdic, J., Hrnjak-Murgić, Z., Kraljić Roković, M., Žic, M., 2017. Stability and synergistic effect of polyaniline/TiO<sub>2</sub> photocatalysts in degradation of azo dye in wastewater. *Nanomaterials* 7 (12), 412.
- Giovannetti, R., Rommozzi, E., Zannotti, M., D'Amato, C.A., 2017. Recent advances in graphene based TiO<sub>2</sub> nanocomposites (GTiO<sub>2</sub>Ns) for photocatalytic degradation of synthetic dyes. *Catalysts* 7 (10), 305.
- Gomes, J., Lincho, J., Domingues, E., Quinta-Ferreira, R.M., Martins, R.C., 2019. N-TiO<sub>2</sub> photocatalysts: A review of their characteristics and capacity for emerging contaminants removal. *Water* 11 (2), 373.
- Gopalan, S.-A., Gopalan, A.-I., Vinu, A., Lee, K.-P., Kang, S.-W., 2018. A new optical-electrical integrated buffer layer design based on gold nanoparticles tethered thiol containing sulfonated polyaniline towards enhancement of solar cell performance. *Sol. Energy Mater. Sol. Cells* 174, 112–123.
- Gopalan, A.-I., Lee, J.-C., Saianand, G., Lee, K.-P., Chun, W.-Y., Hou, Y.-I., Kannan, V., Park, S.-S., Kim, W.-J., 2020. Cost-effective production of TiO<sub>2</sub> with 90-fold enhanced photocatalytic activity via facile sequential calcination and ball milling post-treatment strategy. *Materials* 13 (22), 5072.
- Gopinath, K.P., Madhav, N.V., Krishnan, A., Malolan, R., Rangarajan, G., 2020. Present applications of titanium dioxide for the photocatalytic removal of pollutants from water: A review. *J. Environ. Manag.* 270, 110906.
- Gu, L., Wang, J., Qi, R., Wang, X., Xu, P., Han, X., 2012. A novel incorporating style of polyaniline/TiO<sub>2</sub> composites as effective visible photocatalysts. *J. Mol. Catal. A: Chem.* 357, 19–25.
- Gueye, M.N., Carella, A., Faure-Vincent, J., Demadrille, R., Simonato, J.-P., 2020. Progress in understanding structure and transport properties of PEDOT-based materials: A critical review. *Prog. Mater. Sci.* 108, 100616.
- Hanaor, D.A.H., Sorrell, C.C., 2011. Review of the anatase to rutile phase transformation. *J. Mater. Sci.* 46 (4), 855–874.
- Harraz, F.A., Ismail, A.A., Al-Sayari, S.A., Al-Hajry, A., 2015. Novel  $\alpha$ -Fe<sub>2</sub>O<sub>3</sub>/polypyrrole nanocomposite with enhanced photocatalytic performance. *J. Photochem. Photobiol. A: Chem.* 299, 18–24.
- Hasanpour, M., Hatami, M., 2020. Photocatalytic performance of aerogels for organic dyes removal from wastewaters: Review study. *J. Molecular Liquids* 309, 113094.
- Hashemi Monfared, A., Jamshidi, M., 2019. Synthesis of polyaniline/titanium dioxide nanocomposite (PANI/TiO<sub>2</sub>) and its application as photocatalyst in acrylic pseudo paint for benzene removal under UV/VIS lights. *Prog. Org. Coat.* 136, 105257.
- Haspulat Taymaz, B., Eskizeybek, V., Kamsı, H., 2021. A novel polyaniline/NiO nanocomposite as a UV and visible-light photocatalyst for complete degradation of the model dyes and the real textile wastewater. *Environ. Sci. Pollut. Res.* 28 (6), 6700–6718.
- Hassan, M., Naidu, R., Du, J., Liu, Y., Qi, F., 2020. Critical review of magnetic biosorbents: Their preparation, application, and regeneration for wastewater treatment. *Sci. Total Environ.* 702, 134893.
- Heeger, A.J., 2001. Nobel Lecture: Semiconducting and metallic polymers: The fourth generation of polymeric materials. *Rev. Modern Phys.* 73 (3), 681–700.
- Henderson, M.A., 2011. A surface science perspective on TiO<sub>2</sub> photocatalysis. *Surf. Sci. Rep.* 66 (6), 185–297.
- Heshmatpour, F., Zarrin, S., 2017. A probe into the effect of fixing the titanium dioxide by a conductive polymer and ceramic on the photocatalytic activity for degradation of organic pollutants. *J. Photochem. Photobiol. A: Chem.* 346, 431–443.
- Hiragond, C.B., Khanna, P.K., More, P.V., 2018. Probing the real-time photocatalytic activity of CdS QDs sensitized conducting polymers: Featured PTH, PPy and PANI. *Vacuum* 155, 159–168.
- Hisatomi, T., Kubota, J., Domen, K., 2014. Recent advances in semiconductors for photocatalytic and photoelectrochemical water splitting. *Chem. Soc. Rev.* 43 (22), 7520–7535.
- Hou, D., O'Connor, D., Igalavithana, A.D., Alessi, D.S., Luo, J., Tsang, D.C.W., Sparks, D.L., Yamauchi, Y., Rinklebe, J., Ok, Y.S., 2020. Metal contamination and bioremediation of agricultural soils for food safety and sustainability. *Nat. Rev. Earth Environ.* 1 (7), 366–381.
- Hu, K., E, L., Li, Y., Zhao, X., Zhao, D., Zhao, W., Rong, H., 2020. Photocatalytic degradation mechanism of the visible-light responsive BiVO<sub>4</sub>/TiO<sub>2</sub> core-shell heterojunction photocatalyst. *J. Inorg. Organomet. Polym. Mater.* 30 (3), 775–788.
- Huang, C., Bian, J., Guo, Y., Huang, M., Zhang, R.-Q., 2019. Thermal vacuum de-oxygenation and post oxidation of TiO<sub>2</sub> nanorod arrays for enhanced photoelectrochemical properties. *J. Mater. Chem. A* 7 (10), 5434–5441.
- Huang, Y., Liang, Y., Rao, Y., Zhu, D., Cao, J.-j., Shen, Z., Ho, W., Lee, S.C., 2017. Environment-friendly carbon quantum dots/ZnFe<sub>2</sub>O<sub>4</sub> photocatalysts: Characterization, biocompatibility, and mechanisms for NO removal. *Environ. Sci. Technol.* 51 (5), 2924–2933.
- Hui, Y., Bian, C., Xia, S., Tong, J., Wang, J., 2018. Synthesis and electrochemical sensing application of poly(3, 4-ethylenedioxythiophene)-based materials: A review. *Anal. Chim. Acta* 1022, 1–19.
- Jeong, M.-K., Lee, K., Kang, J., Jang, J., Jung, I.H., 2020. Thiophene backbone-based polymers with electron-withdrawing pendant groups for application in organic thin-film transistors. *New J. Chem.* 44 (22), 9321–9327.
- Jiang, W., Liu, Y., Wang, J., Zhang, M., Luo, W., Zhu, Y., 2016. Separation-free polyaniline/TiO<sub>2</sub> 3D hydrogel with high photocatalytic activity. *Adv. Mater. Interfaces* 3 (3), 1500502.
- Jo, Y.K., Lee, J.M., Son, S., Hwang, S.-J., 2019. 2D inorganic nanosheet-based hybrid photocatalysts: Design, applications, and perspectives. *J. Photochem. Photobiol. C: Photochem. Rev.* 40, 150–190.
- Joseph, S., Saianand, G., Benzigar, M.R., Ramadass, K., Singh, G., Gopalan, A.-I., Yang, J.H., Mori, T., Al-Muhtaseb, A.a.H., Yi, J., Vinu, A., 2020. Recent advances in functionalized nanoporous carbons derived from waste resources and their applications in energy and environment. *Adv. Sustain. Syst.* n/a (n/a), 2000169.
- Kalikeri, S., Kamath, N., Gadgil, D.J., Shetty Kodialbail, V., 2018. Visible light-induced photocatalytic degradation of Reactive Blue-19 over highly efficient polyaniline-TiO<sub>2</sub> nanocomposite: a comparative study with solar and UV photocatalysis. *Environ. Sci. Pollut. Res.* 25 (4), 3731–3744.
- Kanan, S., Moyet, M.A., Arthur, R.B., Patterson, H.H., 2020. Recent advances on TiO<sub>2</sub>-based photocatalysts toward the degradation of pesticides and major organic pollutants from water bodies. *Catal. Rev.* 62 (1), 1–65.
- Kang, X., Liu, S., Dai, Z., He, Y., Song, X., Tan, Z., 2019. Titanium dioxide: From engineering to applications. *Catalysts* 9 (2), 191.
- Kashyap, J., Riaz, U., 2018. Facile synthesis of novel polypyrrole dispersed AgFeO<sub>2</sub> nanohybrid with highly efficient photocatalytic activity towards 2, 4, 6-trichlorophenol degradation. *RSC Adv.* 8 (24), 13218–13225.
- Katančić, Z., Chen, W.-T., Waterhouse, G.I.N., Kušić, H., Lončarić Božić, A., Hrnjak-Murgić, Z., Travas-Sejdic, J., 2020. Solar-active photocatalysts based on TiO<sub>2</sub> and conductive polymer PEDOT for the removal of bisphenol A. *J. Photochem. Photobiol. A: Chem.* 396, 112546.
- Katoch, A., Burkhart, M., Hwang, T., Kim, S.S., 2012. Synthesis of polyaniline/TiO<sub>2</sub> hybrid nanoplates via a sol-gel chemical method. *Chem. Eng. J.* 192, 262–268.
- Kayser, L.V., Lipomi, D.J., 2019. Stretchable conductive polymers and composites based on PEDOT and PEDOT:PSS. *Adv. Mater.* 31 (10), 1806133.
- Khan, S., Narula, A.K., 2019. Ternary photocatalyst based on conducting polymer doped functionalized multiwall carbon nanotubes decorated with nanorods of metal oxide. *Mater. Sci. Eng. B* 243, 86–95.
- Khodagholy, D., Doublet, T., Quilichini, P., Gurfinkel, M., Leleu, P., Ghestem, A., Ismailova, E., Hervé, T., Sanaur, S., Bernard, C., Malliaras, G.G., 2013. In vivo recordings of brain activity using organic transistors. *Nature Commun.* 4 (1), 1575.

- Kim, S.-M., Kim, C.-H., Kim, Y., Kim, N., Lee, W.-J., Lee, E.-H., Kim, D., Park, S., Lee, K., Rivnay, J., Yoon, M.-H., 2018. Influence of PEDOT:PSS crystallinity and composition on electrochemical transistor performance and long-term stability. *Nature Commun.* 9 (1), 3858.
- Kim, M.K., Shanmuga Sundaram, K., Anantha Iyengar, G., Lee, K.-P., 2015. A novel chitosan functional gel included with multiwall carbon nanotube and substituted polyaniline as adsorbent for efficient removal of chromium ion. *Chem. Eng. J.* 267, 51–64.
- Komathi, S., Gopalan, A.I., Muthuchamy, N., Lee, K.P., 2017. Polyaniline nanoflowers grafted onto nanodiamonds via a soft template-guided secondary nucleation process for high-performance glucose sensing. *RSC Adv.* 7 (25), 15342–15351.
- Kraeutler, Bernhard, et al., 1979. Initiation of free radical polymerization by heterogeneous photocatalysis at semiconductor powders. *J. Polym. Sci. Polym. Lett. Ed.* 17 (8), 535–538.
- Kratofil Krehula, L., Stjepanović, J., Perlog, M., Krehula, S., Gilja, V., Travas-Sejdic, J., Hrnjak-Murčić, Z., 2019. Conducting polymer polypyrrole and titanium dioxide nanocomposites for photocatalysis of RR45 dye under visible light. *Polym. Bull.* 76 (4), 1697–1715.
- Kumar, R., 2016. Mixed phase lamellar titania-titanate anchored with Ag<sub>2</sub>O and polypyrrole for enhanced adsorption and photocatalytic activity. *J. Colloid Interface Sci.* 477, 83–93.
- Kumar, R., El-Shishtawy, R.M., Barakat, M.A., 2016. Synthesis and characterization of Ag-Ag<sub>2</sub>O/TiO<sub>2</sub>@polypyrrole heterojunction for enhanced photocatalytic degradation of methylene blue. *Catalysts* 6 (6), 76.
- Kumar, A., Khan, M., He, J., Lo, I.M.C., 2020. Recent developments and challenges in practical application of visible-light-driven TiO<sub>2</sub>-based heterojunctions for PPCP degradation: A critical review. *Water Res.* 170, 115356.
- Lai, K., Wei, W., Zhu, Y., Guo, M., Dai, Y., Huang, B., 2012. Effects of oxygen vacancy and N-doping on the electronic and photocatalytic properties of Bi<sub>2</sub>MO<sub>6</sub> (M=Mo, W). *J. Solid State Chem.* 187, 103–108.
- Lang, X., Saianand, G., Fu, W., Ramakrishna, S., 2020. Photocatalytic water splitting utilizing electrospun semiconductors for solar hydrogen generation: Fabrication, modification and performance. *Bull. Chem. Soc. Japan.*
- Lee, H.-G., Gopalan, A.-I., Sai-Anand, G., Lee, B.-C., Kang, S.-W., Lee, K.-P., 2015a. Facile synthesis of functionalized graphene-palladium nanoparticle incorporated multicomponent TiO<sub>2</sub> composite nanofibers. *Mater. Chem. Phys.* 154, 125–136.
- Lee, J.-C., Gopalan, A.-I., Sai-Anand, G., Lee, K.-P., Kim, W.-J., 2019. Preparation of visible light photocatalytic graphene embedded rutile titanium(IV) oxide composite nanowires and enhanced NO<sub>x</sub> removal. *Catalysts* 9 (2), 170.
- Lee, J.-C., Gopalan, A.-I., Saianand, G., Lee, K.-P., Kim, W.-J., 2020. Manganese and graphene included titanium dioxide composite nanowires: Fabrication, characterization and enhanced photocatalytic activities. *Nanomaterials* 10 (3), 456.
- Lee, H.-G., Sai-Anand, G., Komathi, S., Gopalan, A.-I., Kang, S.-W., Lee, K.-P., 2015b. Efficient visible-light-driven photocatalytic degradation of nitrophenol by using graphene-encapsulated TiO<sub>2</sub> nanowires. *J. Hard Mater.* 283, 400–409.
- Li, W., Elzatahry, A., Aldhayan, D., Zhao, D., 2018a. Core-shell structured titanium dioxide nanomaterials for solar energy utilization. *Chem. Soc. Rev.* 47 (22), 8203–8237.
- Li, X., Wang, D., Cheng, G., Luo, Q., An, J., Wang, Y., 2008. Preparation of polyaniline-modified TiO<sub>2</sub> nanoparticles and their photocatalytic activity under visible light illumination. *Appl. Catal. B* 81 (3), 267–273.
- Li, X., Wang, J., Hu, Z., Li, M., Ogino, K., 2018b. In situ polypyrrole polymerization enhances the photocatalytic activity of nanofibrous TiO<sub>2</sub>/SiO<sub>2</sub> membranes. *Chin. Chem. Lett.* 29 (1), 166–170.
- Li, A., Zhu, W., Li, C., Wang, T., Gong, J., 2019. Rational design of yolk-shell nanostructures for photocatalysis. *Chem. Soc. Rev.* 48 (7), 1874–1907.
- Lin, Y., Li, D., Hu, J., Xiao, G., Wang, J., Li, W., Fu, X., 2012. Highly efficient photocatalytic degradation of organic pollutants by PANI-modified TiO<sub>2</sub> composite. *J. Phys. Chem. C* 116 (9), 5764–5772.
- Liu, X., Cai, L., 2019. A novel double Z-scheme BiOBr-GO-polyaniline photocatalyst: Study on the excellent photocatalytic performance and photocatalytic mechanism. *Appl. Surf. Sci.* 483, 875–887.
- Liu, X., Gao, S., Xu, H., Lou, Z., Wang, W., Huang, B., Dai, Y., 2013. Green synthetic approach for Ti<sup>3+</sup> self-doped TiO<sub>2</sub>-x nanoparticles with efficient visible light photocatalytic activity. *Nanoscale* 5 (5), 1870–1875.
- Liu, W., Kumar, J., Tripathy, S., Senecal, K.J., Samuelson, L., 1999. Enzymatically synthesized conducting polyaniline. *J. Am. Chem. Soc.* 121 (1), 71–78.
- Liu, C., Wang, K., Gong, X., Heeger, A.J., 2016a. Low bandgap semiconducting polymers for polymeric photovoltaics. *Chem. Soc. Rev.* 45 (17), 4825–4846.
- Liu, G., Wang, Y., Xue, Q., Wen, Y., Hong, X., Ullah, K., 2021. TiO<sub>2</sub>/Cu-MOF/PPy composite as a novel photocatalyst for decomposition of organic dyes. *J. Mater. Sci., Mater. Electron.* 32 (4), 4097–4109.
- Liu, M., Zhao, J., Xiao, C., Quan, Q., Li, X., 2016b. PPy-assisted fabrication of Ag/TiO<sub>2</sub> visible-light photocatalyst and its immobilization on PAN fiber. *Mater. Des.* 104, 428–435.
- Liu, J., Zhou, S., Gu, P., Zhang, T., Chen, D., Li, N., Xu, Q., Lu, J., 2020. Conjugate Polymer-clothed TiO<sub>2</sub>@V<sub>2</sub>O<sub>5</sub> nanobelts and their enhanced visible light photocatalytic performance in water remediation. *J. Colloid Interface Sci.* 578, 402–411.
- Liu, Y., Zhou, M., Zhang, W., Chen, K., Mei, A., Zhang, Y., Chen, W., 2019. Enhanced photocatalytic properties of TiO<sub>2</sub> nanosheets@2D layered black phosphorus composite with high stability under hydro-oxygen environment. *Nanoscale* 11 (12), 5674–5683.
- Lu, Y., Wang, Y., Zhang, J., 2021. Semiconductor heterojunction photocatalysts with near-infrared light antennas: a review. *J. Phys. D: Appl. Phys.* 54 (31), 313002.
- Luttrell, T., Halpegamage, S., Tao, J., Kramer, A., Sutter, E., Batzill, M., 2014. Why is anatase a better photocatalyst than rutile? - Model studies on epitaxial TiO<sub>2</sub> films. *Sci. Rep.* 4 (1), 4043.
- Ma, J., Dai, J., Duan, Y., Zhang, J., Qiang, L., Xue, J., 2020. Fabrication of PANI-TiO<sub>2</sub>/rGO hybrid composites for enhanced photocatalysis of pollutant removal and hydrogen production. *Renew. Energy* 156, 1008–1018.
- Ma, M., Yang, Y., Li, W., Ma, Y., Tong, Z., Huang, W., Chen, L., Wu, G., Wang, H., Lyu, P., 2019. Synthesis of yolk-shell structure Fe<sub>3</sub>O<sub>4</sub>/P(MAA-MBAA)-PPy/Au/void/TiO<sub>2</sub> magnetic microspheres as visible light active photocatalyst for degradation of organic pollutants. *J. Alloys Compd.* 810, 151807.
- Majumdar, A., Pal, A., 2020. Recent advancements in visible-light-assisted photocatalytic removal of aqueous pharmaceutical pollutants. *Clean Technol. Environ. Policy* 22 (1), 11–42.
- Manceau, M., Bundgaard, E., Carlé, J.E., Hagemann, O., Helgesen, M., Søndergaard, R., Jørgensen, M., Krebs, F.C., 2011. Photochemical stability of  $\pi$ -conjugated polymers for polymer solar cells: a rule of thumb. *J. Mater. Chem.* 21 (12), 4132–4141.
- Mansor, E.S., Geiushy, R.A., Fouad, O.A., 2021. PANI/BiOCl nanocomposite induced efficient visible-light photocatalytic activity. *J. Mater. Sci., Mater. Electron.* 32 (2), 1992–2000.
- Mehla, S., Kandjani, A.E., Babarao, R., Lee, A.F., Periasamy, S., Wilson, K., Ramakrishna, S., Bhargava, S.K.K., 2020. Porous crystalline frameworks for thermocatalytic CO<sub>2</sub> reduction: An emerging paradigm. *Energy Environ.*
- Meng, A., Zhang, L., Cheng, B., Yu, J., 2019. Dual cocatalysts in TiO<sub>2</sub> photocatalysis. *Adv. Mater.* 31 (30), 1807660.
- MiarAlipour, S., Friedmann, D., Scott, J., Amal, R., 2018. TiO<sub>2</sub>/porous adsorbents: Recent advances and novel applications. *J. Hard Mater.* 341, 404–423.
- Mir, S.H., Nagahara, L.A., Thundat, T., Mokarian-Tabari, P., Furukawa, H., Khosla, A., 2018. Review—Organic-inorganic hybrid functional materials: An integrated platform for applied technologies. *J. Electrochem. Soc.* 165 (8), B3137–B3156.
- Mishra, A., Mehta, A., Basu, S., Shetti, N.P., Reddy, K.R., Aminabhavi, T.M., 2019. Graphitic carbon nitride (g-C<sub>3</sub>N<sub>4</sub>)-based metal-free photocatalysts for water splitting: A review. *Carbon* 149, 693–721.

- Mittal, H., Khanuja, M., 2021. Hydrothermal in-situ synthesis of MoSe<sub>2</sub>-polypyrrole nanocomposite for efficient photocatalytic degradation of dyes under dark and visible light irradiation. *Sep. Purif. Technol.* 254, 117508.
- Mohamed, R.M., Azam, E.S., 2014. Preparation and characterization of core-shell polyaniline/mesoporous Cu<sub>2</sub>O nanocomposites for the photocatalytic oxidation of thiophene. *Appl. Catal. A: Gen.* 480, 100–107.
- Mohd Adnan, M.A., Phoon, B.L., Julkapli, N.Muhd., 2020. Mitigation of pollutants by chitosan/metallic oxide photocatalyst: A review. *J. Cleaner Prod.* 261, 121190.
- Molinari, R., Lavorato, C., Argurio, P., 2017. Recent progress of photocatalytic membrane reactors in water treatment and in synthesis of organic compounds. A review. *Catal. Today* 281, 144–164.
- Mousli, F., Chaouchi, A., Jouini, M., Maurel, F., Kadri, A., Chehimi, M.M., 2019. Polyaniline-grafted RuO<sub>2</sub>-TiO<sub>2</sub> heterostructure for the catalysed degradation of methyl orange in darkness. *Catalysts* 9 (7), 578.
- Mousli, F., Khalil, A.M., Maurel, F., Kadri, A., Chehimi, M.M., 2020. Mixed oxide-polyaniline composite-coated woven cotton fabrics for the visible light catalyzed degradation of hazardous organic pollutants. *Cellulose* 27 (13), 7823–7846.
- Muthirulan, P., Nirmala Devi, C.K., Sundaram, M.M., 2013. Facile synthesis of novel hierarchical TiO<sub>2</sub>@Poly(o-phenylenediamine) core-shell structures with enhanced photocatalytic performance under solar light. *J. Environ. Chem. Eng.* 1 (3), 620–627.
- Naciri, Y., Hsini, A., Bouziani, A., Djellabi, R., Ajmal, Z., Laabd, M., Navío, J.A., Mills, A., Bianchi, C.L., Li, H., Bakiz, B., Albourine, A., 2021. Photocatalytic oxidation of pollutants in gas-phase via Ag<sub>3</sub>PO<sub>4</sub>-based semiconductor photocatalysts: Recent progress, new trends, and future perspectives. *Crit. Rev. Environ. Sci. Technol.* 1–44.
- Nallal, M., Anantha Iyengar, G., Pill-Lee, K., 2017. New titanium dioxide-based heterojunction nano hybrid for highly selective photoelectrochemical-electrochemical dual-mode sensors. *ACS Appl. Mater. Interfaces* 9 (42), 37166–37183.
- Nekooie, R., Shamspur, T., Mostafavi, A., 2021. Novel CuO/TiO<sub>2</sub>/PANI nanocomposite: Preparation and photocatalytic investigation for chlorpyrifos degradation in water under visible light irradiation. *J. Photochem. Photobiol. A: Chem.* 407, 113038.
- Nosrati, R., Olad, A., Najjari, H., 2017. Study of the effect of TiO<sub>2</sub>/polyaniline nanocomposite on the self-cleaning property of polyacrylic latex coating. *Surf. Coat. Technol.* 316, 199–209.
- Nowotny, J., 2008. Titanium dioxide-based semiconductors for solar-driven environmentally friendly applications: impact of point defects on performance. *Energy Environ. Sci.* 1 (5), 565–572.
- Nowotny, M.K., Sheppard, L.R., Bak, T., Nowotny, J., 2008. Defect chemistry of titanium dioxide. Application of defect engineering in processing of TiO<sub>2</sub>-based photocatalysts. *J. Phys. Chem. C* 112 (14), 5275–5300.
- O'Neal Tugaoen, H., Garcia-Segura, S., Hristovski, K., Westerhoff, P., 2018. Compact light-emitting diode optical fiber immobilized TiO<sub>2</sub> reactor for photocatalytic water treatment. *Sci. Total Environ.* 613–614, 1331–1338.
- Ong, C.B., Ng, L.Y., Mohammad, A.W., 2018. A review of ZnO nanoparticles as solar photocatalysts: Synthesis, mechanisms and applications. *Renew. Sustain. Energy Rev.* 81, 536–551.
- Orias, F., Perrodin, Y., 2013. Characterisation of the ecotoxicity of hospital effluents: A review. *Sci. Total Environ.* 454–455, 250–276.
- Ostrovskhova, O., 2016. Organic optoelectronic materials: Mechanisms and applications. *Chem. Rev.* 116 (22), 13279–13412.
- Ovando-Medina, V.M., López, R.G., Castillo-Reyes, B.E., Alonso-Dávila, P.A., Martínez-Gutiérrez, H., González-Ortega, O., Farías-Cepeda, L., 2015. Composite of acicular rod-like ZnO nanoparticles and semiconducting polypyrrole photoactive under visible light irradiation for methylene blue dye photodegradation. *Colloid Polym. Sci.* 293 (12), 3459–3469.
- Pan, H., Liao, W., Sun, N., Muruganathan, M., Zhang, Y., 2018. Highly efficient and visible light responsive heterojunction composites as dual photoelectrodes for photocatalytic fuel cell. *Catalysts* 8 (1), 30.
- Pan, T.J., Zuo, X.W., Wang, T., Hu, J., Chen, Z.D., Ren, Y.J., 2016. Electrodeposited conductive polypyrrole/polyaniline composite film for the corrosion protection of copper bipolar plates in proton exchange membrane fuel cells. *J. Power Sources* 302, 180–188.
- Pang, X., Skillen, N., Gunaratne, N., Rooney, D.W., Robertson, P.K.J., 2021. Removal of phthalates from aqueous solution by semiconductor photocatalysis: A review. *J. Hard Mater.* 402, 123461.
- Park, J., 2017. Visible and near infrared light active photocatalysis based on conjugated polymers. *J. Ind. Eng. Chem.* 51, 27–43.
- Pawar, S.G., Patil, S.L., Chougule, M.A., Mane, A.T., Jundale, D.M., Patil, V.B., 2010. Synthesis and characterization of polyaniline:TiO<sub>2</sub> nanocomposites. *Int. J. Polym. Mater. Polym. Biomater.* 59 (10), 777–785.
- Pei, Z., Ding, L., Lin, H., Weng, S., Zheng, Z., Hou, Y., Liu, P., 2013. Facile synthesis of defect-mediated TiO<sub>2</sub>-x with enhanced visible light photocatalytic activity. *J. Mater. Chem. A* 1 (35), 10099–10102.
- Polarz, S., Strunk, J., Ischenko, V., van den Berg, M.W.E., Hinrichsen, O., Muhler, M., Driess, M., 2006. On the role of oxygen defects in the catalytic performance of zinc oxide. *Angew. Chem. Int. Ed.* 45 (18), 2965–2969.
- Radoičić, M., Čirić-Marjanović, G., Spasojević, V., Ahrenkiel, P., Mitrić, M., Novaković, T., Šaponjić, Z., 2017. Superior photocatalytic properties of carbonized PANI/TiO<sub>2</sub> nanocomposites. *Appl. Catal. B* 213, 155–166.
- Rahimi, N., Pax, R.A., Gray, E.M., 2016. Review of functional titanium oxides. I: TiO<sub>2</sub> and its modifications. *Prog. Solid State Chem.* 44 (3), 86–105.
- Ran, J., Jaroniec, M., Qiao, S.-Z., 2018. Cocatalysts in semiconductor-based photocatalytic CO<sub>2</sub> reduction: Achievements, challenges, and opportunities. *Adv. Mater.* 30 (7), 1704649.
- Razak, S., Nawi, M.A., Haiham, K., 2014. Fabrication, characterization and application of a reusable immobilized TiO<sub>2</sub>-PANI photocatalyst plate for the removal of reactive red 4 dye. *Appl. Surf. Sci.* 319, 90–98.
- Reghunath, S., Pinheiro, D., Kr, S.D., 2021. A review of hierarchical nanostructures of TiO<sub>2</sub>: Advances and applications. *Appl. Surf. Sci. Adv.* 3, 100063.
- Reiche, H., Bard, A.J., 1979. Heterogeneous photosynthetic production of amino acids from methane-ammonia-water at platinum/titanium dioxide. Implications in chemical evolution. *J. Am. Chem. Soc.* 101 (11), 3127–3128.
- Reza, K., Abadi, F.M.H.D., Saeid, M.-P., Leong, O.S., Jiangyong, H., 2019. Polypyrrole- and polyaniline-supported TiO<sub>2</sub> for removal of pollutants from water. *J. Environ. Eng. Sci.* 14 (2), 67–89.
- Reza, K.M., Gurung, A., Bahrami, B., Mabrouk, S., Elbohy, H., Pathak, R., Chen, K., Chowdhury, A.H., Rahman, M.T., Letourneau, S., Yang, H.-C., Saianand, G., Elam, J.W., Darling, S.B., Qiao, Q., 2020. Tailored PEDOT:PSS hole transport layer for higher performance in perovskite solar cells: Enhancement of electrical and optical properties with improved morphology. *J. Energy Chem.* 44, 41–50.
- Riaz, U., Ashraf, S.M., 2014. Synergistic effect of microwave irradiation and conjugated polymeric catalyst in the facile degradation of dyes. *RSC Adv.* 4 (88), 47153–47162.
- Riaz, U., Ashraf, S.M., Kashyap, J., 2015. Role of conducting polymers in enhancing TiO<sub>2</sub>-based photocatalytic dye degradation: A short review. *Polym.-Plast. Technol. Eng.* 54 (17), 1850–1870.
- Saari, J., Ali-Löytty, H., Kauppinen, M.M., Hannula, M., Khan, R., Lahtonen, K., Palmolahti, L., Tukiainen, A., Grönbeck, H., Tkachenko, N.V., Valden, M., 2022. Tunable Ti<sup>3+</sup>-mediated charge carrier dynamics of atomic layer deposition-grown amorphous TiO<sub>2</sub>. *J. Phys. Chem. C* 126 (9), 4542–4554.
- Saha, S., Chaudhary, N., Mittal, H., Gupta, G., Khanuja, M., 2019. Inorganic-organic nanohybrid of MoS<sub>2</sub>-PANI for advanced photocatalytic application. *Int. Nano Lett.* 9 (2), 127–139.
- Sai-Anand, G., Gopalan, A.-I., Lee, K.-P., Venkatesan, S., Qiao, Q., Kang, B.-H., Lee, S.-W., Lee, J.-S., Kang, S.-W., 2016. Electrostatic nanoassembly of contact interfacial layer for enhanced photovoltaic performance in polymer solar cells. *Sol. Energy Mater. Sol. Cells* 153, 148–163.

- Saianand, G., Gopalan, A.-I., Lee, J.-C., Sathish, C., Gopalakrishnan, K., Unni, G.E., Shanbhag, D., Dasireddy, V.D.B.C., Yi, J., Xi, S., Al-Muhtaseb, A.a.H., Vinu, A., 2020. Mixed copper/copper-oxide anchored mesoporous fullerene nanohybrids as superior electrocatalysts toward oxygen reduction reaction. *Small* 16 (12), 1903937.
- Saianand, G., Sonar, P., Wilson, G.J., Gopalan, A.-I., Roy, V.A.L., Unni, G.E., Mamun Reza, K., Bahrami, B., Venkatramanan, K., Qiao, Q., 2021. Current advancements on charge selective contact interfacial layers and electrodes in flexible hybrid perovskite photovoltaics. *J. Energy Chem.* 54, 151–173.
- Sambaza, S.S., Maity, A., Pillay, K., 2020. Polyaniline-coated TiO<sub>2</sub> nanorods for photocatalytic degradation of bisphenol a in water. *ACS Omega* 5 (46), 29642–29656.
- Sangareswari, M., Meenakshi Sundaram, M., 2017. Development of efficiency improved polymer-modified TiO<sub>2</sub> for the photocatalytic degradation of an organic dye from wastewater environment. *Appl. Water Sci.* 7 (4), 1781–1790.
- Schneider, J., Matsuoka, M., Takeuchi, M., Zhang, J., Horiuchi, Y., Anpo, M., Bahnemann, D.W., 2014. Understanding TiO<sub>2</sub> photocatalysis: Mechanisms and materials. *Chem. Rev.* 114 (19), 9919–9986.
- Shanmugasundaram, K., Sai-Anand, G., Gopalan, A.-I., Lee, H.-G., Yeo, H.K., Kang, S.-W., Lee, K.-P., 2016. Direct electrochemistry of cytochrome c with three-dimensional nanoarchitected multicomponent composite electrode and nitrite biosensing. *Sensors Actuators B* 228, 737–747.
- Sheikhsamany, R., Faghihian, H., 2019. Elimination of phenylhydrazine from aqueous solutions by use of a photocatalyst prepared by immobilization of TiO<sub>2</sub> on polyrrrole support. *J. Inorg. Organomet. Polym. Mater.*
- Shi, Q., Zhang, Y., Sun, D., Zhang, S., Tang, T., Zhang, X., Cao, S., 2020. Bi2O<sub>3</sub>-sensitized TiO<sub>2</sub> hollow photocatalyst drives the efficient removal of tetracyclines under visible light. *Inorg. Chem.* 59 (24), 18131–18140.
- Silvestri, S., Burgo, T.A.L., Dias-Ferreira, C., Labrincha, J.A., Tobaldi, D.M., 2020. Polypyrrole-TiO<sub>2</sub> composite for removal of 4-chlorophenol and diclofenac. *React. Funct. Polym.* 146, 104401.
- Silvestri, S., Ferreira, C.D., Oliveira, V., Varejão, J.M.T.B., Labrincha, J.A., Tobaldi, D.M., 2019. Synthesis of PPy-ZnO composite used as photocatalyst for the degradation of diclofenac under simulated solar irradiation. *J. Photochem. Photobiol. A: Chem.* 375, 261–269.
- Sun, X., Sun, B., Gong, Q., Gao, T., Zhou, G., 2019. Double-shell structural polyaniline-derived TiO<sub>2</sub> hollow spheres for enhanced photocatalytic activity. *Transit. Met. Chem.* 44 (6), 555–564.
- Sun, K., Zhang, S., Li, P., Xia, Y., Zhang, X., Du, D., Isikgor, F.H., Ouyang, J., 2015. Review on application of PEDOTs and PEDOT:PSS in energy conversion and storage devices. *J. Mater. Sci., Mater. Electron.* 26 (7), 4438–4462.
- Tada, H., Mitsui, T., Kiyonaga, T., Akita, T., Tanaka, K., 2006. All-solid-state Z-scheme in CdS–Au–TiO<sub>2</sub> three-component nanojunction system. *Nature Mater.* 5 (10), 782–786.
- Taddesse, A.M., Bekele, T., Diaz, I., Adgo, A., 2021. Polyaniline supported CdS/CeO<sub>2</sub>/Ag<sub>3</sub>PO<sub>4</sub> nanocomposite: An A-B type tandem n-n heterojunctions with enhanced photocatalytic activity. *J. Photochem. Photobiol. A: Chem.* 406, 113005.
- Talaiekhosani, A., Rezaei, S., Kim, K.-H., Sanaye, R., Amani, A.M., 2021. Recent advances in photocatalytic removal of organic and inorganic pollutants in air. *J. Cleaner Prod.* 278, 123895.
- Tang, W., Chen, J., Yin, Z., Sheng, W., Lin, F., Xu, H., Cao, S., 2021a. Complete removal of phenolic contaminants from bismuth-modified TiO<sub>2</sub> single-crystal photocatalysts. *Chin. J. Catal.* 42 (2), 347–355.
- Tang, T., Yin, Z., Chen, J., Zhang, S., Sheng, W., Wei, W., Xiao, Y., Shi, Q., Cao, S., 2021b. Novel p-n heterojunction Bi<sub>2</sub>O<sub>3</sub>/Ti<sub>3</sub>O<sub>5</sub>–TiO<sub>2</sub> photocatalyst enables the complete removal of tetracyclines under visible light. *Chem. Eng. J.* 417, 128058.
- Thakare, S.R., Mate, V.R., Urkude, K., Gawande, S.B., 2020. Graphene-TiO<sub>2</sub>-polyaniline nanocomposite: A new green and efficient catalyst as a alternative for noble metal and NaBH<sub>4</sub> induced the reduction of 4-nitro phenol. *FlatChem* 22, 100179.
- Torki, F., Faghihian, H., 2017. Sunlight-assisted decomposition of cephalixin by novel synthesized NiS-PPY-Fe<sub>3</sub>O<sub>4</sub> nanophotocatalyst. *J. Photochem. Photobiol. A: Chem.* 338, 49–59.
- Tryba, B., Rychtowski, P., Markowska-Szczupak, A., Przepiórski, J., 2020. Photocatalytic decomposition of acetaldehyde on different TiO<sub>2</sub>-based materials: A review. *Catalysts* 10 (12), 1464.
- Ullah, H., Tahir, A.A., Mallick, T.K., 2017. Polypyrrole/TiO<sub>2</sub> composites for the application of photocatalysis. *Sensors Actuators B* 241, 1161–1169.
- Vajihinejad, V., Gumfekar, S.P., Bazoubandi, B., Najafabadi, Z.Rostami., Soares, J.B.P., 2019. Water soluble polymer flocculants: Synthesis, characterization, and performance assessment. *Macromol. Mater. Eng.* 304 (2), 1800526.
- Venieri, D., Mantzavinos, D., Binias, V., 2020. Solar photocatalysis for emerging micro-pollutants abatement and water disinfection: A mini-review. *Sustainability* 12 (23), 10047.
- Wang, H., Han, B., Lu, J., Wu, P., Cui, W., 2020a. Excellent photoelectrocatalytic degradation and superior charge separation of polyaniline nanosheets wrapped TiO<sub>2</sub> nanotube arrays. *Mater. Lett.* 260, 126906.
- Wang, H., Liu, X., Liu, X., Huo, P., Guan, Q., 2015a. Preparation of polypyrrole–TiO<sub>2</sub> and its adsorption and photocatalytic degradation of salicylic acid. *Desalin. Water Treat.* 54 (12), 3291–3299.
- Wang, D., Pillai, S.C., Ho, S.-H., Zeng, J., Li, Y., Dionysiou, D.D., 2018. Plasmonic-based nanomaterials for environmental remediation. *Appl. Catal. B* 237, 721–741.
- Wang, J., Wang, B., Zhang, W., Xiao, Y., Xu, H., Liu, Y., Liu, Z., Zhang, J., Jiang, Y., 2022. Visible-light-driven double-shell SnIn<sub>4</sub>S<sub>8</sub>/TiO<sub>2</sub> heterostructure with enhanced photocatalytic activity for MO removal and Cr(VI) cleanup. *Appl. Surf. Sci.* 587, 152867.
- Wang, J., Wang, X., Zhao, S., Sun, B., Wang, Z., Wang, J., 2020b. Robust superhydrophobic mesh coated by PANI/TiO<sub>2</sub> nanoclusters for oil/water separation with high flux, self-cleaning, photodegradation and anti-corrosion. *Sep. Purif. Technol.* 235, 116166.
- Wang, Z., Yang, C., Lin, T., Yin, H., Chen, P., Wan, D., Xu, F., Huang, F., Lin, J., Xie, X., Jiang, M., 2013a. H-doped black titania with very high solar absorption and excellent photocatalysis enhanced by localized surface plasmon resonance. *Adv. Funct. Mater.* 23 (43), 5444–5450.
- Wang, Z., Yang, C., Lin, T., Yin, H., Chen, P., Wan, D., Xu, F., Huang, F., Lin, J., Xie, X., Jiang, M., 2013b. Visible-light photocatalytic, solar thermal and photoelectrochemical properties of aluminium-reduced black titania. *Energy Environ. Sci.* 6 (10), 3007–3014.
- Wang, Y.J., Yu, G., 2019. Conjugated polymers: From synthesis, transport properties, to device applications. *J. Polym. Sci. B* 57 (23), 1557–1558.
- Wang, Y., Zhang, P., Zhang, T.C., Xiang, G., Wang, X., Pehkonen, S., Yuan, S., 2020c. A magnetic  $\gamma$ -Fe<sub>2</sub>O<sub>3</sub>@PANI@TiO<sub>2</sub> core-shell nanocomposite for arsenic removal via a coupled visible-light-induced photocatalytic oxidation-adsorption process. *Nanoscale Adv.* 2 (5), 2018–2024.
- Wang, Q., Zheng, L., Chen, Y., Fan, J., Huang, H., Su, B., 2015b. Synthesis and characterization of novel PPy/Bi<sub>2</sub>O<sub>2</sub>CO<sub>3</sub> composite with improved photocatalytic activity for degradation of Rhodamine-B. *J. Alloys Compd.* 637, 127–132.
- Wei, J., Zhang, Q., Liu, Y., Xiong, R., Pan, C., Shi, J., 2011. Synthesis and photocatalytic activity of polyaniline–TiO<sub>2</sub> composites with bionic nanopapilla structure. *J. Nanopart. Res.* 13 (8), 3157–3165.
- Wen, M., Wang, J., Tong, R., Liu, D., Huang, H., Yu, Y., Zhou, Z.-K., Chu, P.K., Yu, X.-F., 2019. A low-cost metal-free photocatalyst based on black phosphorus. *Adv. Sci.* 6 (1), 1801321.
- Wu, H., Kong, X.Y., Wen, X., Chai, S.-P., Lovell, E.C., Tang, J., Ng, Y.H., 2021. Metal-organic framework decorated cuprous oxide nanowires for long-lived charges applied in selective photocatalytic CO<sub>2</sub> reduction to CH<sub>4</sub>. *Angew. Chem. Int. Ed.* 60 (15), 8455–8459.
- Xiao, Y., Sun, X., Li, L., Chen, J., Zhao, S., Jiang, C., Yang, L., Cheng, L., Cao, S., 2019. Simultaneous formation of a C/N-TiO<sub>2</sub> hollow photocatalyst with efficient photocatalytic performance and recyclability. *Chin. J. Catal.* 40 (5), 765–775.
- Xing, X., Tang, S., Hong, H., Jin, H., 2020. Concentrated solar photocatalysis for hydrogen generation from water by titania-containing gold nanoparticles. *Int. J. Hydrogen Energy* 45 (16), 9612–9623.

- Xiong, S., Wang, Q., Xia, H., 2004. Template synthesis of polyaniline/TiO<sub>2</sub> bilayer microtubes. *Synth. Met.* 146 (1), 37–42.
- Xu, X., Gao, X., Lu, T., Liu, X., Wang, X., 2015. Hybrid material based on a coordination-complex-modified polyoxometalate nanorod (CC/POMNR) and PPy: a new visible light activated and highly efficient photocatalyst. *J. Mater. Chem. A* 3 (1), 198–206.
- Xu, B., Gopalan, S.-A., Gopalan, A.-I., Muthuchamy, N., Lee, K.-P., Lee, J.-S., Jiang, Y., Lee, S.-W., Kim, S.-W., Kim, J.-S., Jeong, H.-M., Kwon, J.-B., Bae, J.-H., Kang, S.-W., 2017. Functional solid additive modified PEDOT:PSS as an anode buffer layer for enhanced photovoltaic performance and stability in polymer solar cells. *Sci. Rep.* 7 (1), 45079.
- Xu, C., Ravi Anusuyadevi, P., Aymonier, C., Luque, R., Marre, S., 2019. Nanostructured materials for photocatalysis. *Chem. Soc. Rev.* 48 (14), 3868–3902.
- Xu, C., Song, Y., Lu, L., Cheng, C., Liu, D., Fang, X., Chen, X., Zhu, X., Li, D., 2013. Electrochemically hydrogenated TiO<sub>2</sub> nanotubes with improved photoelectrochemical water splitting performance. *Nanoscale Res. Lett.* 8 (1), 391.
- Yang, H., 2021. A short review on heterojunction photocatalysts: Carrier transfer behavior and photocatalytic mechanisms. *Mater. Res. Bull.* 142, 111406.
- Yang, C., Dong, W., Cui, G., Zhao, Y., Shi, X., Xia, X., Tang, B., Wang, W., 2017. Enhanced photocatalytic activity of PANI/TiO<sub>2</sub> due to their photosensitization-synergetic effect. *Electrochim. Acta* 247, 486–495.
- Yang, L., Lv, M., Song, Y., Yin, K., Wang, X., Cheng, X., Cao, K., Li, S., Wang, C., Yao, Y., Luo, W., Zou, Z., 2020. Porous SnO<sub>2</sub> nanosheets on PPy hollow rod with photo-induced electrons oriented migration for enhanced visible-light hydrogen production. *Appl. Catal. B* 279, 119341.
- Yao, T., Shi, L., Wang, H., Wang, F., Wu, J., Zhang, X., Sun, J., Cui, T., 2016. A simple method for the preparation of TiO<sub>2</sub>/Ag-AgCl@Polypyrrole composite and its enhanced visible-light photocatalytic activity. *Chem. – Asian J.* 11 (1), 141–147.
- Yi, S.-S., Zhang, X.-B., Wulan, B.-R., Yan, J.-M., Jiang, Q., 2018. Non-noble metals applied to solar water splitting. *Energy Environ. Sci.* 11 (11), 3128–3156.
- Yu, J., Pang, Z., Zheng, C., Zhou, T., Zhang, J., Zhou, H., Wei, Q., 2019. Cotton fabric finished by PANI/TiO<sub>2</sub> with multifunctions of conductivity, anti-ultraviolet and photocatalysis activity. *Appl. Surf. Sci.* 470, 84–90.
- Yuan, X., Floresyona, D., Aubert, P.-H., Bui, T.-T., Remita, S., Ghosh, S., Brisset, F., Goubard, F., Remita, H., 2019. Photocatalytic degradation of organic pollutant with polypyrrole nanostructures under UV and visible light. *Appl. Catal. B* 242, 284–292.
- Yuan, X., Kobylanski, M.P., Cui, Z., Li, J., Beaunier, P., Dragoe, D., Colbeau-Justin, C., Zaleska-Medynska, A., Remita, H., 2020. Highly active composite TiO<sub>2</sub>-polypyrrole nanostructures for water and air depollution under visible light irradiation. *J. Environ. Chem. Eng.* 8 (5), 104178.
- Zarrin, S., Heshmatpour, F., 2018. Photocatalytic activity of TiO<sub>2</sub>/Nb<sub>2</sub>O<sub>5</sub>/PANI and TiO<sub>2</sub>/Nb<sub>2</sub>O<sub>5</sub>/RGO as new nanocomposites for degradation of organic pollutants. *J. Hard Mater.* 351, 147–159.
- Žerjav, G., Scandura, G., Garlisi, C., Palmisano, G., Pintar, A., 2020. Sputtered vs. sol-gel TiO<sub>2</sub>-doped films: Characterization and assessment of aqueous bisphenol a oxidation under UV and visible light radiation. *Catal. Today* 357, 380–391.
- Zeynali, S., Taghizadeh, M.T., 2019. Highly efficient TiO<sub>2</sub>/AgBr/PANI heterojunction with enhanced visible light photocatalytic activity towards degradation of organic dyes. *J. Mater. Sci., Mater. Electron.* 30 (18), 17020–17031.
- Zhang, L., Liu, P., Su, Z., 2006. Preparation of PANI-TiO<sub>2</sub> nanocomposites and their solid-phase photocatalytic degradation. *Polym. Degrad. Stab.* 91 (9), 2213–2219.
- Zhang, L., Ran, J., Qiao, S.-Z., Jaroniec, M., 2019. Characterization of semiconductor photocatalysts. *Chem. Soc. Rev.* 48 (20), 5184–5206.
- Zhang, L., Wan, M., 2003. Polyaniline/TiO<sub>2</sub> composite nanotubes. *J. Phys. Chem. B* 107 (28), 6748–6753.
- Zhang, G., Zhang, X., Meng, Y., Pan, G., Ni, Z., Xia, S., 2020. Layered double hydroxides-based photocatalysts and visible-light driven photodegradation of organic pollutants: A review. *Chem. Eng. J.* 392, 123684.
- Zhao, J., Biswas, M.R.U.D., Oh, W.-C., 2019a. A novel BiVO<sub>4</sub>-GO-TiO<sub>2</sub>-PANI composite for upgraded photocatalytic performance under visible light and its non-toxicity. *Environ. Sci. Pollut. Res.* 26 (12), 11888–11904.
- Zhao, J., Han, P., Tian, S., Shi, H., He, J., Xiao, C., 2019b. Polypyrrole/cadmium sulfide hollow fiber with high performance contaminant removal and photocatalytic activity fabricated by layer-by-layer deposition and fiber-sacrifice template approach. *J. Colloid Interface Sci.* 557, 94–102.
- Zhao, Z., Zhou, Y., Wang, F., Zhang, K., Yu, S., Cao, K., 2015. Polyaniline-decorated {001} facets of Bi<sub>2</sub>O<sub>2</sub>CO<sub>3</sub> nanosheets: In situ oxygen vacancy formation and enhanced visible light photocatalytic activity. *ACS Appl. Mater. Interfaces* 7 (1), 730–737.
- Zhou, Q., Zhao, D., Sun, Y., Sheng, X., Zhao, J., Guo, J., Zhou, B., 2020. G-C<sub>3</sub>N<sub>4</sub>- and polyaniline-co-modified TiO<sub>2</sub> nanotube arrays for significantly enhanced photocatalytic degradation of tetrabromobisphenol A under visible light. *Chemosphere* 252, 126468.
- Zhu, X., Song, Z., Wang, Z., Liu, W., Hong, B., Bao, J., Gao, C., Sun, S., 2020. Selective formation of interfacial bonding enables superior hydrogen production in organic-inorganic hybrid cocatalyzed photocatalysts. *Appl. Catal. B* 274, 119010.
- Zhu, Z., Tang, X., Ma, C., Song, M., Gao, N., Wang, Y., Huo, P., Lu, Z., Yan, Y., 2016. Fabrication of conductive and high-dispersed Ppy@Ag/g-C<sub>3</sub>N<sub>4</sub> composite photocatalysts for removing various pollutants in water. *Appl. Surf. Sci.* 387, 366–374.
- Zia, J., Ajeer, M., Riaz, U., 2019. Visible-light driven photocatalytic degradation of bisphenol-a using ultrasonically synthesized polypyrrole/k-birnessite nanohybrids: Experimental and DFT studies. *J. Environ. Sci.* 79, 161–173.